DISRUPTION OF MITOCHONDRIAL FITNESS IN HUMAN PREADIPOCYTES BY FATTY ACIDS

By

Artie Carlyle Rogers

June 2013

Director of Dissertation: Jacques Robidoux Ph.D.

Major Department: Pharmacology and Toxicology

Adipose tissue lies at the core of energy metabolism, by not only releasing and taking up fatty acids (FA) according to the individuals energy requirements, but also signaling other tissues to regulate their own metabolism. If adipose tissue function is lost, insulin resistance, hypertriglyceridemia and hepatic steatosis can develop. Despite understanding how adipocytes function in normal and diseased states, preadipocytes, which can safeguard against adipocyte dysfunction by differentiating and joining the adipocyte pool, have been overlooked. Furthermore, how preadipocytes, which have a diminished capacity to esterify FA compared to adipocytes, are able to survive constant FA fluctuations within the adipose tissue depot without succumbing to lipotoxicity remains unclear. Therefore, how human preadipocytes sense and resist a mixture of FA (oleate, palmitate, stearate and linoleate) that resembles a healthy individual's adipose tissue microenvironment was investigated.

Experiments using a novel real-time flow cytometry device show that the maximal rate of mitochondrial superoxide accumulation, hydrogen peroxide (H_2O_2) production, and lipid

peroxidation occurred within seconds of exposure to FA. Although mitochondrial ROS occurred in a transient fashion (within 2 hours), preadipocytes still experienced a loss in respiration through depletion of NAD+ and NADH that manifested into overt oxidative stress and cell death after 24 hours of FA exposure. Despite observing cell death in 35% of our population, the majority of preadipocytes were able to mount a protective response through increases in the mitochondrial antioxidant buffering capacity. Investigation into FOXO1, one of the transcription factors that govern mitochondrial antioxidant gene transcription, revealed an increase in deacetylation as soon as six hours post FA exposure. Inhibition of FOXO1 or SIRT1, which deacetylates FOXO1, exacerbated the toxic effects of FA suggesting that the SIRT1-FOXO1 axis may play a beneficial role in protecting preadipocytes from constant exposure to FA. Furthermore, SIRT1, FOXO1 and mitochondrial antioxidant gene expression from human adipose tissue was correlated to insulin sensitivity further highlighting the potential importance of mitochondrial antioxidant buffering systems in adipose tissue function. Altogether, this study suggests that the preadipocyte survivability is centered on mitochondrial resistance to FA-induced ROS through up regulation of mitochondrial antioxidant systems.

DISRUPTION OF MITOCHONDRIAL FITNESS IN HUMAN PREADIPOCYTES BY FATTY ACIDS

A Dissertation

Presented To

The Faculty of the Department of Pharmacology and Toxicology

The Brody School of Medicine at East Carolina University

In Partial Fulfillment of the Requirements for the Degree

Doctor of Philosophy in Pharmacology and Toxicology

By

Artie Carlyle Rogers

June 2013

DISRUPTION OF MITOCHONDRIAL FITNESS IN HUMAN PREADIPOCYTES BY FATTY ACIDS

By

Artie Carlyle Rogers

APPROVED BY:

DIRECTOR OF DISSERTATION:

_____

Jacques Robidoux, Ph.D.

COMMITTEE MEMBER:

_____

Ethan Anderson, Ph.D.

COMMITTEE MEMBER:

_____

David Brown, Ph.D.

COMMITTEE MEMBER:

_____

Jingbo Pi, Ph.D.

COMMITTEE MEMBER AND

CHAIR OF THE DEPARTMENT OF

PHAMACOLOGY AND TOXICOLOGY _____

David A. Taylor, Ph.D.

DEAN OF THE GRADUATE SCHOOL

_____

Paul J. Gemperline, Ph.D.

DEDICATION

This work is dedicated to my mother, Marsha Manning Rogers and to my grandfather, J. Carlyle Manning, whose namesake I am proud to carry.

ACKNOWLEDGEMENTS

I would like to extend the upmost thanks to my Heavenly Father, and to my family and to my friends for their support throughout my time at East Carolina University. To my mother, without your constant guidance and support throughout my education I would have never been able to make it this far. I could not have been blessed with a more wonderful mother. To my two brothers, Christopher and Christian, I thank you for helping me during tough times and always providing comic relief when needed. To my grandfather and grandmother, I would like to say thanks for always believing in me.

Secondly, I would like to thank the wonderful staff and faculty in the Pharmacology and Toxicology Department at The Brody School of Medicine. Without providing me a sound foundation in Pharmacology and Toxicology, I would not have developed into the scientist I am today. Furthermore, the helpfulness of the office staff (Mrs. Pam Wynne, Mrs. Jackie Hooker, Ms. Amber Hardie, and Mrs. Judy Melendez) with ordering, paperwork or just simple chats about life helped to make my time as a graduate student much easier.

Next, I would like to thank my committee members, Dr. Jacques Robidoux, Dr. David Taylor, Dr. Ethan Anderson, Dr. David Brown and Dr. Jingbo Pi. Without your input, advice, time and comments, I would not have been able to advance my scientific ideas in a meaningful way. I would like to give a special mention to my mentor, Dr. Jacques Robidoux, whose constant efforts and use of resources to guide and develop my ideas has helped me immensely. Without the contribution of Dr. Robidoux's time and effort, my exploits into adipose tissue would have been a lot more difficult. I hope our time together has helped to begin the foundation of the "Robidoux Dynasty" you dreamed of.

Lastly, I would like to thank the other members of the Robidoux Laboratory. Mrs. Barbara Davis thank you, for having the magical touch with the “cell children”, always keeping the snack drawer full and being one of the nicest people I have ever had the pleasure of working with. I would also like to give a special thanks to our extended lab family of Mrs. Jackie Masterson and Dr. James Gibson. Mrs. Jackie, I would like to thank you for guidance, providing me an opportunity to test my “handyman skills” and supplying me with candy. To Dr. Gibson, I would like to thank you for your scientific wisdom, your endless supply of jokes and always pushing me to be even better. I would also like to thank all the graduate students who have shared a laugh, cried a tear or had a discussion with me during these past years. I wish you all the best in all of your future endeavors.

TABLE OF CONTENTS

LIST OF TABLES

LIST OF FIGURES

LIST OF SYMBOLS OR ABBREVIATIONS

BMI	Body Mass Index
BSA	Bovine Serum Albumin
Ca^{2+}	Calcium
CAT	Catalase
CDC	Center for Disease Control
cDNA	Complementary DNA
CM-H_2DCFDA	5-(and-6)-Chloromethyl-2',7'-Dichlorodihydrofluorescein Diacetate, Acetyl Ester
CoA	Coenzyme A
CRT	Continuous Real Time
Cu^{2+}	Copper
dL	Deciliter
DMEM	Dulbecco's Modified Eagle Medium
DMSO	Dimethyl Sulfoxide
DN	Dominant Negative
DNA	Deoxyribonucleic Acid
DPBS	Dubellco's Phophate Buffered Saline
ETC	Electron Transport Chain
FA	Fatty Acid
FAD	Flavin Adenine Dinucleotide
$FADH_2$	Reduced Flavin Adenine Dinucleotide

FasL	FAS Receptor Ligand
FCCP	p-Trifluoromethoxy Carbonyl Cyanide Phenyl Hydrazone
Fe^{2+}	Iron
FFA	Free Fatty Acid
FKHR	Forkhead (Drosophila) Homolog 1 (rhabdomyosarcoma)
FOXO	Forkhead Box Class O
FRE	Foxo Response Element
FSC	Forward Scatter
GAPDH	Glyceraldehyde 3-Phosphate Dehydrogenase
GPX1	Glutathione Peroxidase 1
GSR	Glutathione Reductase
H_2O	Water
H_2O_2	Hydrogen Peroxide
$HO^{\cdot}$	Hydroxyl Radical
HOMA-IR	Homeostatic Model Assessment of Insulin Resistance
IgG	Immunoglobulin G
IRO	Insulin Resistant Obese
IRS	Insulin Receptor Substrate
ISL	Insulin Sensitive Lean
ISNO	Insulin Sensitive Non-Obese
IU	International Unit
Kg	Kilogram

M	Molar
m	Meter
MFI	Mean Fluorescence Intensity
Mg^{2+}	Magnesium
mL	Mililiter
mM	Millimolar
µM	Micromolar
mPTP	Mitochondrial Permeability Transition Pore
mRNA	Messenger Ribonucleic Acid
NAD+	Nicotinamide Adenine Dinucleotide
NADH+	Reduced Nicotinamide Adenine Dinucleotide
NADPH	Reduced Nicotinamide Adenine Dinucleotide Phosphate
NAM	Nicotinamide
NEFA	Non-Esterified Fatty Acid
nM	Nanomolar
nm	Nanometer
O_2^-	Superoxide
OCR	Oxygen Consumption Rate
P53	Tumor Protein 53
PBS	Phosphate Buffered Saline
PRX3	Peroxiredoxin 3
RNA	Ribonucleic Acid

ROS	Reactive Oxygen Species
rt-PCR	Real-time Polymerase Chain Reaction
SD	Standard Deviation
SEM	Standard Error of the Mean
SI	Insulin Sensitivity
SIRT1	Sirtuin 1
SOD2	Superoxide Dismutase 2
SSC	Side Scatter
T2DM	Type 2 Diabetes Mellitus
TMRE	Tetramethylrhodamine Ethyl Ester Perchlorate
TXNRD2	Thioredoxin Reductase 2

CHAPTER 1: REVIEW OF THE LITERATURE

In the developing world, rates of obesity are reaching epidemic proportions (Dinsa, Goryakin, Fumagalli, & Suhrcke, 2012). An accumulating body of literature suggests that adipose tissue dysfunction in obesity leads to ectopic fat accumulation and the development of an array of diseases (Abbasi, Brown, Lamendola, McLaughlin, & Reaven, 2002; A. Gastaldelli et al., 2002; Ravussin & Smith, 2002). However, irrespective of body weight, adipose tissue dysfunction can cause insulin resistance, hypertriglyceridemia and hepatic steatosis, suggesting that adipose tissue susceptibility should not be looked at in terms of obesity alone (P. Arner et al., 2011). One proposed mechanism as how adipose tissue dysfunction occurs is from failure of adipose tissue turnover by either a loss in preadipocyte number or differentiation capacity (J. Smith, Al-Amri, Dorairaj, & Sniderman, 2006). Once a reduction in preadipocyte number or differentiation capacity occurs, mature adipocytes will store an overabundance of fatty acids (FA) and enter a hypertrophic/dysfunctional state (E. Arner et al., 2010; Heilbronn, Smith, & Ravussin, 2004; J. Smith et al., 2006). Although numerous studies have focused on the role of the adipocyte (Ahmadian, Wang, & Sul, 2010; DeFronzo, 2004; Varlamov et al., 2010; Wang et al., 2010), how preadipocytes function in an environment of constant exposure to FA levels has not been investigated.

Preadipocytes, which are located within close proximity to lipid filled mature adipocytes, are in constant exposure to FA at much higher levels than other cell types of the body in both the healthy and diseased state (Tahiri, Karpe, Tan, & Cianflone, 2007). However, the elevation in intracellular levels of FA, seen during overnight fasting, may come at a price of increased reactive oxygen species (ROS) generation, specifically mitochondrial superoxide and hydrogen peroxide (H_2O_2) (Lambertucci et al., 2008; P Schönfeld & L Wojtczak, 2008). If preadipocytes

fail to mount a protective response in the face of increased ROS generation, oxidative stress and cell death can occur. Studies on the effects of FA on preadipocytes revealed a transient increase in mitochondrial superoxide, H_2O_2 and lipid peroxidation. This initial mitochondrial superoxide and/or alkyl radical production is linked to a cascade of events that lead to decreased NAD^+ levels, a loss of mitochondrial inner membrane potential (MIMP), diminished mitochondrial respiration, reduced ATP, and ultimately lead to the preadipocytes' demise. Although almost one-third of cells died, the majority of cells survived, suggesting a protective mechanism against FA toxicity existed. Gene expression from preadipocytes indicated an upregulation of mitochondrial antioxidant genes following FA exposure. Examination of FOXO1, one of the transcription factors that govern mitochondrial antioxidant gene transcription, revealed an increase in deacetylation as soon as six hours post FA exposure. Inhibition of FOXO1 or SIRT1, which deacetylates FOXO1, exacerbated the toxic effects of FA suggesting that the SIRT1-FOXO1 axis may play a beneficial role in protecting preadipocytes from constant exposure to FA. Gene expression profiles between adipose tissue obtained from insulin-sensitive and insulin-resistant individuals revealed that antioxidant genes regulated by the SIRT1-FOXO1 axis were lower in insulin resistance suggesting the protective effect of mitochondrial antioxidant gene expression in preserving adipose tissue function.

The survey of literature will examine why the choice was made to investigate the effects of FA in preadipocytes rather than adipocytes. Highlights from this section include how adipose tissue and preadipocytes function within an adipose tissue environment in the context of daily fluctuations of FA, the impact of FA on mitochondrial fitness and how the prototypical SIRT1-FOXO1 stress response may serve to protect against FA-induced lipotoxicity.

Adipose Tissue: The Body's Fat Stores

From the beginning of human history, the ability to survive required that individuals store calories in the form of triacylglycerol that is used as fuel during periods of low food availability. The main cell type that performs this process of lipid storage and release is the white adipocyte (Frayn, 2002). Two other main adipocyte cell types have been identified, the brown and beige adipocyte. Unlike white adipocytes, brown and beige adipocytes use FA almost exclusively for thermogenesis rather than storage (Cinti, 2006; Lidell et al., 2013). The locations of brown adipose tissue are found exclusively around the thorax, neck, and vertebrata, while beige adipocytes are located within white adipose tissue (Wu et al., 2012). Since an increase in caloric intake can involve expansion of white adipose tissue to store excess calories as fat (Gray & Vidal-Puig, 2007; J. Y. Kim et al., 2007; J. Smith et al., 2006), the focus of this review of literature will be on the role of white adipocytes, and specifically their progenitors, the white preadipocytes.

White adipose tissue develops around sites of loose connective tissue such as subcutaneous layers between the muscle and the dermis; however, adipose specific depots also form around the heart, kidneys and other internal organs (Gray & Vidal-Puig, 2007). The three main adipose tissue depots responsible for FA trafficking are 1) visceral, the adipose tissue surrounding the major abdominal organs, 2) lower body subcutaneous and 3) upper body subcutaneous (Paolisso, Gambardella, et al., 1995). Although each adipocyte depot functions to store FA, their contribution to the uptake and release of FA is different. For example, although visceral fat has a higher rate of FA release than subcutaneous fat, it contributes very little to systemic levels of non-esterified fatty acids (NEFA) (P. Arner, 2005; Gil, Olza, Gil-Campos, Gomez-Llorente, & Aguilera, 2011). Therefore, the major contributor to circulating NEFA is

from subcutaneous adipose tissue, and specifically from the upper body region (Koutsari, Ali, Mundi, & Jensen, 2011; Koutsari, Snozek, & Jensen, 2008). Because of its preponderant role in extracting circulating FA, it has been hypothesized that failure of subcutaneous adipose tissue to store FA into neutral lipids essentially triacylglycerol, causes an efflux of FA to ectopic sites including visceral adipose tissue, liver and muscle (Ravussin & Smith, 2002). As FA are recognized to be cytotoxic for most non-adipocyte cells, increased FA exposure could explain the onset of systemic metabolic abnormalities (Unger, Clark, Scherer, & Orci, 2010a).

The Preadipocyte: Guardian of Adipose Tissue Turnover

Adipocytes are renewed throughout our lifetime, with roughly 10% of fat cells being renewed annually between the ages of 20 and 50 (Spalding et al., 2008). Therefore, preadipocytes, the progenitors that differentiate into new adipocytes, are an important adipose tissue cell type in their own right. Irrespective of body weight, if adipose tissue turnover fails to store FA, preexisting adipocytes will take up an overabundance of FA and enter a hypertrophic (abnormally enlarged) state (DeFronzo, 2004; Ravussin & Smith, 2002; Sethi & Vidal-Puig, 2007). Ultimately, hypertrophic adipocytes become insulin resistant and fail to take up FA leading to an elevation in the basal circulating NEFA level and perhaps furthering exacerbating an already dysfunctional adipose tissue depot (E. Arner et al., 2010; Gray & Vidal-Puig, 2007; J. Smith et al., 2006). Although the current understanding of how adipocytes function in a diseased state is characterized (DeFronzo, 2004; Hegele, Joy, Al-Attar, & Rutt, 2007), how other adipose tissue cell types function in diseased states or even in healthy environment is not as clear. One of these cell types that has the biggest impact on overall adipocyte function, is the preadipocyte. A reduction in preadipocyte number or adipogenic potential has been correlated with the increase in hypertrophic adipocytes and the onset of metabolic abnormalities (E. Arner et al., 2010;

Tchoukalova, Koutsari, & Jensen, 2007). The reason why there is a decrease in the number of preadipocytes, preadipocyte fitness and/or preadipocyte adipogenenic potential is not known.

As discussed earlier, adipose tissue, serves to convert cytotoxic FA into less damaging neutral lipids, thereby protecting other tissues from their lipotoxicity (DeFronzo, 2004). Since preadipocytes are located near FA-releasing adipocytes, they are periodically exposed to high FA concentrations even in healthy individuals. For example, Tahiri *et al.*, demonstrated that the adipose venous NEFA concentrations far exceeds the arterial NEFA concentration, indicating that cells within the adipose depot are exposed to two to three times higher FA concentrations than non-adipose depot cells independent of the diseased state (Tahiri et al., 2007). Although the role of FA on adipocytes has been the focus of several studies (DeFronzo, 2004; Koutsari et al., 2011; M. Nguyen et al., 2005; Shadid, Koutsari, & Jensen, 2007; A. Subauste & C. Burant, 2007; Wang et al., 2010; Wang, Zang, Ling, Corkey, & Guo, 2003), FA effects on preadipocytes have been overlooked for some time. This may be due to the misguided thought that the adipocyte lineage is immune to the deleterious effects of FA because of their efficiency to neutralize FA into triacylglycerol; however, it has recently been shown that a supraphysiological concentration of 250 μM of palmitate when bound to 85 μM BSA can increase death in both rat and mouse preadipocytes (Guo, Wong, Xie, Lei, & Luo, 2007).

Fatty Acids: Too Much For Too Long

In humans, circulating NEFA and adipose tissue represents the largest reservoir of FA (Bernardi, Penzo, & Wojtczak, 2002). In the circulation, FA are present at FA: albumin ratios that rarely exceed 1:1 except during prolonged exercise, fasting, disease and at locations directly around adipose tissue where FA release/uptake is the highest (Curry, Brick, & Franks, 1999; Don

& Kaysen, 2004; Yamazaki, Inagaki, Kurita, & Inoue, 2005). Although the plasma NEFA concentration is often lumped together as one entity, it represents a mixture of individual FA with different characteristics. The four main FA that comprise nearly 95% of circulating NEFA are the saturated FA, palmitate and stearate, and the unsaturated FA, oleate and linoleate. Mittendorfer *et al*, demonstrated that during the fasting basal state, the total plasma NEFA concentration was comprised of 26% palmitate, 13% stearate, 38% oleate, and 17% linoleate (Mittendorfer, Liem, Patterson, Miles, & Klein, 2003). Surprisingly, infusion of epinephrine to stimulate adipocyte lipolysis did not change the percent of each FA although the total NEFA concentration had increased from a mean of 371 μM to 1048 μM (Mittendorfer et al., 2003). Studies measuring NEFA levels during fasting from plasma of obese and lean children, and patients with metabolic syndrome reported similar individual FA percentages, with the mean difference in percent composition of each FA differing less than 5% between lean or obese children or adults with metabolic syndrome (Novgorodtseva et al., 2011; Sabin et al., 2007). Although fasting NEFA mixture levels appear to be similar after fasting, following a meal containing fat, the composition can vary based on what fat the meal contained. In a process called spillover, FA hydrolyzed from chylomicrons and not taken up by adipocytes, will join the circulating plasma NEFA pool influencing the mixture of FA (Fielding et al., 1996; Heimberg, Dunn, & Wilcox, 1974). Therefore, the biggest influence on the NEFA composition comes directly after a meal. The change in fatty acid composition, however, is short lived, as NEFA composition appears to equilibrate rapidly during the postprandial period. Throughout our experiments, this basal FA composition will be used to try to mimic physiological situations in which FA are elevated for a prolonged period of time like postabsorptive or fasting periods. It

will help us to define the threshold at which lipotoxicity may occur and the mechanisms involved.

Impact of Fatty Acids on Mitochondrial Reactive Oxygen Species Emission

Although reactive oxygen species (ROS) serve in normal physiological signaling, if ROS are generated at a rate above the buffering capacity of the cell, they can become a toxic by-product, and have been linked to a wide variety of metabolic diseases including T2DM (Murphy, 2009). In mammalian tissues, four main types of ROS exist: the free radicals superoxide anion (O_2^-) and hydroxyl radical ($HO^\cdot$), and the non-radical species H_2O_2 and singlet oxygen ($^1O_2$) (Orrenius, Gogvadze, & Zhivotovsky, 2007; P Schönfeld & L Wojtczak, 2008). If ROS generation is above the buffering capacity of the mitochondrion, lipid peroxidation as well as redox-dependent protein modifications can occur leading to a loss in mitochondrial electron transport efficiency, membrane potential and inner membrane permeabilization (Orrenius et al., 2007). This is of importance because these consequences have a negative impact on cellular respiration and result in cell death.

After they enter the cell, FA are activated by the addition of a free coenzyme group, generating a fatty acyl CoA that can be either esterified or oxidized (Binas et al., 2003; Schaap, Binas, Danneberg, van der Vusse, & Glatz, 1999). The fraction of fatty acyl CoA channeled for β-oxidation is shuttled into the matrix of the mitochondria by CPT1, CPT2 and Carnitine translocase (Drynan, Quant, & Zammit, 1996). Once in the mitochondrial matrix, fatty acyl Co-A is oxidized to generate NADH and $FADH_2$. NADH and $FADH_2$ then pass electrons to the electron transport chain (ETC) due to their own negative redox potential, thus allowing electrons to travel down the chain to more positive redox potentials until they reduce oxygen, the final

electron acceptor to water (Brand, 2005; Brand & Nicholls, 2011). As electrons are passed along the chain, protons are pumped from the matrix through Complexes I, III, and IV and into the inner membrane space to generate a proton motive force that is used by the ATP synthase complex to form ATP (MITCHELL, 1961; Mitchell & Moyle, 1968). When ATP synthesis is low or the ability to pass electrons from complex to complex is interrupted, the ETC can become highly reduced (Wallace, Fan, & Procaccio, 2010). Once the ETC is reduced, electrons and oxygen accumulate at electron carriers within the ETC, thereby increasing the probability of electrons interacting with oxygen to form superoxide (Skulachev, 1996).

Several other hypotheses describing the mechanism by which FA induce ROS generation have been proposed. One explanation is that FA directly affects mitochondrial ETC machinery. Wojtczak et al., demonstrated in permeabilized mitochondria that Complex III becomes inactivated when exposed to palmitate in a concentration-dependent manner (P. Schönfeld & Wojtczak, 2007). Furthermore, inhibitory effects of palmitate on Complex I and depletion of cytochrome c by arachidonic acid have been observed (Cocco, Di Paola, Papa, & Lorusso, 1999; Di Paola, Cocco, & Lorusso, 2000; Loskovich, Grivennikova, Cecchini, & Vinogradov, 2005). FA can also change mitochondrial membrane fluidity and affect the ability of electrons to pass freely along the ETC, causing an increased probability of superoxide formation (P. Schönfeld & Struy, 1999; P. Schönfeld & Wojtczak, 2007; Stillwell, Jenski, Crump, & Ehringer, 1997).

Once superoxide is formed, it is dismutated by superoxide dismutase 2 (SOD2) into H_2O_2. Following dismutation of superoxide to H_2O_2, detoxifying systems such as the glutathione peroxidases and peroxiredoxins reduce H_2O_2 to H_2O. Mitochondrial glutathione peroxidases, especially GPX1, use reduced glutathione (GSH) to reduce H_2O_2 and release water and oxidized

glutathione (GSSG)(Cox, Peskin, Paton, Winterbourn, & Hampton, 2009; Lu, 2000). GSSG thereafter is restored to its reduced form by glutathione reductase (GSR), which sequentially uses two NADPH to reduce the prosthetic flavin adenine dinucleotide group that, in turn, reduces GSSG (Lei, 2002). Mitochondrial peroxiredoxins, specifically PRDX3, can interact with H_2O_2 to become oxidized and release water (Chae, Uhm, & Rhee, 1994; Cox et al., 2009). Thioredoxin, and its mitochondrial isoform, TRX2, serves to reduce the oxidized cysteine groups on proteins including oxidized PRX3 (Chae, Chung, & Rhee, 1994). By utilizing intra-mitochondrial NADPH a source of reducing equivalents, reduced TRX2 is regenerated by thioredoxin reductase (trxR) (Hansen, Zhang, & Jones, 2006; M. Liang & Pietrusz, 2007; Nonn, Williams, Erickson, & Powis, 2003). Other mitochondrial antioxidant defenses, such as phospholipid hydroperoxide glutathione peroxidase 4 (GPX4) can reduce hydroperoxide groups on phospholipids, lipoproteins and cholesteryl esters, in addition to being able to reduce H_2O_2 (Pushpa-Rekha, Burdsall, Oleksa, Chisolm, & Driscoll, 1995).

The NAD+ and SIRT1 Connection

During fasting conditions, the level of carbohydrates in the blood goes down and the level of FA rises. This increased availability of FA for oxidation within the mitochondria of most cells leads to an increase in the mitochondrial level of reduced nicotinamide adenosine dinucleotide (NADH). At the same time, lower availability of glucose maintains or slightly increases the level of oxidized nicotinamide adenosine dinucleotide (NAD+). By having higher cytosolic and nuclear NAD+ concentrations, SIRT1, a cytosolic/nuclear nicotinamide adenosine dinucleotide (NAD+) dependent deacetylase, is activated. Once activated, SIRT1 will start deacetylation of target proteins within the nucleus. SIRT1 has a wide variety of targets that include several transcription factors including the tumor suppressor protein p53, FOXO1,

FOXO3, PPARγ, PGC1-α, and NFκB (H Huang & Tindall, 2007). When the body returns to a high carbohydrate state, the breakdown of glucose by glycolysis reduces the cytosolic NAD+ level, and SIRT1 is inactivated (Wallace et al., 2010). Since SIRT1 absolutely requires NAD+ for its enzymatic activity, it is important to understand the role of NAD+ synthesis and supply in the activation of SIRT1.

There are two main pathways of NAD+ synthesis: the novo pathway, in which NAD+ is synthesized from L-tryptophane (Rongvaux, Andris, Van Gool, & Leo, 2003; Sauve, 2008), and the salvage pathway (Revollo, Grimm, & Imai, 2007). Nicotinic acid phosphoribosyltransferase (NAMPT) initiates the salvage pathway by converting nicotinamide, and 5'phospho-ribosyl-1-pyrophohosphate (5'PRPP) to nicotinamide monoculecotide (NMN), which is the rate limiting step of this NAD+ synthetic pathway (Imai, 2011). Completion of NAD+ biosynthesis occurs by nicotinamide/nicotinic acid mononucleotide adenylyltransferae (NMNAT), which transfers adenine from ATP to NMN to form NAD+. Dietary niacin and its derivative, nicotinamide, are thought to be the main NAD+ precursors (Rongvaux et al., 2003).

Deacetylation of FOXO: The Difference Between Life and Death

Members of the FOXO family of proteins, in particular FOXO1 and FOXO3, function primarily as a transcription factor in the nucleus that modulate the expression of genes involved in apoptosis, cell cycle, DNA damage repair, oxidative stress, cell differentiation and glucose metabolism. High affinity DNA-binding studies have identified a consensus FOXO-recognized element (FRE) (Furuyama, Nakazawa, Nakano, & Mori, 2000). Functional FRE sites that match the consensus have been shown to correspond to the promoter of pro-apoptotic sequence genes such as Fas ligand (FASL) and tumor-necrosis-factor-related apoptosis-inducing ligand (TRAIL)

and antioxidant detoxification genes such as catalase, glutathione peroxidase and SOD2 (Brunet et al., 1999; Malik & Storey, 2011; Modur, Nagarajan, Evers, & Milbrandt, 2002). Because FOXO proteins have a diverse array of transcriptional targets, regulation of FOXO proteins is essential in propagating the correct transcriptional changes that may serve to determine survival versus death for the cell. FOXO1, the best-characterized member of the FOXO family, has three main post-translational modifications, phosphorylation, ubiquitylation and acetylation have been identified.

AKT-phosphorylated FOXO1 binds to the chaperone protein, 14-3-3β, and becomes sequestered in the cytoplasm, where both are unable to regulate gene expression (Brunet et al., 1999). Alternatively, FOXO1 can also be phosphorylated by several different kinases that lead to its sequestration to the cytoplasm (Brunet et al., 2001; H. Huang, Regan, Lou, Chen, & Tindall, 2006; Woods et al., 2001). The c-Jun N-terminal kinase (JNK) can indirectly effect FOXO1, by phosphorylating 14-3-3β, which leads to dissociation of 14-3-3β from FOXO1, and nuclear localization of FOXO1 (Accili & Arden, 2004). Once in the nucleus, FOXO1 can be ubiquitylated by S-phase kinase-associated protein 2, ultimately leading to FOXO's degradation (H Huang & Tindall, 2007).

The third post-translational modification that can affect FOXO transcriptional activity is acetylation/deacetylation. Acetylation of FOXO1 by p300 or cAMP response element-binding protein-binding protein (CBP) causes FOXO1 to become more negatively charged (Daitoku et al., 2004; Kitamura et al., 2005). While CBP can acetylate FOXO1 directly, it plays a dual role by enhancing FOXO1 transcription, by acetylating histones and by allowing the formation the preinitiation complex (Daitoku et al., 2004; M. Li, Luo, Brooks, & Gu, 2002). SIRT1 can form a complex with, and deacetylate, FOXO1 in the nucleus. Deacetylated FOXO1 favors increased

binding to the promoters of genes encoding for antioxidant enzymes (Higuchi et al., 2012; G. R. Smith & Shanley, 2010). Silencing of FOXO1 has been demonstrated to blunt increases in SOD2, catalase and glutathione peroxidase (Higuchi et al., 2012). In combination with FOXO1, SIRT1 appears to inhibit the transcriptional activity of p53, and shift the FOXO1 function from cell death to survival (Langley et al., 2002; Vaziri et al., 2001).

In mature adipocytes, it has been demonstrated that resveratrol, an allosteric activator of SIRT1, can increase FOXO1 protein levels, and increase SOD2 expression, in the presence of FA (Hubbard et al., 2013; A. R. Subauste & C. F. Burant, 2007). Therefore, for preadipocytes, the ability of FA to influence the SIRT1-FOXO1 axis may be important to resist lipotoxicity, to improve survival, and ultimately to protect adipose tissue turnover.

Central Hypothesis

Based on these observations, the central hypothesis to be tested is that preadipocyte exposure to a mixture of FA in the context of daily FA concentrations causes the production of intra-mitochondrial superoxide-derived reactive oxygen species (ROS) or alkyl radical overloads. ROS overloads ultimately lead to a loss of respiration through increased mitochondrial inner membrane permeabilization and inner membrane depolarization, thereby decreasing ATP synthetic and H_2O_2 dissipating capacities. This loss in preadipocyte mitochondrial fitness would ultimately cause cell death. Despite preadipocyte susceptibility to FA, preadipocytes are able to survive FA fluctuations through initiation of the SIRT1-FOXO1 axis that governs mitochondrial antioxidant gene expression.

Specific Aim #1. Determine the impact of FA on mitochondrial fitness and cell viability using a human SAT-derived preadipocyte cell line.

This is the topic of Chapters 2 -4:

Specific Aim #2. Determine whether a SIRT1-FOXO1 axis elicits an antioxidant response that protects against sustained FA exposure. As a sub-aim investigate whether the loss of mitochondrial antioxidant gene expression, SIRT1 and FOXO1 is lower in insulin resistant versus insulin sensitive individuals.

This is the topic of Chapters 5 and 6.

CHAPTER 2: INTEGRATED MATERIALS AND METHODS

Subjects

All 32 subjects were women from eastern North Carolina, recruited through participating physicians performing abdominal surgery at Vidant Medical Center, and all subjects had given informed written consent. Subjects for this study were previously used in Rogers et al. to compare EGF Receptor (ERBB1) abundance in adipose tissue to markers of adipogenesis and proliferation (Rogers et al., 2012a). Their ages ranged from 25 to 61 years and their body mass indices (BMI) ranged from 20.7 to 54.7 kg/ m2. The protocol was approved by the East Carolina University Institutional Review Board (Appendix 1). All subjects were undergoing hysterectomies and were not taking drugs that could affect lipid or glucose homeostasis. BMI was calculated from body mass and height recorded at the time of surgery to the nearest 0.5 kg and centimeter, respectively. Fasting glucose was quantified from blood collected the day of the surgery using the 2300 Stat Plus System (Yellow Springs Instruments, Inc., Yellow Springs, OH). Insulin was quantified using the Beckman-Coulter Access Immunoassay System (Beckman-Coulter, Fullerton, CA). Abdominal subcutaneous adipose tissue (outside the fascia superficialis) was chosen because it constitutes the primary site of fatty acid storage and release, and hence would likely be a location where turnover is critical to maintaining fatty acid homeostasis (Koutsari & Jensen, 2006). The tissue was immediately frozen in liquid nitrogen, transported to the laboratory, and stored at -80^0 C. For comparison purposes, the subjects were subdivided into four groups: the insulin-sensitive lean (ISNO) [BMI_30 kg/m^2, homeostasis model of assessment for insulin resistance (HOMA-IR) _2.6 (actual highest value was 1.7), fasting insulin 10 _IU/ml, and fasting glucose_110 mg/dL]; the insulin-sensitive obese (ISO) (BMI_30 kg/m^2, HOMA-IR _2.6, fasting insulin _10 _IU/mLl, and fasting glucose _110 mg/dl);

the insulin-resistant obese (IRO) [BMI _30 kg/m^2, HOMA-IR _2.6 (actual lowest value was 3.0), fasting insulin _10_IU/mL, and fasting glucose_126 mg/dL], and the T2DM (fasting glucose ≥126 mg/dL on two occasions). The HOMA-IR cutoff of 2.6 was determined from our data bank of 38 lean individuals with normal glucose tolerance based on the commonly used 75th percentile, and it is in line with previously reported cutoffs (Ascaso et al., 2003). For some comparisons, the subjects from the first and fourth quartiles were compared with respect to insulin sensitivity, regardless of their body weight. Analysis of data from 81 subjects for which there were both HOMA-IR and iv glucose tolerance tests, minimal model values established that the first and last quartiles of HOMA have a sensitivity of 0.9 to identify subjects belonging to the last and first tertiles of SI, respectively. These are more stringent HOMA-IR cutoffs than the above-described insulin-sensitive and insulin-resistant cutoffs. For other comparisons, we compared the subjects from the first and fourth quartiles with respect to SIRT1 and FOXO1 protein levels.

Cell Culture and Transfection

XA15A1 human preadipocytes (Lonza Walkersville, Inc., Walkersville, MD) were cultured as described in Skurk et al.,(Skurk, Ecklebe, & Hauner, 2007) using Dulbecco's modified Eagle's medium: F12 (DMEM:F12; Mediatech, Manassas, VA) with 10% calf serum, 15 mM glucose, 33 µM biotin, 17 µM D-pantothenate, 100 nM insulin, and 10 nM hydrocortisone (all from Sigma Aldrich), 1 nM epidermal growth factor and 1 nM basic fibroblast growth factor (Gemini, West Sacrameto, CA). This medium also contained 50 IU/ml penicillin, 50 µg/ml of streptomycin and 2.5 µg/ml amphotericin B (Mediatech). The XA15A1 cells were propagated at 33 C. When the cells reached 80% confluence, growth factors were omitted from the media and the cells were placed at 37 C for at least 24 hours prior to the

experiment. The XA15A1 cells express a temperature-sensitive mutant of the SV 40 Large T-antigen (u19tsA58) and needs to be incubated at 37 C for 24 hours to revert to a phenotype that resembles that of primary cells and are able to differentiate. For some experiments, XA15A1 cells were transiently transfected with Mito-HyPer or Cyto-HyPer plasmids (Evrogen, Moscow, Russia), which encode mitochondrion- or cytosol-targeted H_2O_2-sensitive ratiometric reporter proteins. For other experiments, the cells were transfected with plasmids coding for SIRT1 or FOXO1 dominant negative (DN) mutants obtained through the AddGene repository (Herscovitch, Perkins, Baltus, & Fan, 2012; J. Nakae, Barr, & Accili, 2000; Vaziri et al., 2001). The Sirt1 DN mutation causes an alteration of the catalytic site and leads to a loss in deacetylation activity (Vaziri et al., 2001). The Foxo1 DN mutant contains a deletion that truncates the transactivation domain (J. Nakae et al., 2000). Both the Sirt1 DN and Foxo1 DN plasmid encode for the puromycin resistance gene, for the selection of stably transfected cells. The two types of transfection were performed identically. Briefly, 5×10^6 cells were transfected in a 100 μL final volume of the nucleofection solution V containing 1μg of plasmid DNA and the application of the T-030 program from the Amaxa Nucleofactor 2b electroporator (Lonza Walkersville) list. For experiments using transiently transfected cells, the cells were used 48 hours later. For experiments using stably transfected cells, 10 ug/mL puromycin was added to the medium after 24 hours to select for cells that stably integrated the Puromycin resistance gene. The cells were used 4 to 6 passages later.

Preparation of Fatty Acids

A 50 mM stock of each single fatty acid was prepared in 0.1 M NaOH. Each fatty acid stock was added to Dulbecco's modified Eagle's medium: F12 (DMEM:F12) containing 600 µM BSA, 5% calf serum, 10 mM glucose, 33 µM biotin, 17 µM D-pantothenate, containing 50 IU/ml penicillin, 50 µg/ml of streptomycin, and 2.5 µg/ml amphotericin B to reach a mixture consisting of 40% oleate, 25% palmitate, 20% linoleate, and 15% stearate. Each concentration was pre-equilibrated for one hour with 600 µM BSA at 37^0C. For all experiments, cells were incubated in 600 µM BSA for at least 2 hours prior to the addition of the drugs or fatty acids (FA). To start the experiment FA mixtures were added to the 600 µM BSA at a 2x concentration to equal a final FA concentration of 1x.

RNA Isolation, Reverse Transcription, and Quantitative Real-Time PCR

RNA was isolated from frozen adipose tissue samples or from cell culture samples after various treatments. Pieces of frozen adipose tissue of approximately 100 mg were allowed to unfreeze in 1 mL of RNA later ICE (Applied Biosystems, Foster City, CA). These pieces were homogenized and RNA isolated using the TriReagent procedure as described by the supplier (Sigma Aldrich). TriReagent was used, as well, for the cell culture experiments. First-strand cDNA was synthesized from 5 µg total RNA with the High-Capacity cDNA Reverse Transcription Kit (Applied Biosystems). Relative real-time TaqMan PCR was performed with primers and 6-carboxyfluorescein dye-labeled TaqMan probes (Applied Biosystems). Glyceraldehyde-3-phosphate dehydrogenase (GAPDH) was used as an endogenous control because it was found to be the most stable when compared to HPRT and POLII. Each reaction contained 5 ng cDNA from total RNA, in a total reaction volume of 10 µl. To prevent bias

toward a specific group, the relative expression was determined by the comparative threshold method (Δct) using all samples as reference.

MitoSox Red and CM-H_2-DCFDA Fluorescence Measurements

MitoSox Red, the fluorescent probe hydroethidine coupled to the mitochondrion-targeting hexyl triphenylphosphonium (TPP) cation was used as a mitochondrion-localized superoxide indicator (Invitrogen, Carlsbad, CA). The fluorescent probe 5-(and-6)-chloromethyl-2',7'-dichlorodihydrofluorescein diacetate acetyl ester (CM-H_2-DCFDA; also from Invitrogen) was used as a cytosol-localized mitochondrial crisis indicator. As the majority of DCF fluorescence relies on cytochrome c release from the mitochondria and cytosolic H_2O_2 oxidation of cytochrome C (Brömme, Zühlke, Silber, & Simm, 2008; Karlsson, Kurz, Brunk, Nilsson, & Frennesson, 2010). These detection methods were used for end point as well as real-time experiments. At the end of the incubation periods for end point experiments, cells were washed with Dulbecco's phosphate buffered saline, containing calcium and magnesium (DPBS) and incubated at 37°C, with 4 µM MitoSox Red or 6 µM of CM-H_2DCFDA in DPBS for 35 and 45 minutes, respectively. After loading of the fluorescence probe, cells were washed twice with DPBS. After preloading, cells were dissociated from the dishes by adding 1 mL of 10x TrpLe dissociation buffer (Life Technologies, Grand Island, NY) for 30 seconds, and after adding 1 mL of DPBS, collected through repeated aspirations and ejections. MitoSox fluorescence was measured using an Accuri C6 flow cytometer (BD, Franklin Lakes, New Jersey) at an excitation wavelength of 488 and a 585 ± 40 nm emission filter. H_2-DCFDA fluorescence was measured using an excitation wavelength of 488 and a 535 ± 30 nm emission filter. The real-time approach will be described separately in addition to being the subject of an independent chapter.

Continuous Real-Time Flow Cytometry Analysis

To quantify changes in fluorescence on a cell-by-cell basis over the course of minutes to hours an apparatus was invented that could be retrofitted to any flow cytometers not operating under pressurized conditions like the BD Accuri C6. Briefly, the apparatus consists of an open 30 mL polypropylene receptacle (vial) surrounded by a water coil jacket, supplied by a heated-circulating water bath, set to maintain the temperature at 37°C. The vessel is sitting on a stir plate allowing a rapid dispersion of FA or drugs without interruption, as well as maintaining homogeneous cell sampling. After loading of the fluorescence probe as described in their respective method subsection, cells were processed similarly, except for the final addition of 1 mL of flow buffer, which consisted of Krebs's ringer bicarbonate buffer (Sigma-Aldrich Co., St. Louis, MO) containing 600 µM fatty acid-free bovine serum albumin, 5% fetal calf serum, 33 µM Biotin, 17 µM D-Pantothenate, 50 IU/ml penicillin, and 50 µg/ml of streptomycin instead of DPBS. Cells were counted by gating the single cell population in the Forward Scatter (FCS-H) versus Side Scatter (SSC-H) density plot. The counted cells were suspended in flow buffer to obtain a final concentration of about $1x10^6$ cells in a total volume of 7 mL. The suspended cells were transferred into the 30 ml vial. A stir bar was added and rotated at 400 rpm to maintain the oxygen tension constant, to quickly distribute the added compounds, and to prevent cell clumping. The flow rate was adjusted to have a flow rate of 66 µL/minute and a core size of 22 µm in order to analyze fluorescence levels from about 2000 cells in the live cell region per minute. Baseline fluorescence in each sample was measured for 3-5 minutes prior to the addition of 600 µM BSA (basal). After 5 minutes, different compounds were added directly to the sample.

Detection of Lipid Peroxide Formation

Mitochondrial inner membrane localized lipid peroxidation was assessed using a C11-BODIPY$^{581/591}$ probe conjugated to a TPP cation moiety (MitoPerOx: Dr. Michael Murphy, MRC Mitochondrial Biology Unit; Cambridge, England, UK) (Prime et al., 2012). The reduced C11-BODIPY$^{581/591}$ probe has a maximum emission wavelength of ~590 while the oxidized product displays a maximum emission wavelength of ~520 nm in response to lipid peroxidation by hydroxyl and peroxy radicals (Drummen, Gadella, Post, & Brouwers, 2004). Briefly, cells were incubated, at 37°C, in DPBS with 150 nM MitoPerOx for 30 minutes. After loading, cells were collected and CRT flow cytometry or fluorescent microscopy was performed. For the CRT flow cytometry experiments, MitoPerOx was excited at a wavelength of 488 and emission captured through a 585 ± 40 nm and 535 ± 30 nm emission filters for the reduced and oxidized form of MitoPerOx, respectively. For the microscopy based experiments, cells were washed with 1x PBS and 1 mL of flow buffer was added. Following an addition of flow buffer, images were taken at multiple time points with an EVOS fluorescent microscope (AMG, a part of life technologies, Grand Island, NY) using the GFP light cube, which couples a 470 ± 22 nm excitation and a 525 ± 50 nm emission filter, as well as the RFP light cube, which couples a 531 ± 40 nm excitation to a 593 ± 40 nm emission filter.

Detection of Mitochondrial and Cytosolic H_2O_2

H_2O_2 levels in the mitochondrial or cytosolic compartment were measured using the genetically encoded sensors Mito-HyPer (has a mitochondria targeted sequence) or Cyto-HyPer (which resides in the cytosol) that encode for a mutated OxyR protein that is sensitive to submicromolar (or physiological) levels of H_2O_2 (Belousov et al., 2006; Choi et al., 2001). HyPer has an emission of ~516 nm and an excitation of 420 and 500 nm. In the presence of

H_2O_2, the excitation peak of HyPer at ~420 nm decreases proportionally to the increase of the excitation peak at 500 nm, allowing for the ratiometric measurement of H_2O_2. For the studies, measurements of the ~516 nm emission peak was used with a 530± 30 nm emission filter, after using an excitation wavelength of 488 only. Cells were plated in six well dishes and grown for 48 hours before CRT flow cytometry was performed. The cells were lifted as described in the CRT flow cytometry subsection and the FA added similarly.

Cell Death

Cell death was measured by Calcein AM and Ethidium Homodimer-1 (Life Technologies, Grand Island, NY). Calcein AM is a live cell dye that accumulates in intact cells where it acquires a strong green fluorescence upon cleavage by intracellular esterases (Papadopoulos et al., 1994). Because intracellular esterase activity is quickly lost as cells die, little to no gain in fluorescence occurs in dead or dying cells. Ethidium Homodimer-1 is a dye that enters the damaged plasma membrane and interacts with nucleic acids. As Ethidium Homodimer-1 interacts with nucleic acids the red fluorescence of the dye increases by 40 Fold, indicating dying or dead cells (Papadopoulos et al., 1994). At the end of the 6, 12 or 24 hour FA incubation periods, cells were collected and incubated for 15 minutes at room temperature in DPBS containing Calcein AM and Ethidium Homodimer 1 at a final concentration of 0.05 µM and 4 µM. To detect Calcein AM fluorescence an excitation wavelength of 488 and a 530± 30 nm emission filter was used. Ethidium Homodimer 1 fluorescence was detected using an excitation wavelength of 488 and a 675 ± 25 emission filter. After subtraction of auto-fluorescence, the live cell region was determined by examining an untreated sample and a sample containing only 600 µM BSA. Dead cells were determined by treating a control sample

with 0.01% Triton-X for 15 minutes. All values for cell death represent the percent of dead cells found in the gated region of the cell population of interest.

Mitochondrial Inner Membrane Permeabilization

As mentioned in the description of the use of Calcein AM for the identification of live cells, Calcein AM enters cells and has access to every compartment. Cobalt is known to quench Calcein fluorescence, but since cobalt does not freely enter mitochondria, Calcein AM fluorescence within the mitochondria is not quenched unless there is an increase in membrane permeability (Petronilli et al., 1998). Briefly, cells are incubated with Calcein AM at a final concentration of 0.05 µM in DPBS for 30 minutes, followed by 200 µM $CoCl_2$ for 15 minutes. Calcein AM fluorescence was measured using an excitation wavelength of 488 and a 535 ±30 nm emission filter. Mean fluorescence and percent of cells experiencing mitochondrial inner membrane permeabilization was determined by histogram plots of Calcein AM after the subtraction of auto fluorescence.

Detection of Changes in Inner Mitochondrial Membrane Potential

Changes in inner mitochondrial membrane potential was measured by using the lipohilic cationic dye tetramethylrhodamine ethyl (TMRE) ester (Sigma-Aldrich Co) that accumulates in direct proportion to the inner mitochondrial membrane potential according to the Nernst Equation. Each sample was incubated with 50 nM TMRE in DPBS for 20 minutes at 37^0C. TMRE was measured using an excitation wavelength of 488 and a 585 ±40 nm emission filter. Mean fluorescence was determined by histogram plots of TMRE fluorescence after the subtraction of auto fluorescence.

Measurement of the Ratio of Acetylated versus Total FOXO1 Proteins

Following treatment with FA, $1.0x10^6$ cells were collected, fixed in 5% formaldehyde and permeabilized in 100% methanol. The non-specific binding of antibody on cells was blocked by incubating the cells for 60 minutes in an incubation buffer consisting of PBS containing 0.5 % BSA. After blocking, primary antibodies directed against total FOXO1 (sc-9808; Santa Cruz Biotechnology, Dallas, TX) or Ac-FOXO1 (sc-49437, Santa Cruz) were added at a 1:100 dilution ratio in the incubation buffer. Cells were washed once and incubated with a 1:1000 dilution of anti-goat IgG (H+L) Alexa Fluor 568 (A11057; Life technologies) and a 1:1000 dilution of anti-rabbit IgG (H+L) Alexa Fluor 488 (4412; Cell Signaling Technology) for 30 minutes to reveal the total and acetylated FOXO1 antibody, respectively. Alexa Fluor 488 has an excitation of 488 nm and an emission of 520 nm. Alexa Fluor 568 has an excitation of 568 nm and an emission of 600 nm. After 30 minutes, cells were washed twice and suspended in 300 µL of PBS and analyzed on a flow cytometer. Auto fluorescence and nonspecific staining were determined by using either normal anti-rabbit IgG (Sc-2027; Santa Cruz) or normal anti-goat IgG (Sc-2028; Santa Cruz Biotechnology) as isotype controls, after gating on the live cell population. Gates were applied to each histogram that corresponded to either the 530 ±30 nm band pass filter or the 585 ±40 nm band pass filter. Mean fluorescence intensity (MFI) for each histogram was determined after gating. The ratio of Ac-Foxo MFI to Total-Foxo2 MFI was calculated and plotted using GraphPad Prism.

Cellular Respiration Assay

Approximately 20,000 preadipocytes in growth media without growth factors were seeded to each well of Seahorse XF24 plates (Seahorse Bioscience, MA) and grown for 24 hours at 37°C before treatment with various inhibitors or FA. Four to six hours before the experiments, the media was changed to DMEM, containing 5% calf serum, 25 mM Hepes, 10 mM glucose and 600 µM FA-free BSA. An hour before FA treatments, inhibitors or their vehicle was added to the cells, and then FA were added at various concentrations (0 – 1000 µM) for 24 hours. At the end of the incubation, cells were washed two times with 1 ml of phosphate-buffered saline with magnesium and calcium. Finally, 500 µL of Seahorse XF-DMEM medium containing 10 mM glucose and 2 mM sodium pyruvate was added to the cells. Cellular respiration was measured as described previously by Herscovitch et. al., (Herscovitch et al., 2012) with the following slight modifications determined to be optimal in preliminary experiments. First, the measurement cycle consisted of 1 minute mix, 1 minute wait and three minutes measurement. Second, three basal rate measurements were taken, three after oligomycin injection, three after Carbonyl cyanide 4-(trifluoromethoxy) phenylhydrazone (FCCP) injection and three after Rotenone injection. Drugs were delivered through the ports at final concentrations of 1 µM for oligomycin, 500 nM for FCCP and 1 µM for Rotenone. Each of the three independent experiments were performed in triplicate.

NAD^+ and NADH Levels

Following FA exposure, cells were washed twice with PBS. NAD+ levels were determined using a NAD+/NADH cell-based assay kit as described in the manual (Cayman Chemical, Ann Arbor, MI). After washing, cells were lysed, centrifuged and the supernatant was

used to measure NAD+ and NADH levels. In this assay, alcohol dehydrogenase converts ethanol to acetoaldehyde and yields NADH from the NAD+ present in the supernatant. After NADH is formed, it reduces the tetrazolium salt substrate (WST-1) into a highly colored formazan dye that absorbs at the 450 nm wavelength. An Infinite 200 Pro Series plate reader was used to quantify absorbance. As more than 95% of the NAD in cells is oxidized this assay is essentially a NAD+ assay.

ATP Determination

Following FA exposure, cells were washed twice with PBS, and ATP was extracted by using the boiling water extraction method (Yang, Ho, Chen, & Hu, 2002). Following extraction, ATP levels were determined using an ATP determination kit, as described by the supplier (Life Technologies). An Infinite 200 Pro Series plate reader was used to quantify luminescence.

Statistical Analysis

Statistical analysis was performed with PRISM (GraphPad Software, San Diego, CA) version 5.00 for Windows. Differences between ISL, ISNO, IRO and T2DM individuals were assessed by a one-way ANOVA, followed by Tukey's multiple comparison tests. Differences between the first and last quartiles of insulin sensitivity or gene expression were assessed using a two-tailed unpaired Student's T test. For in-vitro studies, differences between H_2O_2, Diamide, Tert-Butyl Hydroperoxide, FA concentrations, 600 µM BSA and/or pretreatment with MitoTempo, Etomoxir, Carnosine, Cyclosporin A or Nicotinamide were assessed by a one-way ANOVA with a Tukey's multiple comparison test. All values are reported as $\pm$ SD. In all cases, a *P* value of less that 0.05 was used to indicate statistical significance between conditions.

CHAPTER 3: A NEW FLOW CYTOMETRY APPROACH SHOWS THAT FATTY ACIDS DO NOT CAUSE ACUTE OXIDATIVE STRESS IN HUMAN PREADIPOCYTES

Carlyle Rogers, Barbara Davis and Jacques Robidoux

[1] Department of Pharmacology and Toxicology and [2] The East Carolina Diabetes and Obesity Institute , East Carolina University, Greenville, North Carolina.

Abstract

A reduction in preadipocyte number or adipogenic potential correlates with the onset of several metabolic abnormalities. Although the underlying cause of preadipocyte dysfunction is unknown, one potential hypothesis is that preadipocytes are unable to resist the lipotoxic effects of fatty acids (FA) in the adipose tissue microenvironment, leading to an overall increase in preadipocyte oxidative stress. For preadipocytes, dynamic changes in FA associated uptake and oxidative stress can occur within a matter of seconds and can vary dramatically from cell to cell, making it a challenge to measure these short-lived events in a representative portion of the population in real-time. For this purpose, a device that maintains physiological temperature, evenly mixes compounds and can be retrofitted to an existing flow cytometer was developed to measure millisecond changes in preadipocyte FA uptake, oxidative stress and cytosolic H_2O_2. Results demonstrate that FA uptake rapidly reaches equilibrium within 10 seconds. However, despite observing mitochondrial crisis and H_2O_2 accumulation, with exogenous H_2O_2, tert-butyl hydroperoxide and diamide, the occurrence of oxidative stress or H_2O_2 emission during FA exposure was not observed. Together this data provides a foundation for use of continuous real-time flow cytometry to study rapid changes in biological systems and suggests that while

preadipocyte take up FA within seconds, FA oxidative effects are compartmentalized within the first 3 hours of exposure.

Introduction

"As articulated so clearly by Skulachev, "Living with the risk of oxidative stress is a price that aerobic organisms must pay for more efficient bioenergetics" (Skulachev, 1996). The term oxidative stress is defined loosely as a series of interrelated phenomena including an elevated generation of reactive oxygen species (ROS) and oxidative damage to cell constituents (Andreyev, Kushnareva, & Starkov, 2005). Since the intracellular generation of ROS is considered an inevitable outcome of aerobic metabolism, balancing ROS production with detoxification mechanisms is an important contributor in shaping cellular processes. Therefore, measuring intrinsic rates of ROS generation is important for understanding the pathology of oxidative stress and associated disease states. For adipose tissue extracellular concentrations of fatty acids (FA) can levels that can lead to ROS and oxidative stress for most cells of the body (Frayn, Coppack, & Humphreys, 1993). The sensitivity of these cells depends on many factors; however, the two dominant factors are the energy required to perform their intended function and their triacylglycerol synthetic capacity (Unger, Clark, Scherer, & Orci, 2010b). Based on research performed in a variety of cell type, it has been hypothesized that mismatches between nutrient overload and ATP demand can manifest into excessive reductive pressures on the electron transport chain leading to superoxide-derived H_2O_2 production and eventually emission toward other compartments, in particular the cytosol (E. J. Anderson et al., 2009; Bonnard et al., 2008; Fisher-Wellman & Neufer, 2012; Murphy, 2009). Although transient bidirectional mismatches serve to fine-tune metabolic and signaling pathways, excessive H_2O_2 emission disrupts normal cellular functions including insulin sensitivity (Fisher-Wellman & Neufer, 2012;

Houstis, Rosen, & Lander, 2006). For preadipocytes, which have a diminished capacity to esterify FA, the influence of FA on preadipocyte function may increase H_2O_2 emission from the mitochondria leading to an increase in cytosolic oxidative stress, and ultimately the preadipocytes demise, which can have a grave impact on the overall health of the adipose tissue depot.

Although a number of approaches are currently available to measure FA uptake, oxidative stress and cytosol H_2O_2 levels, several limitations exist. For example, plate reader-based approaches have the unfortunate limitation of merging the individual cellular responses into combined readings while losing sight of cellular heterogeneity. Microscopy approaches follow events within a selected group of cells, but this is also their main limitation as only few cells at a time can be sampled. Recently, Vines et al. reported that changes in intracellular Ca^{2+} concentrations could be monitored on a single cell basis in a large cell population, using a non-pressurized flow cytometer (Vines, McBean, & Blanco-Fernández, 2010). Using a similar approach, a device that could be retrofitted to a non-pressurized flow cytometer was developed to study in real-time the effects of FA on preadipocytes.

The overall goal of this study was 1) to establish a method that allows for the real-time measurement of rapidly occurring biological process in living cells and 2) to determine the effect of FA exposure on preadipocyte FA uptake, oxidative stress and cytosolic H_2O_2. Data suggest that despite FA uptake occurring within seconds of FA exposure, H_2O_2 emission and subsequent oxidative stress does not occur within the first 3 hours of FA exposure. Furthermore, the data demonstrate that continuous real-time flow cytometry can be a useful tool that expands the ability of researchers to understand dynamic changes in cellular processes.

Materials and Methods

Fatty Acid Preparation

A 50 mM stock of each FA was prepared in 0.1 M NaOH. Each FA stock was added to Dulbecco's modified Eagle's medium:F12 (DMEM: F12) containing 600 µM BSA, 5% calf serum, 10 mM glucose, 33 µM Biotin, 17 µM D-Pantothenate, 50 IU/ml penicillin, 50 µg/ml of streptomycin, and 2.5 µg/ml amphotericin B to reach a mixture consisting of 40% oleate, 25% palmitate, 20% linoleate, and 15% stearate. Each concentration was pre-equilibrated for one hour with 600 µM BSA at 37^0C. For all experiments, cells were incubated in 600 µM BSA for at least 2 hours prior to the addition of drugs or FA. To start the experiments, FA mixtures were added at 2X concentrations. For the FA uptake experiments, 4,4-difluoro-5,7-dimethyl-4-bora-3a,4a-diaza-s-indacene-3-hexadecanoic acid (BODIPY FL C_{16}; Invitrogen, Carlsbad, CA) replaced 4% of the palmitate in the mixture.

Loading of the Cells with CM-H2-DCFDA

The fluorescent probe 5-(and-6)-chloromethyl-2',7'-dichlorodihydrofluorescein diacetate acetyl ester (CM-H_2-DCFDA referred to here as H_2-DCFDA; Invitrogen) was used as a cytosol-localized mitochondrial crisis indicator (Brömme et al., 2008; Karlsson et al., 2010). Cells were washed with Dulbecco's phosphate buffered saline containing calcium and magnesium (DPBS) and incubated for 45 minutes at 37°C with 6 µM of CM-H_2DCFDA in DPBS. After loading, cells were washed twice with DPBS and the dye-loaded cells were dissociated from the dishes by adding 1 mL of TrpLe dissociation buffer (Life Technologies, Grand Island, NY) for 30 seconds. Cells were collected through repeated aspirations and ejections after adding 1 mL of flow buffer which consisted of Krebs's ringer bicarbonate buffer (Sigma-Aldrich Co., St. Louis, MO)

containing 600 µM fatty acid-free bovine serum albumin, 5% fetal calf serum, 33 µM Biotin, 17 µM D-Pantothenate, 50 IU/ml penicillin, and 50 µg/ml of streptomycin.

Continuous Real-Time Flow Cytometry Analysis

To quantify changes in fluorescence over the course of seconds to hours, a device that could be retrofitted to any flow cytometer not operating under pressurized conditions was built. We used a BD Accuri C6 was used (Figure 1). Briefly, the apparatus consists of an open 30 ml polypropylene receptacle (tube) surrounded by a water coil jacket supplied by a heated-circulating water bath set to maintain the temperature at 37°C. The receptacle sits on a stir plate allowing a rapid dispersion of FA or drugs without interruption, as well as maintaining homogeneous cell sampling. For all experiments, cells were counted after gating the single and live cell population. The counted cells were suspended in flow buffer to obtain a final concentration of about 400,000 cells in a total volume of 7 mL. The suspended cells were transferred into the 30 mL vial. A stir bar was added, and the suspension was rotated at 400 rpm. The flow rate of the pump was adjusted to 66 µL per minute and the core size set to 22 µm in order to analyze fluorescence levels from about 4,000 cells per minute before, and 2,000 cells per minute after the addition of test compounds as the final volume reached 14 mL. For the FA uptake experiments, the cells were suspended in the flow buffer (described in the loading of the cells with H_2-DCFDA section). At time zero, flow buffer containing various concentrations of FA was added in order to achieve a final FA concentration ranging from 0 to 1000 µM. Fluorescence was measured using an excitation wavelength of 488 and a 585 ± 40 nm emission filter. For the H_2-DCFDA experiments, the baseline fluorescence of the loaded cells was measured for 2 to 3 minutes prior to the addition of various concentrations of FA (0 to 1000

μM), H_2O_2 (0 to 100 μM), 100 μM tert-butyl hydroperoxide (t-BHP) or 1 μM of diamide. H_2-DCFDA fluorescence was measured continuously for up to 3 hours (FA) or 20 minutes (everything else) at an excitation wavelength of 488 and a 535 ± 30 nm emission filter. Although pHyPer Cyto is a dual-excitation ratiometric H_2O_2 sensor, the Accuri C6 can only detect the oxidized pHyPer; therefore, an excitation laser wavelength of 488 coupled to a 535 ± 30 nm emission filter was used.

Results and Discussion

Fatty acids (FA) have been shown to elicit cytotoxic effects in a large variety of cell types including preadipocytes and adipocytes. The goal of this study was to develop an approach that can be used to characterize various events involved in FA-induced preadipocyte dysfunction in real-time. To accomplish this task, a device that maintains physiological temperature, evenly mixes compounds and can be retrofitted to non-pressurized flow cytometers was developed (Figure 1). For traditional flow cytometers, samples are placed in tubes that are then pressurized by the flow cytometer in order to draw the sample into the machine. Therefore, addition of compound requires the sample to be taken off the cytometer and a loss in recording occurs. By using a flow cytometer that uses a peristaltic pump to draw up the sample, the sample tube can be open and allows for the addition of compounds to the sample without interrupting the recording of events.

Although preadipocytes belong to the adipocyte lineage, the effect on FA exposure on preadipocytes is not known, especially in the context of FA concentrations found in the adipose tissue microenvironment. Before examining how FA exposure affects preadipocyte oxidation, the ability of preadipocytes to take up FA and if the real-time flow cytometry device could detect

rapid changes in FA entrance into preadipocytes was explored. As shown in Figure 2*B* to 2*F*, there was a rapid increase in BODIPY FL C_{16}/FA fluorescence after the addition of FA. This increase in fluorescence was proportional to the FA concentration. To ensure that cellular uptake of fatty acids was being observed, two control experiments were performed. In the experiments illustrated in Figure 1*G*, cells were incubated with 1000 μM unlabeled FA to ascertain that the measured increase in fluorescence was not due to auto-fluorescence. Furthermore, Figure 1*H* illustrates cells fixed prior to FA exposure showed no measurable increase in fluorescence, indicating nonspecific FA absorption was not the cause of the increased fluorescence in live cells. As no increase in fluorescence was observed in both these control experiments, it can be confidently reported that there is true documentation of FA uptake. Also noteworthy is the time necessary to reach the apparent equilibrium of FA inside versus outside, as seen in Figure 1*B* to 1*F*. This observation is in line with results reported by others (Caserta et al., 2001; Kampf, Parmley, & Kleinfeld, 2007). For example, Kampf *et al* (Kampf et al., 2007)have shown rapid uptake of oleate by murine preadipocyte cell lines that were injected with the fluorescent fatty acid sensor ADIFAB and Caserta *et al* (Caserta et al., 2001) have shown rapid uptake of oleate by rat and human preadipocytes that were loaded with the pH indicator 2',7'-bis(2-carboxyethyl)-5,(6)-carboxyfluorescein (BCECF). Nevertheless, the flow cytometry data reported here gave comparable results to microscopy (data not shown), however, the flow cytometry methods allowed for a sampling rate in the thousands, dramatically increasing the power of the analysis.

The second method illustrates that the device renders flow-cytometry suitable to document, also in real-time, events that may develop over periods of minute to hours. For this purpose, measurements of H_2DCFDA fluorescence, which is an index of mitochondrial and/or

oxidative stress, were taken. To ensure our device was able to measure changes H_2DCFDA fluorescence a variety of widely utilized oxidative agents were used (Figure 2). As shown in Figure 2*A* to 2*D*, the addition of increasing concentrations of H_2O_2 led to a rapid increase in H_2DCFDA fluorescence. The rate of appearance of H_2DCFDA fluorescence was clearly higher at the highest concentration of exogenously added H_2O_2 (Figure 2*D*). How H_2O_2 increases cytochrome c release from the mitochondria is not fully elucidated. However, oxidation of cardiolipins and mitochondrial outer membrane permeabilization are two important steps in the process (Ott, Robertson, Gogvadze, Zhivotovsky, & Orrenius, 2002). Therefore, the higher H_2O_2 concentrations leading to faster release of cytochrome c was consistent with this hypothesis. Figure 2*E* shows that tert-butyl-hydroperoxide, an analog of lipid peroxides that mimics lipid peroxidation products, causes an increase in H_2DCFDA fluorescence, likely due to cytochrome c release, as well as mitochondrial H_2O_2 emission (Haidara, Morel, Abalea, Gascon Barre, & Denizeau, 2002). Finally, Figure 2*F* shows that diamide, a general thiol-oxidizing agent that reacts with glutathione and decreases its availability for enzymes like glutathione S-transferases or glutathione peroxidases, also increases H_2DCFDA fluorescence (Edelhauser, Van Horn, Miller, & Pederson, 1976). Consistent with diamide mechanism of action, figure 2*F* additionally shows that the rate of appearance of H_2DCFDA fluorescence was slow, but progressive. Altogether, these results presented in figure 2 confirm that flow cytometry can be used to monitor processes occurring over several minutes in real-time.

Although FA have been shown to induce oxidative stress in adipocytes, high FA concentrations will put an even greater reductive pressure on the mitochondria of preadipocytes, since preadipocyte have a diminished capacity to esterify FA, and potential causing an increase in H_2O_2 emission and oxidative stress (Gao et al., 2010; A. R. Subauste & C. F. Burant, 2007;

Yeop Han et al., 2010). Figure 3*A* shows that normal fasting FA concentrations (1000 μM FA conjugated to 600 μM BSA) did not cause overt oxidative stress within the first hour. Figure 3*B* illustrates that increasing the FA concentration to a level only seen during prolonged fasting (starvation) or a bout of exercise (2000 μM) did not cause signs of oxidative stress within an hour either. In fact, increasing the incubation time to almost three hours was insufficient to cause an increase in H_2DCFDA fluorescence (Figure 3*C*). To directly measure H_2O_2 emission the cells were transfected with pHyPer Cyto, a selective cytosolic H_2O_2 sensor that displays nanomolar sensitivity (Figure 3*D*). As Figure 3*D* illustrates, while 100 μM extracellular H_2O_2 was able to transiently (back to basal levels by 30 minutes) increase cytosolic concentration of H_2O_2 to measurable levels, 1000 μM of FA did not. This is consistent with the published time course of H_2O_2 handling by living cells, which shows that it takes between 15-20 minutes for Hela or NIH-3T3 cells to dissipate 100 μM H_2O_2 (Markvicheva et al., 2011). More importantly, it confirms the relative resistance of preadipocytes to FA-induced oxidative stress by use of a mixture of FA at physiological FA: BSA ratios. Additionally, there is the possibility that much longer incubation times are required to establish mitochondrial crisis, as most of the cited studies exposed the cells to FA for at least 24 hours.

Although no changes in FA induced oxidative stress or H_2O_2 emission occurred, the ability of the continuous real time flow cytometry device to measure rapid changes in FA uptake and cytosolic oxidation by H_2O_2, tert-butyl hydroperoxide and diamide was observed. As any fluorescent probe can be used, the repertoire of applications is almost limitless and permits the simultaneous measurement of multiple readouts. Furthermore, the ability of real-time flow cytometry to measure a large portion of the population has a clear advantage over other methods that do not have the sampling power to identify subsets of the population.

Figure 1: Mixing and sampling device that allows for continuous real-time (CRT) flow cytometry.

Cells are loaded into the receptacle (sample tube). The maintenance of the sample temperature is assured by a heated water coil jacket connected to a heated circulating water bath. A stir plate serves not only to keep the cells in a homogeneous suspension, but also allows the added compounds to equilibrate and reach all the cells rapidly. The apparatus was placed in a manner such that the cytometer could aspirate sample without interference.

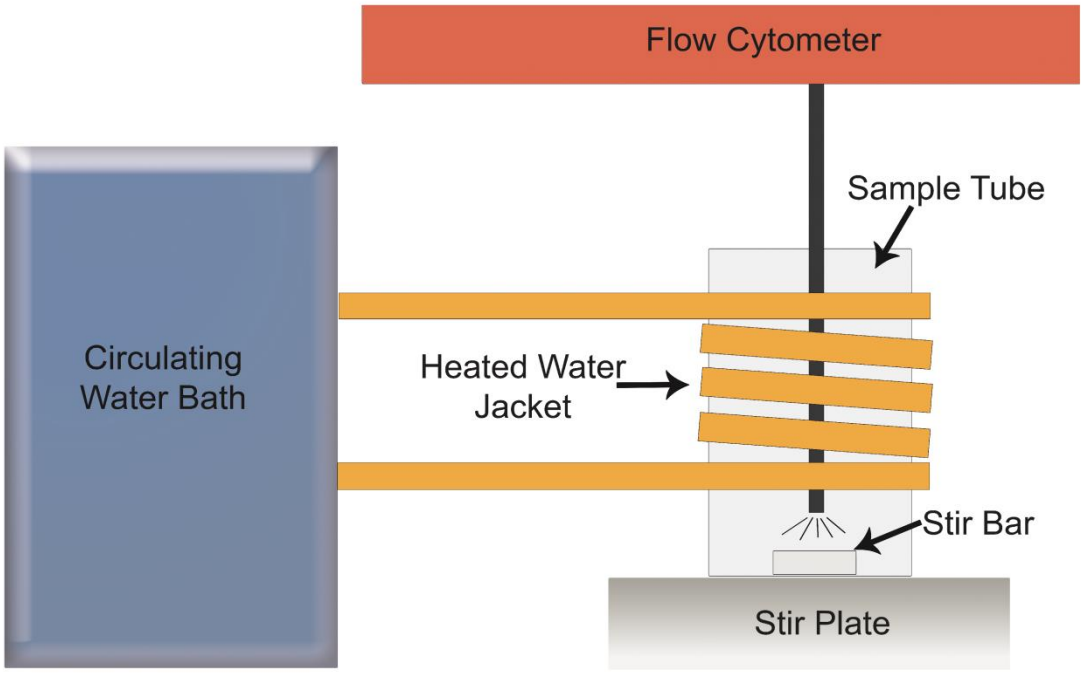
Flow Cytometer
Sample Tube
Circulating
Water Bath
Heated Water
Jacket
Stir Bar
Stir Plate

Figure 2. Uptake of fatty acids by human preadipocytes is rapid.

Time course of uptake of fatty acids in human preadipocytes evaluated using BODIPY FL C_{16} (fluorescent palmitate that has an excitation wavelength of 488 and emission wavelength of 590 nm) uptake as an index of fatty acid uptake as described in the materials and methods section. Cellular autofluorescence before and after (arrow) the addition of fresh 600 μM BSA was measured (A). Concentration-dependent increases in fluorescence after the addition of 200 (B), 400 (C), 600 (D), 800 (E) or 1000 (F) μM of FA. No increase in fluorescence was measured with label-free 1000 μM FA (G) or in cells that were fixed prior to the addition of 1000 μM of FA (H). The arrows indicate the time at which fatty acids were added.

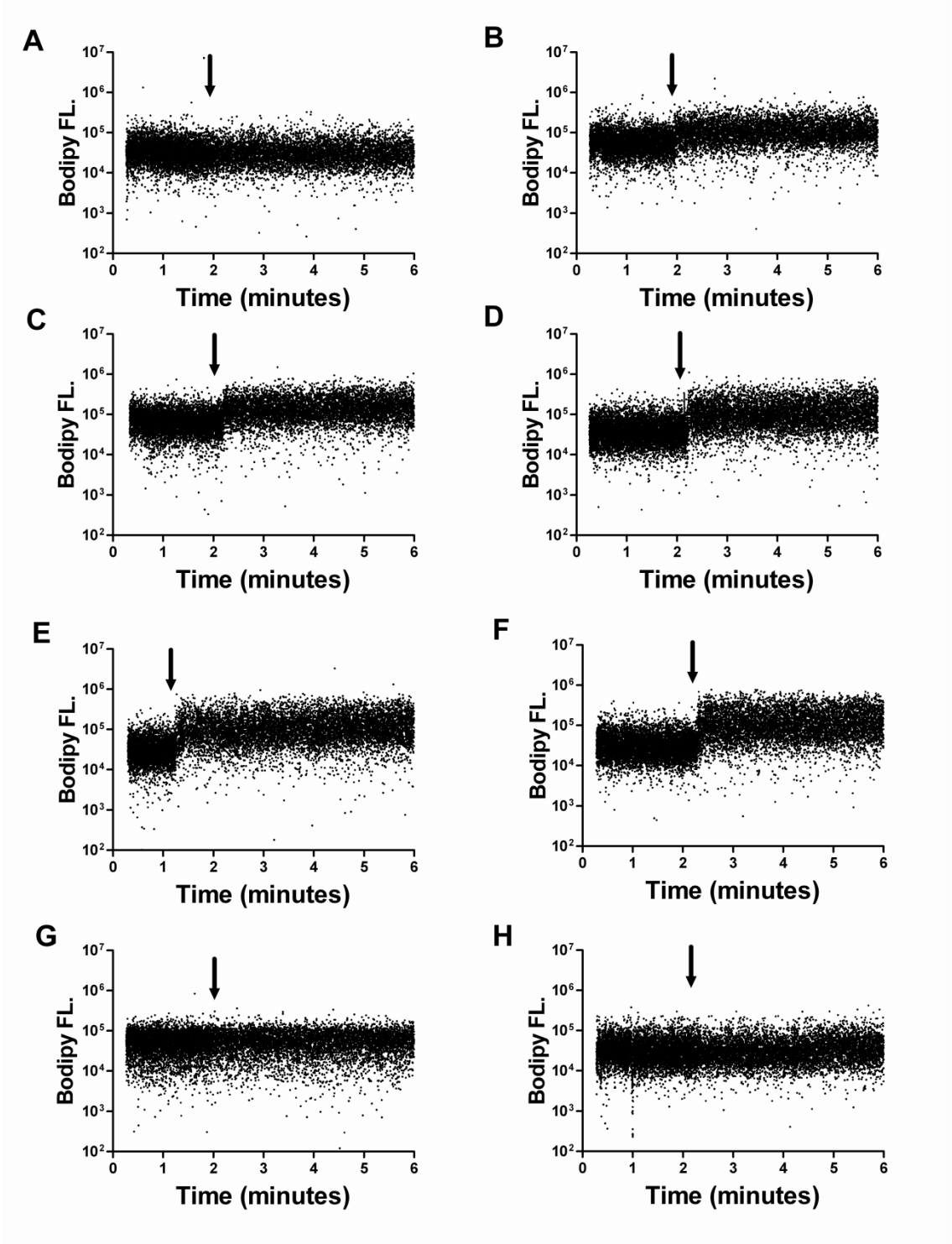
A
B
C
D
E
F
G
H
Bodipy FL.
Time (minutes)

Figure 3. Various models of oxidative stress-induced mitochondrial crisis.

Time course of H_2DCFDA fluorecence measured with an excitation wavelength of 488 and an emission filter 535 ± 30 nm as described in the materials and methods section (A-F). The arrows indicate the time at which the agents were added. H_2DCFDA fluorescence was measured up to 12 minutes after the addition of buffer alone (A) or freshly prepared 5 (B), 50 (C) 100 (D) µM H_2O_2. Similar time courses were performed with 100 µM Tert-butyl hydroperoxide (E) or 1 µM Diamide (F).

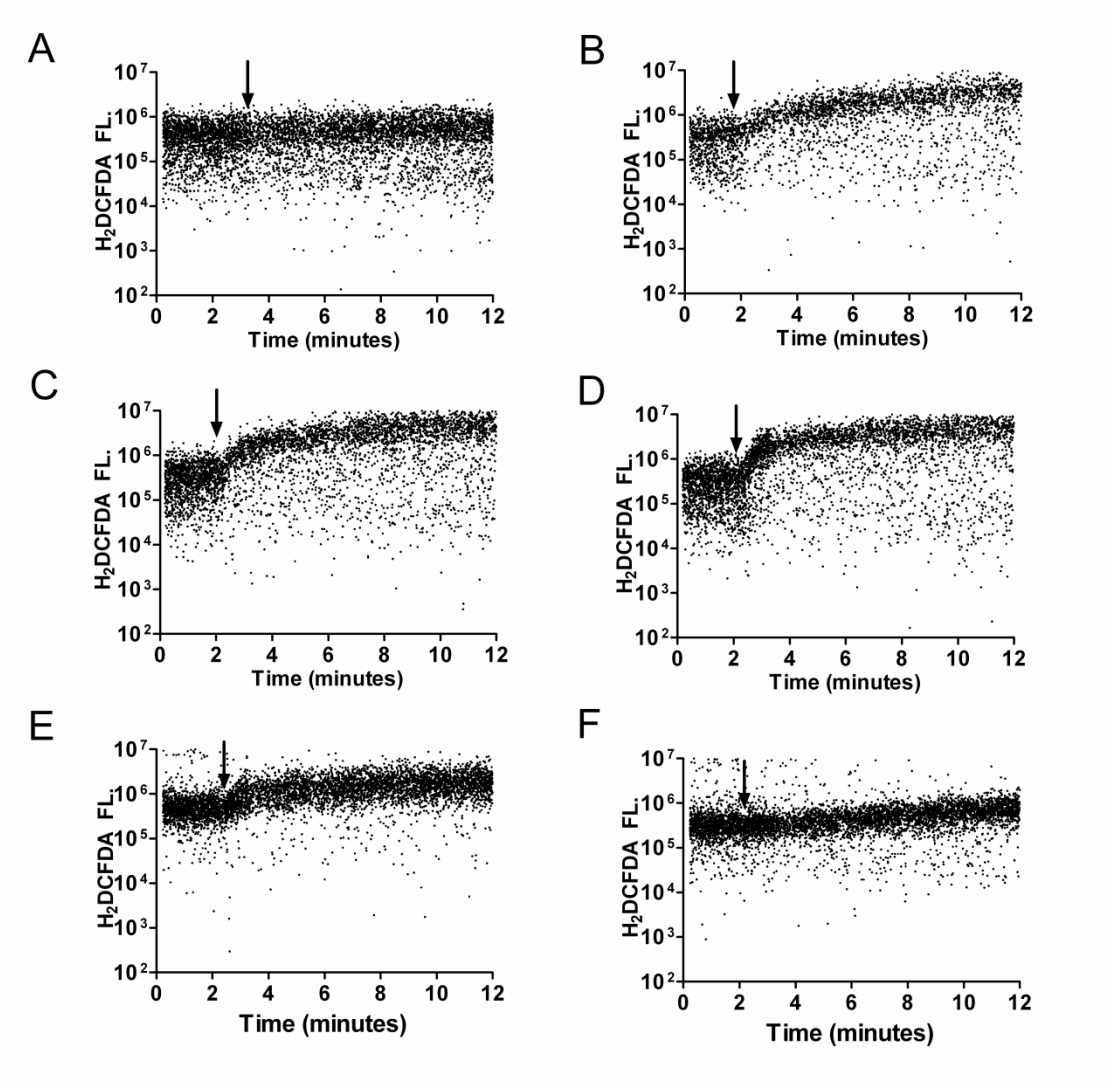
A
B
C
D
E
F
H2DCFDA FL.
Time (minutes)
10^2
10^3
10^4
10^5
10^6
10^7
0
2
4
6
8
10
12

Figure 4. Fatty acids do not promote acute mitochondrial crisis nor do they promote cytosolic H_2O_2 accumulation

Time course of H_2DCFDA fluorecence measured with an excitation wavelength of 488 and an emission filter 535 ± 30 nm as described in the materials and methods section (A-C). The arrows indicate the time at which the agents were added. In three independent experiments, H_2DCF fluorescence was measured for 60 minutes after the addition of 1000 (A) or 2000 (B) μM FA. In two experiments, H_2DCFDA fluorescence was measured for at least 160 minutes after the addition of 1000 (c) μM FA. In those experiments, there was no significant increase in fluorescence. Alternatively, we measured H_2O_2 directly using cells transfected with pHyPer Cyto (D). This method confirmed the absence of H_2O_2 emission following FA exposure and confirmed that H_2O_2 levels are only transiently increased, even after the addition of a supra-physiological concentration of H_2O_2. In the bar graph data are the mean ± SD of three independent experiments. * $P \leq 0.05$ when compared to 600 μM BSA.

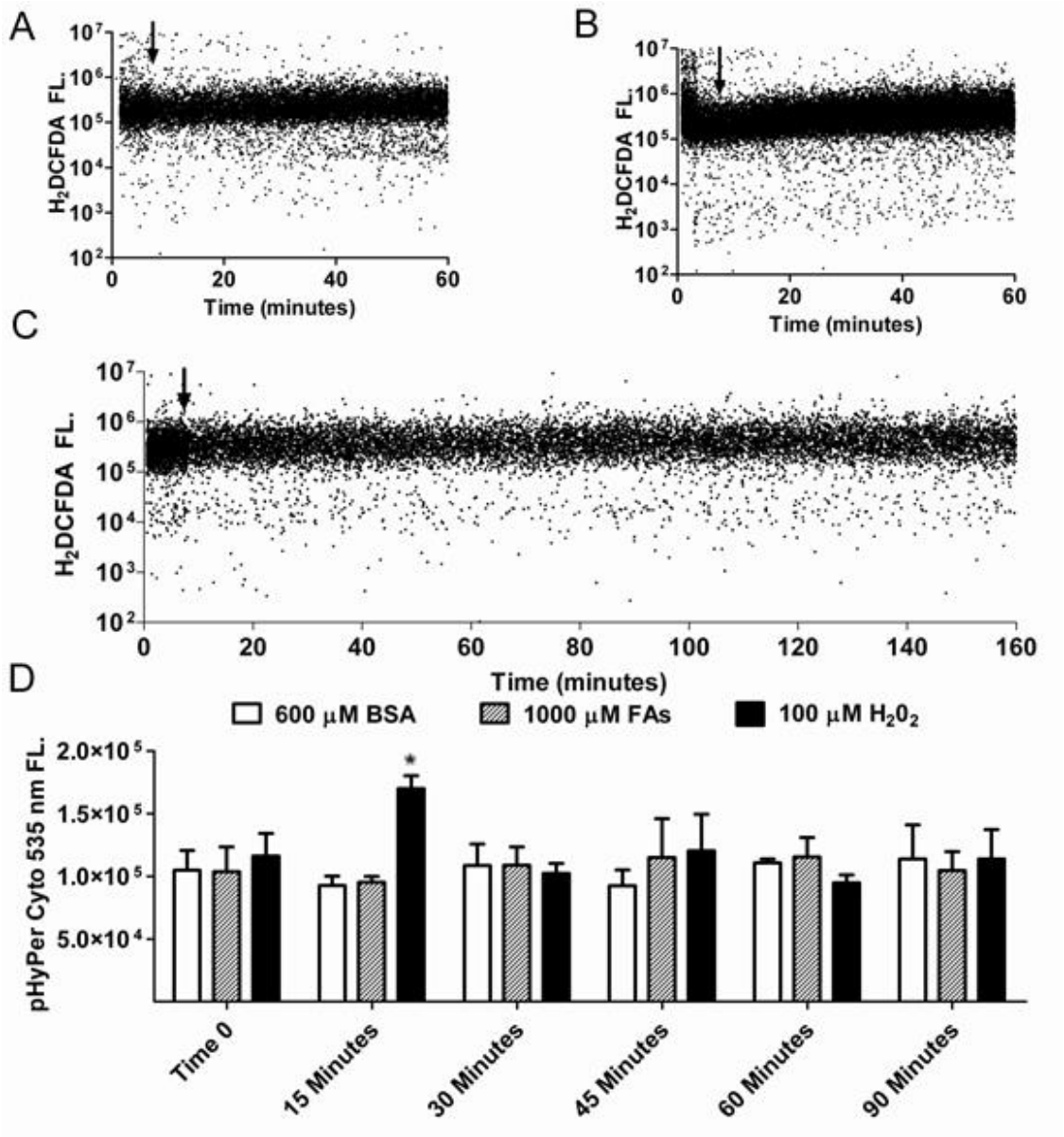
A
B
C
D
H2DCFDA FL.
Time (minutes)
600 μM BSA
1000 μM FAs
100 μM H2O2
pHyPer Cyto 535 nm FL.
Time 0
15 Minutes
30 Minutes
45 Minutes
60 Minutes
90 Minutes

CHAPTER 4: FATTY ACIDS INDUCE A TRANSIENT INCREASE IN MITOCHONDRIAL SUPEROXIDE AND H_2O_2, WHICH PRIMES HUMAN PREADIPOCYTES TO THE METABOLIC CONSEQUENCES OF NAD+ DEPLETION

Carlyle Rogers[1,2], Barbara Davis[1,2], Ethan Anderson[1,2], Michael Murphy[3] and Jacques Robidoux[1,2]

[1] Department of Pharmacology and Toxicology and [2] The East Carolina Diabetes and Obesity Institute , East Carolina University, Greenville, North Carolina. [3]MRC Dunn Nutrition Unit, Hills Road, Cambridge CB2 OXY, U.K.

Abstract

Elevated circulating non-esterified fatty acids (NEFA), a key feature of obesity, are a risk factor for Type 2 Diabetes (T2DM) and several cardiovascular diseases (CVDs). Since a lessened ability of adipocytes to store and retain fatty acids (FA) underlies the elevation of NEFA that is observed in obesity, understanding the cause of this elevation in NEFA due to adipose tissue dysfunction is important in preventing the development of metabolic disease. One potential hypothesis as to how adipose tissue dysfunction develops is due to a loss in preadipocyte number or adipogenic potential. One potential way that preadipocyte loss occurs is through an increased susceptibility to the constant flux of FA in and out of the adipose tissue depot.Furthermore how changes in FA levels affect preadipocyte function is not known. Using conditionally immortalized human preadipocytes, the effects of a physiologically relevant mixture of FA on mitochondrial and cellular redox, metabolic fitness and cell viability were tested. A FA concentration above 600 µM initiated a transient, rather than a persistent elevation of intra-mitochondrial superoxide (< 30 min), H_20_2 (< 60 min) and inner mitochondrial

membrane lipid peroxide (< 120 min) production that could be prevented by use of mitochondrial selective scavengers of superoxide and alkyl radicals. Similar changes in cytosolic redox parameters were not observed within the first twelve hours, demonstrating that mitochondrial reactive oxygen species (ROS) buffering systems were able to buffer this initial surge. A delayed and massive surge in cytosolic reactive oxygen species eventually occurs, but it is preceded by a progressive depletion of NAD+ and coincides with the collapse of the inner membrane potential ($\Delta\Psi$), the opening of the mitochondrial permeability transition pore (mPTP), as well as a decrease in ATP synthesis and ultimately death. Together the results reveal that FA induced ROS production does not follow the current paradigm of a massive ROS/oxidative event leading to cell death, but rather suggests that transient changes in redox homeostasis can prime preadipocytes for mitochondrial dysfunction and cell death.

Introduction

Currently, more than one-third of adults in the United States have a body mass index (BMI) above 30, which is accompanied by an escalation in obesity-associated health problems (Z. Li, Bowerman, & Heber, 2005; Olshansky, 2005; Shah & Braverman, 2012). Although the link between obesity and obesity-related-disorders, such as insulin resistance, has been demonstrated in several epidemiological and interventional studies, the underlying mechanism is unclear (P. J. Anderson et al., 1997; Pories & Dohm, 2009; Ravussin & Smith, 2002). To meet the storage requirements for increased intracellular lipids, adipocytes can increase in either size (hypertrophy) or number (hyperplasia) by recruiting preadipocytes to join the adipocyte pool and share the increased lipid load (P. Arner et al., 2011). While hyperplasia and hypertrophy play a role in obesity, the ability of the adipose tissue depot to replace dysfunctional adipocytes, as well as to increase the number of mature adipocytes is compromised (P. Arner et al., 2011; Paolisso,

Gambardella, et al., 1995; Paolisso, Tataranni, et al., 1995). If adipose tissue turnover fails, ectopic fat accumulation occurs in the liver, muscle and other non-adipose tissue (A Gastaldelli et al., 2004; A. Gastaldelli et al., 2002; Moro, Bajpeyi, & Smith, 2008). One potential mechanism as to why adipose tissue turnover failure occurs is through a diminished preadipocyte pool due to an increased susceptibility to lipotoxicity within the normal day to day fluctuations in fatty acids (FA) (Tchoukalova et al., 2007).

Depending on the equilibrium of FA outside versus inside the cell, FA can rapidly enter through the cellular membrane, interact with coenzyme A (CoA), and form fatty acyl-CoA (Kiens & Roepstorff, 2003). Once formed, fatty acyl-CoA can be shuttled into the mitochondria to be oxidized and generate reducing equivalents for ATP production via the electron transport chain (Wojtczak, 1976). If the NADH levels outweigh the preadipocytes ATP demand, one-electron reduction of oxygen can occur at the level of the electron transport chain (ETC), forming superoxide and subsequently H_2O_2 (P Schönfeld & L Wojtczak, 2008) . Although levels of FA below a certain concentration pose no risk to mitochondrial or cellular functions, FA concentrations well-above physiological limits have been shown to increase mitochondrial complex I and III reactive oxygen species (ROS) generation in preadipocytes, and has been suggested based on work in other cell types to open the mitochondrial permeability transition pore (mPTP) and cause cell death (Guo et al., 2007; P Schönfeld & Bohnensack, 1997; P. Schönfeld & L. Wojtczak, 2008). Although reactive oxygen species (ROS) production of preadipocytes or adipocytes following fixed or prolonged (45 min to 7 days) FA exposure has been demonstrated, none have performed an extensive time course evaluation of fatty acid induced ROS production in preadipocytes (Guo et al., 2007). Additionally, understanding how FA influence mitochondrial fitness and survival have not been studied.

The objective of this study was to observe how human preadipocytes, in vitro, would respond to a FA-enriched environment. The findings are that FA exposure initiates a transient rather than a persistent elevation of mitochondrial superoxide and H_20_2 production that primes preadipocytes for cell death through depletion of NADH and NAD+. Together these results suggest that FA-induced ROS production does not follow the current paradigm of a massive ROS/oxidative event leading to cell death, but rather suggests a mechanism by which transient changes in mitochondrial ROS production can lead to mitochondrial dysfunction and cell death.

Materials and Methods

Cell Culture

XA15A1 human preadipocytes (Lonza Walkersville, Inc., Walkersville, MD) were cultured as described in Skurk et al.,(Skurk et al., 2007) using Dulbecco's modified Eagle's medium: F12 (DMEM:F12; Mediatech, Manassas, VA) with 10% calf serum, 15 mM glucose, 33 µM biotin, 17 µM D-pantothenate, 100 nM insulin, and 10 nM hydrocortisone (all from Sigma Aldrich), 1 nM epidermal growth factor and 1 nM basic fibroblast growth factor (Gemini, West Sacrameto, CA). This medium also contained 50 IU/ml penicillin, 50 µg/ml of streptomycin and 2.5 µg/ml amphotericin B (Mediatech). The XA15A1 cells were propagated at 33 C. When the cells reached 80% confluence, growth factors were omitted from the media and the cells were placed at 37 C for at least 24 hours prior to the experiment. The XA15A1 cells express a temperature-sensitive mutant of the SV 40 Large T-antigen (u19tsA58) and needs to be incubated at 37 C for 24 hours to revert to a phenotype that resembles that of primary cells and are able to differentiate. For experiments, XA15A1 cells were transiently transfected with Mito-HyPer or Cyto-HyPer plasmids (Evrogen, Moscow, Russia), which encode mitochondrion- or

cytosol-targeted H_2O_2-sensitive ratiometric reporter proteins. Briefly, 5 x 10^6 cells were transfected in a 100 µL final volume of the nucleofection solution V containing 1µg of plasmid DNA and the application of the T-030 program from the Amaxa Nucleofactor 2b electroporator (Lonza Walkersville) list. For experiments using transiently transfected cells, the cells were used 48 hours later.

Preparation of Fatty Acids

A 50 mM stock of each single fatty acid was prepared in 0.1 M NaOH. Each fatty acid stock was added to Dulbecco's modified Eagle's medium: F12 (DMEM:F12) containing 600 µM BSA, 5% calf serum, 10 mM glucose, 33 µM biotin, 17 µM D-pantothenate, containing 50 IU/ml penicillin, 50 µg/ml of streptomycin, and 2.5 µg/ml amphotericin B to reach a mixture consisting of 40% oleate, 25% palmitate, 20% linoleate, and 15% stearate. Each concentration was pre-equilibrated for one hour with 600 µM BSA at 37^0C. For all experiments, cells were incubated in 600 µM BSA for at least 2 hours prior to the addition of the drugs or fatty acids (FA). To start the experiment FA mixtures were added to the 600 µM BSA at a 2x concentration to equal a final FA concentration of 1x.

MitoSox Red and CM-H2-DCFDA Fluorescence Measurements

MitoSox Red, the fluorescent probe hydroethidine coupled to the mitochondrion-targeting hexyl triphenylphosphonium (TPP) cation was used as a mitochondrion-localized superoxide indicator (Invitrogen, Carlsbad, CA). The fluorescent probe 5-(and-6)-chloromethyl-2',7'-dichlorodihydrofluorescein diacetate acetyl ester (CM-H_2-DCFDA; also from Invitrogen) was used as a cytosol-localized mitochondrial crisis indicator. As the majority of DCF fluorescence relies on cytochrome c release from the mitochondria and cytosolic H_2O_2 oxidation

of cytochrome C (Brömme et al., 2008; Karlsson et al., 2010). These detection methods were used for end point as well as real-time experiments. At the end of the incubation periods for end point experiments, cells were washed with Dulbecco's phosphate buffered saline, containing calcium and magnesium (DPBS) and incubated at 37°C, with 4 µM MitoSox Red or 6 µM of CM-H_2DCFDA in DPBS for 35 and 45 minutes, respectively. After loading of the fluorescence probe, cells were washed twice with DPBS. After preloading, cells were dissociated from the dishes by adding 1 mL of 10x TrpLe dissociation buffer (Life Technologies, Grand Island, NY) for 30 seconds, and after adding 1 mL of DPBS, collected through repeated aspirations and ejections. MitoSox fluorescence was measured using an Accuri C6 flow cytometer (BD, Franklin Lakes, New Jersey) at an excitation wavelength of 488 and a 585 ± 40 nm emission filter. H_2-DCFDA fluorescence was measured using an excitation wavelength of 488 and a 535 ± 30 nm emission filter. The real-time approach will be described separately in addition to being the subject of an independent chapter.

Continuous Real-Time Flow Cytometry Analysis

To quantify changes in fluorescence on a cell-by-cell basis over the course of minutes to hours an apparatus was invented that could be retrofitted to any flow cytometers not operating under pressurized conditions like the BD Accuri C6. Briefly, the apparatus consists of an open 30 mL polypropylene receptacle (vial) surrounded by a water coil jacket, supplied by a heated-circulating water bath, set to maintain the temperature at 37°C. The vessel is sitting on a stir plate allowing a rapid dispersion of FA or drugs without interruption, as well as maintaining homogeneous cell sampling. After loading of the fluorescence probe as described in their respective method subsection, cells were processed similarly, except for the final addition of 1

mL of flow buffer, which consisted of Krebs's ringer bicarbonate buffer (Sigma-Aldrich Co., St. Louis, MO) containing 600 µM fatty acid-free bovine serum albumin, 5% fetal calf serum, 33 µM Biotin, 17 µM D-Pantothenate, 50 IU/ml penicillin, and 50 µg/ml of streptomycin instead of DPBS. Cells were counted by gating the single cell population in the Forward Scatter (FCS-H) versus Side Scatter (SSC-H) density plot. The counted cells were suspended in flow buffer to obtain a final concentration of about $1x10^6$ cells in a total volume of 7 mL. The suspended cells were transferred into the 30 ml vial. A stir bar was added and rotated at 400 rpm to maintain the oxygen tension constant, to quickly distribute the added compounds, and to prevent cell clumping. The flow rate was adjusted to have a flow rate of 66 µL/minute and a core size of 22 µm in order to analyze fluorescence levels from about 2000 cells in the live cell region per minute. Baseline fluorescence in each sample was measured for 3-5 minutes prior to the addition of 600 µM BSA (basal). After 5 minutes, different compounds were added directly to the sample.

Detection of Lipid Peroxide Formation

Mitochondrial inner membrane localized lipid peroxidation was assessed using a C11-BODIPY$^{581/591}$ probe conjugated to a TPP cation moiety (MitoPerOx: Dr. Michael Murphy, MRC Mitochondrial Biology Unit; Cambridge, England, UK) (Prime et al., 2012). The reduced C11-BODIPY$^{581/591}$ probe has a maximum emission wavelength of ~590 while the oxidized product displays a maximum emission wavelength of ~520 nm in response to lipid peroxidation by hydroxyl and peroxy radicals (Drummen et al., 2004). Briefly, cells were incubated, at 37°C, in DPBS with 150 nM MitoPerOx for 30 minutes. After loading, cells were collected and CRT flow cytometry or fluorescent microscopy was performed. For the CRT flow cytometry experiments, MitoPerOx was excited at a wavelength of 488 and emission captured through a

585 ± 40 nm and 535 ± 30 nm emission filters for the reduced and oxidized form of MitoPerOx, respectively. For the microscopy based experiments, cells were washed with 1x PBS and 1 mL of flow buffer was added. Following an addition of flow buffer, images were taken at multiple time points with an EVOS fluorescent microscope (AMG, a part of life technologies, Grand Island, NY) using the GFP light cube, which couples a 470 ± 22 nm excitation and a 525 ± 50 nm emission filter, as well as the RFP light cube, which couples a 531 ± 40 nm excitation to a 593 ± 40 nm emission filter.

Detection of Mitochondrial and Cytosolic H_2O_2

H_2O_2 levels in the mitochondrial or cytosolic compartment were measured using the genetically encoded sensors Mito-HyPer (has a mitochondria targeted sequence) or Cyto-HyPer (which resides in the cytosol) that encode for a mutated OxyR protein that is sensitive to submicromolar (or physiological) levels of H_2O_2 (Belousov et al., 2006; Choi et al., 2001). HyPer has an emission of ~516 nm and an excitation of 420 and 500 nm. In the presence of H_2O_2, the excitation peak of HyPer at ~420 nm decreases proportionally to the increase of the excitation peak at 500 nm, allowing for the ratiometric measurement of H_2O_2. For the studies, measurements of the ~516 nm emission peak was used with a 530± 30 nm emission filter, after using an excitation wavelength of 488 only. Cells were plated in six well dishes and grown for 48 hours before CRT flow cytometry was performed. The cells were lifted as described in the CRT flow cytometry subsection and the FA added similarly.

Cell Death

Cell death was measured by Calcein AM and Ethidium Homodimer-1 (Life Technologies, Grand Island, NY). Calcein AM is a live cell dye that accumulates in intact cells where it acquires a strong green fluorescence upon cleavage by intracellular esterases (Papadopoulos et al., 1994). Because intracellular esterase activity is quickly lost as cells die, little to no gain in fluorescence occurs in dead or dying cells. Ethidium Homodimer-1 is a dye that enters the damaged plasma membrane and interacts with nucleic acids. As Ethidium Homodimer-1 interacts with nucleic acids the red fluorescence of the dye increases by 40 Fold, indicating dying or dead cells (Papadopoulos et al., 1994). At the end of the 6, 12 or 24 hour FA incubation periods, cells were collected and incubated for 15 minutes at room temperature in DPBS containing Calcein AM and Ethidium Homodimer 1 at a final concentration of 0.05 µM and 4 µM. To detect Calcein AM fluorescence an excitation wavelength of 488 and a 530± 30 nm emission filter was used. Ethidium Homodimer 1 fluorescence was detected using an excitation wavelength of 488 and a 675 ± 25 emission filter. After subtraction of auto-fluorescence, the live cell region was determined by examining an untreated sample and a sample containing only 600 µM BSA. Dead cells were determined by treating a control sample with 0.01% Triton-X for 15 minutes. All values for cell death represent the percent of dead cells found in the gated region of the cell population of interest.

Mitochondrial Inner Membrane Permeabilization

As mentioned in the description of the use of Calcein AM for the identification of live cells, Calcein AM enters cells and has access to every compartment. Cobalt is known to quench Calcein fluorescence, but since cobalt does not freely enter mitochondria, Calcein AM fluorescence within the mitochondria is not quenched unless there is an increase in membrane

permeability (Petronilli et al., 1998). Briefly, cells are incubated with Calcein AM at a final concentration of 0.05 µM in DPBS for 30 minutes, followed by 200 µM $CoCl_2$ for 15 minutes. Calcein AM fluorescence was measured using an excitation wavelength of 488 and a 535 ±30 nm emission filter. Mean fluorescence and percent of cells experiencing mitochondrial inner membrane permeabilization was determined by histogram plots of Calcein AM after the subtraction of auto fluorescence.

Detection of Changes in the Inner Mitochondrial Membrane Potential

Changes in inner mitochondrial membrane potential was measured by using the lipohilic cationic dye tetramethylrhodamine ethyl (TMRE) ester (Sigma-Aldrich Co) that accumulates in direct proportion to the inner mitochondrial membrane potential according to the Nernst Equation. Each sample was incubated with 50 nM TMRE in DPBS for 20 minutes at 37^0C. TMRE was measured using an excitation wavelength of 488 and a 585 ±40 nm emission filter. Mean fluorescence was determined by histogram plots of TMRE fluorescence after the subtraction of auto fluorescence.

Cellular Respiration Assay

Approximately 20,000 preadipocytes in growth media without growth factors were seeded to each well of Seahorse XF24 plates (Seahorse Bioscience, MA) and grown for 24 hours at 37°C before treatment with various inhibitors or FA. Four to six hours before the experiments, the media was changed to DMEM, containing 5% calf serum, 25 mM Hepes, 10 mM glucose and 600 µM FA-free BSA. An hour before FA treatments, inhibitors or their vehicle was added to the cells, and then FA were added at various concentrations (0 – 1000 µM) for 24 hours. At the end of the incubation, cells were washed two times with 1 ml of phosphate-buffered saline

with magnesium and calcium. Finally, 500 µL of Seahorse XF-DMEM medium containing 10 mM glucose and 2 mM sodium pyruvate was added to the cells. Cellular respiration was measured as described previously by Herscovitch et. al., (Herscovitch et al., 2012) with the following slight modifications determined to be optimal in preliminary experiments. First, the measurement cycle consisted of 1 minute mix, 1 minute wait and three minutes measurement. Second, three basal rate measurements were taken, three after oligomycin injection, three after Carbonyl cyanide 4-(trifluoromethoxy) phenylhydrazone (FCCP) injection and three after Rotenone injection. Drugs were delivered through the ports at final concentrations of 1 µM for oligomycin, 500 nM for FCCP and 1 µM for Rotenone. Each of the three independent experiments were performed in triplicate.

NAD+ and NADH Levels

Following FA exposure, cells were washed twice with PBS. NAD+ levels were determined using a NAD+/NADH cell-based assay kit as described in the manual (Cayman Chemical, Ann Arbor, MI). After washing, cells were lysed, centrifuged and the supernatant was used to measure NAD+ and NADH levels. In this assay, alcohol dehydrogenase converts ethanol to acetoaldehyde and yields NADH from the NAD+ present in the supernatant. After NADH is formed, it reduces the tetrazolium salt substrate (WST-1) into a highly colored formazan dye that absorbs at the 450 nm wavelength. An Infinite 200 Pro Series plate reader was used to quantify absorbance. As more than 95% of the NAD in cells is oxidized this assay is essentially a NAD+ assay.

ATP Determination

Following FA exposure, cells were washed twice with PBS, and ATP was extracted by using the boiling water extraction method (Yang et al., 2002). Following extraction, ATP levels were determined using an ATP determination kit, as described by the supplier (Life Technologies). An Infinite 200 Pro Series plate reader was used to quantify luminescence.

Statistical Analysis

Statistical analysis was performed with PRISM (GraphPad Software, San Diego, CA) version 5.00 for Windows. Differences between FA concentrations, 600 µM BSA and/or pretreatment with MitoTempo, Etomoxir, Carnosine, Cyclosporin A or Nicotinamide were assessed by a one-way ANOVA with a Tukey's multiple comparison test. All values are reported as $\pm$ SD. In all cases, a *P* value of less that 0.05 was used to indicate statistical significance between conditions.

Results

24 Hour exposure to fatty acids in human preadipocytes leads to cell death

Conditionally immortalized human subcutaneous adipose tissue preadipocytes were treated with a physiological mixture of FA in a concentration range and a FA to albumin ratio that resembles the physiological state within adipose tissue. Preadipocytes were treated with increasing concentrations of FA for 6, 12, 24 hours and changes in fluorescence of Calcein AM and Ethidium Homodimer 1 were examined using flow cytometry or microcopy). Figure 5A illustrates two representative flow cytometry dot-blots comparing the BSA control to 1000 µM FA-treated cells. Figure 5B illustrates two representative microscopy observations from the same comparison. Figure 5C is the average of three independent experiments that shows that it takes

24 hours of constant exposure to FA and concentrations of 800 µM FA and 1000 µM FA to observe a significant amount of cells death. No difference in cell death among the different FA concentrations was observed at the 6 and 12 hour time point (Figure 5C).

To test the hypothesis that FA entry into the mitochondria and/or ROS production could cause cell death, cells were pretreated for 10 minutes with 10 µM Etomoxir, a carnitine palmitoyl transferase I inhibitor that blocks entry of fatty acyl CoA into the mitochondria or 10 µM MitoTempo, a mitochondrial specific superoxide and alkyl radical scavenger. Pretreatment with Etomoxir or MitoTempo, followed by 1000 µM FA exposure, resulted in a significant decrease in cell death compared to 1000 µM FA alone (Figure 5D), suggesting that FA entry into the mitochondria and ensuing superoxide or alkyl radical production was the main source of cell death. Since retention of Ethidium Homodimer 1 occurs in the late stages of cell death, 6 and 12 hours of constant FA exposure followed by 18 and 12 hours of 600 µM BSA respectively, was investigated. No change in cell death at 24 hours after treating for 6 or 12 hours was observed (data not shown) indicating that FA exposure only caused cell death after 12 hours of constant FA exposure. Interestingly, the addition either Etomoxir or MitoTempo two hours after the onset of the FA treatment totally abrogated their protective effects (Figure 5E).

Fatty acids cause a transient and a delayed increase in superoxide and H2O2 within the first hour of exposure

Once an elevation in superoxide or alkyl radicals occurs, the resulting oxidation of proteins, lipid and/or nucleotides can lead to cellular dysfunction, and ultimately cell death (Girotti, 1998). To observe if cell death was accompanied or preceded by an increase in mitochondrial and cytosolic oxidation, changes in the mean fluorescence of MitoSox Red and

H_2DCFDA was measured. At the 24 hour time point a statistically significant increase in the mean fluorescence of H_2DCFDA (Figure 6A and C) and MitoSox Red (Figure 6B and D) was observed suggesting that mitochondrial and cytosolic compartments were in the presence of an oxidative environment. Pretreatment with Etomoxir or MitoTempo prevented the increase in CM-H_2DCFDA (Figure 6C) and MitoSox Red (Figure 6D) fluorescence induced by 24 hours exposure to 1000 µM FA, suggesting that FA entry into the mitochondria and subsequent superoxide or alkyl radical production were the cause of the increased oxidative environment at 24 hours. To confirm that FA exposure initiated a sustained increase in ROS and oxidative environment, MitoSox Red and H_2DCFDA fluorescence at 3 and 12 hours following FA exposure were measured. Surprisingly, no change in MitoSox Red or H_2DCFDA fluorescence was observed at the 3 or 12 hour time points (Figure 6A and B).

The greatest protective effect of Etomoxir or MitoTempo pretreatment against cell death was seen during the first hour of FA exposure. However, no changes in MitoSox or H_2DCFDA fluorescence were observed after 3 hours of FA exposure. Therefore, we directly investigated the existence of a transient increase in mitochondrial superoxide following the addition of FA. To characterize such a rapid changes in superoxide levels, preadipocytes were preloaded with MitoSox Red and changes in fluorescence measured using continuous real time (CRT) flow cytometry, a method that we recently developed (Chapter 3). Representative traces demonstrate that MitoSox fluorescence rapidly increases upon FA exposure. At the end of one hour, 57.9 ± 2.6 % of preadipocytes treated with 1000 µM FA had high MitoSox Red fluorescence compared to just 14.03 ± 3.7 % of the cells in 600 µM BSA (Figure 7B). Since MitoSox Red is not reversible once oxidized, no oscillations in fluorescence could be observed once reaching the fluorescent plateau. Therefore, cells were treated with FA for 0, 15, 30, 45 or 60 minutes,

followed by intermediate loading of MitoSox Red at -15, 0, 15, 30, 45 or 60 minutes. Comparison of 1000 µM FA versus 600 µM BSA revealed a waxing and waning of MitoSox Red fluorescence that occurred within 60 minutes of FA exposure (Figure 7C). Pretreatment of Etomoxir or MitoTempo followed this increase in MitoSox Red mean fluorescence (Figure 7C).

To examine H_2O_2 production, cells were transfected with pHyPer, a genetically encoded reversible H_2O_2-selective fluorescent sensor, that is capable of detection of intracellular H_2O_2 in the physiological or nanomolar range (Belousov et al., 2006). cells were transfected with pHyPer Mito. Since H_2O_2 production is a product of the dismutation of superoxide, CRT flow cytometry was used to characterize rapid (second to minutes) changes in pHyPer fluorescence. Figure 8A illustrates a transient elevation in the number of events with a higher pHyPer Mito fluorescence following 1000 µM FA (Red dots) exposure versus 600 µM BSA (black dots). Single time point analysis of pHyPer Mito fluorescence revealed an increase and decrease in pHyPer Mito fluorescence within the first 60 minutes of FA exposure (Figure 8B) that could be blocked by pretreatment of Etomoxir or MitoTempo (Figure 8B).

Mitochondrial lipid peroxidation occurs within two hours of exposure to fatty acids

Mitochondrial lipid peroxidation, which is a free radical-mediated degradation process by which lipids are oxidized leading to alteration of their structure and functions (Girotti, 1998). To examine mitochondrial lipid peroxidation, CRT flow cytometry and fluorescent microscopy of the fluorescent probe MitoPerOx, which in response to lipid peroxidation shifts its fluorescence from ~590 nm to ~520 nm, were measured (Prime et al., 2012). Figure 9A shows a representative dot blot of the shift in fluorescence after treatment with 1000 µM FA over a 150 minute timespan. Figure 9B displays microscopic imaging of a similar experiment where 600

μM BSA and 1000 μM FA are compared with respect to MitoPerOx oxidation. These images were obtained by merging the fluorescence at each wavelength observed after 1 hour of exposure to either 1000 μM FA or 600 μM BSA. Analysis of the mean fluorescence of MitoPerOx following treatment with 600 μM BSA or 1000 μM FA at 0, 30, 60, 90, 120 and 150 minutes showed that the ratio of 530/585 mean fluorescence reached a plateau after 120 minutes of 1000 μM FA exposure (Figure 9C). Figure 9C also shows the increase in MitoPerOx green fluorescence was prevented by pretreatment with MitoTempo or 10 μM carnosine. Carnosine is a compound identified as a scavenger of both α,β-unsaturated aldehydes such as hydroxynonenal or acrolein and dialdehydes like malondialdehyde or glyoxal that prevents peroxidation as well as carbonylation of lipids (Aldini et al., 2006; M. Y. Kim, Kim, Kim, Choi, & Lee, 2011). Endpoint analysis, in which MitoPerOx was incorporated into the cells during FA exposure, confirmed the absence of active lipid peroxidation at 3, 6 or 12 hours after the addition of 1000 μM FA (Figure 9D).

Entry of fatty acids into the mitochondria and subsequent increase in ROS leads to mitochondrial crisis

Although transient increases in mitochondrial superoxide, H_2O_2 and lipid peroxidation occurred within hours of FA exposure, the link between transient increases in mitochondrial ROS and cell death was unclear. One potential hypothesis was that the secondary phase of ROS accumulation and cell death was a consequence of a loss in mitochondrial fitness (i.e. the ability of the mitochondrion to maintain equilibrium between substrate availability versus substrate utilization) that manifested into mitochondrial crisis (i.e. a state of the mitochondrion characterized by a unrecoverable loss in mitochondrial respiration, inner mitochondrial membrane potential and ATP synthesis). To establish the time course of the possible effects of

FA on the respiratory capacity, the oxygen consumption rate (OCR) was measured in real-time using respirometry. As shown in Figure 10A, the two concentrations of FA that increased ROS and cell death, also significantly altered respiration. Compared to the 600 µM BSA control condition, OCR was significantly decreased after 10 hours of FA to 1000 µM FA and by 14 hours at the concentration of 800 µM, indicating that changes in mitochondrial respiration occurred well before any observed cell death. Next, the ability of increasing FA concentrations to decrease mitochondrial inner membrane potential was investigated. Surprisingly, Figure 10 B shows that tetramethylrhodamine ethyl (TMRE) fluorescence, a cationic dye that collects in the mitochondria in direct proportion to the mitochondrial inner membrane potential, was decreased 24 hours after the addition of 800 or 1000 µM of FA, but not after 3 or 12 hours. As with ROS production and cell death, loss of OCR and inner mitochondrial membrane potential could be prevented by pretreatment with Etomoxir or MitoTempo (Figure 10C and D).

The mitochondrial inner membrane potential, or more accurately the mitochondrial inner membrane proton gradient, is a driving force for multiple functions including ATP and NADPH synthesis (Brand & Nicholls, 2011). Therefore, ATP levels were measured every 2 hours for 20 hours (Figure 10 E). As shown in Figure 10E, drops in ATP levels occurred well ahead of 24 hours, with a statistically significant loss in ATP levels occurring between 12 to 14 hours with 1000 µM FA and 16 to 18 hours at 800 µM FA. The observed decrease in ATP levels occurred about 2 hours after the observed decrease in OCR. For ATP production to occur, reducing equivalents, such as NADH, must pass their electrons to the electron transport chain (ETC) to generate a proton motive force that can drive ATP synthase to make ATP (GM, 2000). NAD^+ and NADH levels were measured every 2 hours up to 20 hours. Interestingly, NAD^+ and NADH levels were significantly decreased within 8 hours of 1000 µM and 12 to 14 hours of 800 µM FA

exposure. The drop in NAD^+ and NADH preceded the decrease in OCR by about 2 hours (Figure 10F). Pretreatment with either Etomoxir or MitoTempo prevented the decrease of both NAD^+ and NADH and ATP measured at 18 and 24 hours respectively (Figure 10H and I) indicating that the transient increase in ROS was the triggering event in NAD^+ and NADH and ATP loss.

Opening of the mPTP can cause the mitochondrial membrane to become permeable to any molecule less than 1.5 kDa, leading to loss of inner mitochondrial membrane potential and exit and potential degradation of NAD+ (P Schönfeld & Bohnensack, 1997). To look at the opening of the mPTP, preadipocytes were stained with Calcein AM in the presence of $CoCl_2$. Calcein AM will enter both the cytosol and mitochondria, while $CoCl_2$ will reside only within the cytosol and will quench cytosolic Calcein AM fluorescence (Petronilli et al., 1998). Upon opening of the mPTP, $CoCl_2$ can enter and quench mitochondrial Calcein AM fluorescence (Petronilli et al., 1998). The percentage of cells with a lower Calcein AM fluorescence, indicative of mPTP opening, was statistically significant in 1000 µM and 800 µM FA at the 12 and 24 hour time point compared to 600 µM BSA (Figure 10I). Pretreatment with Etomoxir or MitoTempo prevented the increase in the number of cells that had lower Calcein AM (Figure 10J). Together these data suggest that transient increases in ROS leads to a loss of mitochondrial fitness as observed by decreases in OCR, inner mitochondrial membrane potential, ATP, NAD^+ and NADH and opening of the mPTP.

Nicotinamide supplementation prevents both the loss or mitochondrial fitness and cell death

Of all the different mitochondrial readouts examined, decreases in NAD^+ + NADH levels occurred earliest. To test if loss of NAD^+ and NADH was one of the primary triggers for loss of mitochondrial fitness, nicotinamide was added to cells for 30 minutes prior to FA exposure.

Decreases in OCR, inner mitochondrial membrane potential, ATP and NAD^+ and NADH were prevented by pretreatment with 40 µM nicotinamide (Figure 11A, B, C and D). Although nicotinamide supplementation prevented the deleterious effects brought on by 1000 µM FA exposure, the percentage of cells with open mPTP was only partly reduced (Figure 11E). Examination of MitoSox Red and CM-H_2DCFDA fluorescence at 24 hours revealed that nicotinamide supplementation also prevented the delayed oxidative stress phase (Figure 11F and G) and the cell death that was associated with 1000 µM FA treatment (Figure 11H).

As alluded to above, one possible explanation for depletion of NAD^+ and NADH levels is opening of the mPTP. Pretreatment with 10 µM Cyclosporin A, which interacts with cyclophilin D to prevent formation of the mPTP did not prevent the decrease in NAD^+ and NADH induced by 1000 µM FA (Figure 11J).

Discussion

Although the effects of individual FA on preadipocytes have been studied (Guo et al., 2007), none have exposed human preadipocytes to a FA mixture that resembles the physiological state of adipose tissue. The novel FA mixture used in this study included the four main FA: oleate, linoleate, palmitate and stearate. The relative percentage of each FA within each total concentration was kept constant, as it has been shown the percentage of each FA is independent of increasing or decreasing FA levels (Mittendorfer et al., 2003). Although the FA mixture accounted for 95% of the FA found in circulation, the other 5%, which includes myristate, polyunsaturated FA, etc. may have an impact on preadipocyte function. For example, 3T3-L1 adipocytes treated for 7 days with 250 µM myristate increased expression of inflammatory factors such as MCP-1 (Yeop Han et al., 2010). Furthermore, 25 µM docosahexaenoic acid

(DHA) has been shown to increase apoptosis and inhibit differentiation of 3T3-L1 adipocytes (H. K. Kim, Della-Fera, Lin, & Baile, 2006). Although these results would suggest that additional FA would make our FA mixture more toxic, this may not be the case as both studies used a FA to albumin ratio greater than 4:1 (H. K. Kim et al., 2006; Yeop Han et al., 2010) . In circulation, FA to albumin ratios rarely exceeds 1:1 except during prolonged exercise, fasting, or locations within the adipose tissue depot(Curry et al., 1999; Yamazaki et al., 2005). For this study, FA was conjugated to 600 µM BSA to maintain a ratio below or around 1:1. Despite mimicking the physiological environment with respect to FA, limitations exist. One major limitation is that preadipocytes are not exposed to a single dose of FA, but rather constant fluctuations of FA, glucose and insulin throughout a 24-hour time period (Tahiri et al., 2007). Nevertheless, even with a single dose of FA, increases in ROS and lipid peroxidation occurred, suggesting that preadipocytes, although within the adipocyte lineage, are a target for lipotoxicity.

In this study, for cell death to occur, preadipocytes must experience a loss of mitochondrial fitness. Interestingly, the loss of mitochondrial fitness appears to occur through transient rather than sustained increases in superoxide, H_2O_2, and lipid peroxidation during the first 1-3 hours of FA exposure that primes preadipocytes for death. Although the initial spike in ROS ultimately leads to cell death, preadipocytes still had to be exposed for more than 12 hours for death to occur. One possible explanation is that the initial influx of FA into the mitochondria causes an increase in ROS above the buffering capacity. Once the equilibrium of FA in and outside the preadipocyte establishes, the buffering capacity of the cell is able to return ROS levels back to the basal state. Although the elevation of ROS above the buffering capacity subsides within an hour, oxidation of processes that lead to NAD^+ and NADH depletion have already been initiated. Although NAD^+ and NADH loss is observed as soon as 8 hours, it may

take more than 12 hours to pass the threshold that leads to an effect on mitochondrial fitness and ultimately cell death. Furthermore, by replacing FA with 600 µM BSA at the 12 hour time point the need of NAD^+ and NADH for FA β-oxidation and respiration in the mitochondria may have been reduced. For both Cyclosporin A and Carnosine, limiting opening of the mPTP and reducing the toxic effect of lipid peroxides on mitochondrial function may delay, rather than prevent the detrimental effects of NAD^+ and NADH depletion, as cell death was observed after 48, but not 24 hours of FA exposure.

In addition to loss of NAD^+ and NADH, a loss in mitochondria fitness was observed. For mitochondria, once the mPTP is in a constant open state, disruption of the inner mitochondrial membrane, loss of respiration, outer membrane permeabilization and mitochondrial swelling can occur (Gottlieb, Armour, Harris, & Thompson, 2003; Mather & Rottenberg, 2001). Although opening of the mPTP was observed at 12 hours, this did not translate to a loss in inner mitochondrial membrane potential. However, the sensitivity of TMRE to change in response to mPTP opening is lower than that of Calcein AM, since a 5-fold increase in the number of cells with lower Calcein AM fluorescence did not result in a similar change in TMRE fluorescence after 24 hour exposure to 1000 µM FA. Furthermore, since all of the FA concentrations and flow experiments were used with a threshold and gate based on 600 µM BSA, an underestimation of FA effects could have occurred, since dying cells would have shifted out of the live region. Nevertheless, time course evaluation did show decreases in the OCR, ATP and NAD^+ and NADH before any measurable death was observed, suggesting that the loss of mitochondrial fitness was not dependent on cell death.

In summary, preadipocytes are susceptible to FA through transient (1-2 hours) increases in ROS that lead to depletion of NAD^+ and NADH and ATP, reduction of OCR, opening of the mPTP, decrease of the mitochondrial inner membrane potential, and ultimately to cell death. The initial increase in ROS is initiated through FA entry into the mitochondria and superoxide production. Despite FA causing a delayed increase in cytosolic ROS it does not appear to cause cell death. Finally, nicotinamide supplementation prevented the loss of mitochondrial fitness that was associated with FA exposure, suggesting that nicotinamide could provide protection against the ill effects of FA.

Figure 5. Fatty acids cause cell death after 24 hours of exposure

Preadipocytes were exposed to FA for 24 hours. Flow cytometry dot plots (A) and microscopy (B) analysis of Calcein-AM vs. Ethidium Homodimer 1 fluorescence demonstrates a shift in live cells (green) to dead cells (red) at 1000 μM FA concentrations. In addition to 1000 μM FA, 800 μM FA treated cells also had a significant increase in the percentage of dead cells at 24 hours, but not at 6 or 12 hours (C). Increases in the percentage of dead cells could be prevented by pretreatment with Etomoxir or MitoTempo followed by 1000 μM FA exposure, indicating that FA entry and superoxide and/or alkyl radical production was the cause of cell death (D). To test if the initial hour was important in preventing cell death, pretreatment or post-treated either 1 or 2 hours after FA exposure with Etomoxir and MitoTempo was performed (E). Post-treatment with either Etomoxir or MitoTempo restored the elevation in the percentage of cell death that was associated with 1000 μM FA. Percentage of dead cells and mean fluorescence is expressed as $\pm$ SD (n=three independent experiments for C, D and E). * $P \leq 0.05$ when compared to 600 μM BSA. + $P \leq 0.05$ when compared to 1000 μM FA.

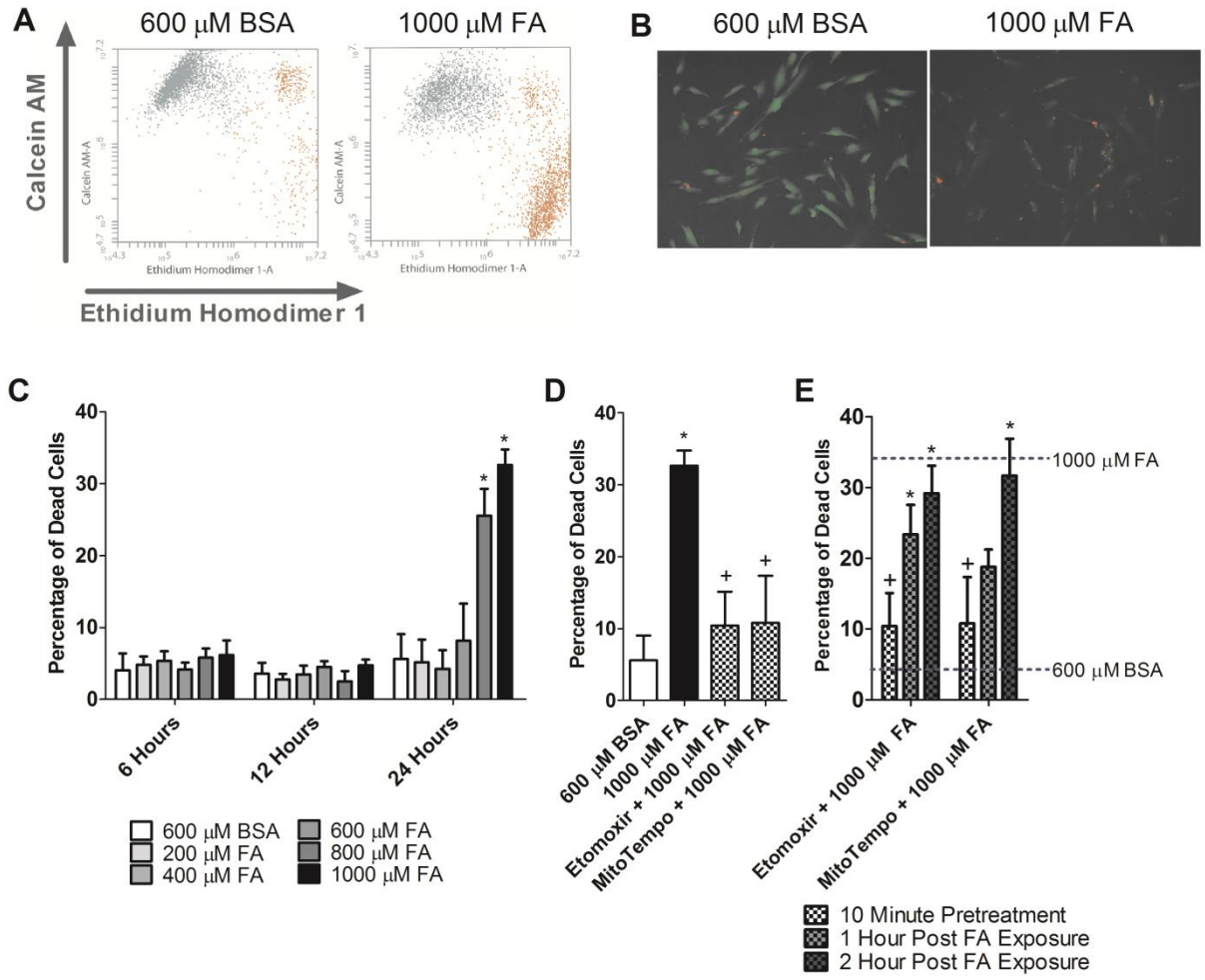
A
600 μM BSA
1000 μM FA
Calcein AM
Ethidium Homodimer 1
B
600 μM BSA
1000 μM FA
C
Percentage of Dead Cells
6 Hours
12 Hours
24 Hours
600 μM BSA
200 μM FA
400 μM FA
600 μM FA
800 μM FA
1000 μM FA
D
Percentage of Dead Cells
600 μM BSA
1000 μM FA
Etomoxir + 1000 μM FA
MitoTempo + 1000 μM FA
E
Percentage of Dead Cells
1000 μM FA
600 μM BSA
Etomoxir + 1000 μM FA
MitoTempo + 1000 μM FA
10 Minute Pretreatment
1 Hour Post FA Exposure
2 Hour Post FA Exposure

Figure 6. Fatty acids cause an increase in oxidative stress at 24, but not 3 and 12 hours

Preadipocytes were exposed to FA for 24, 12 and 3 hours. Flow cytometry histograms of the 24, 12 and 3 hour time point of CM-H_2DCFDA (A) or MitoSox Red (B) showed only increases in 1000 µM FA at 24 hours (Shaded Gray =Unstained, Solid Line=600 µM BSA and Dotted Line=1000 µM FA). Measurements of mean fluorescence at 24 hours across the FA concentration dose range show increases in CM-H_2DCFDA (C) or MitoSox Red (D) fluorescence when treated with 800 and 1000 µM FA. Pretreatment with either Etomoxir or MitoTempo followed by 1000 µM FA exposure prevented the increase in mean fluorescence of CM-H_2DCFDA (C) or MitoSox Red (D). Mean fluorescence is expressed as $\pm$ SD (n=three independent experiments for C and D). * $P \leq 0.05$ when compared to 600 µM BSA. + $P \leq 0.05$ when compared to 1000 µM FA.

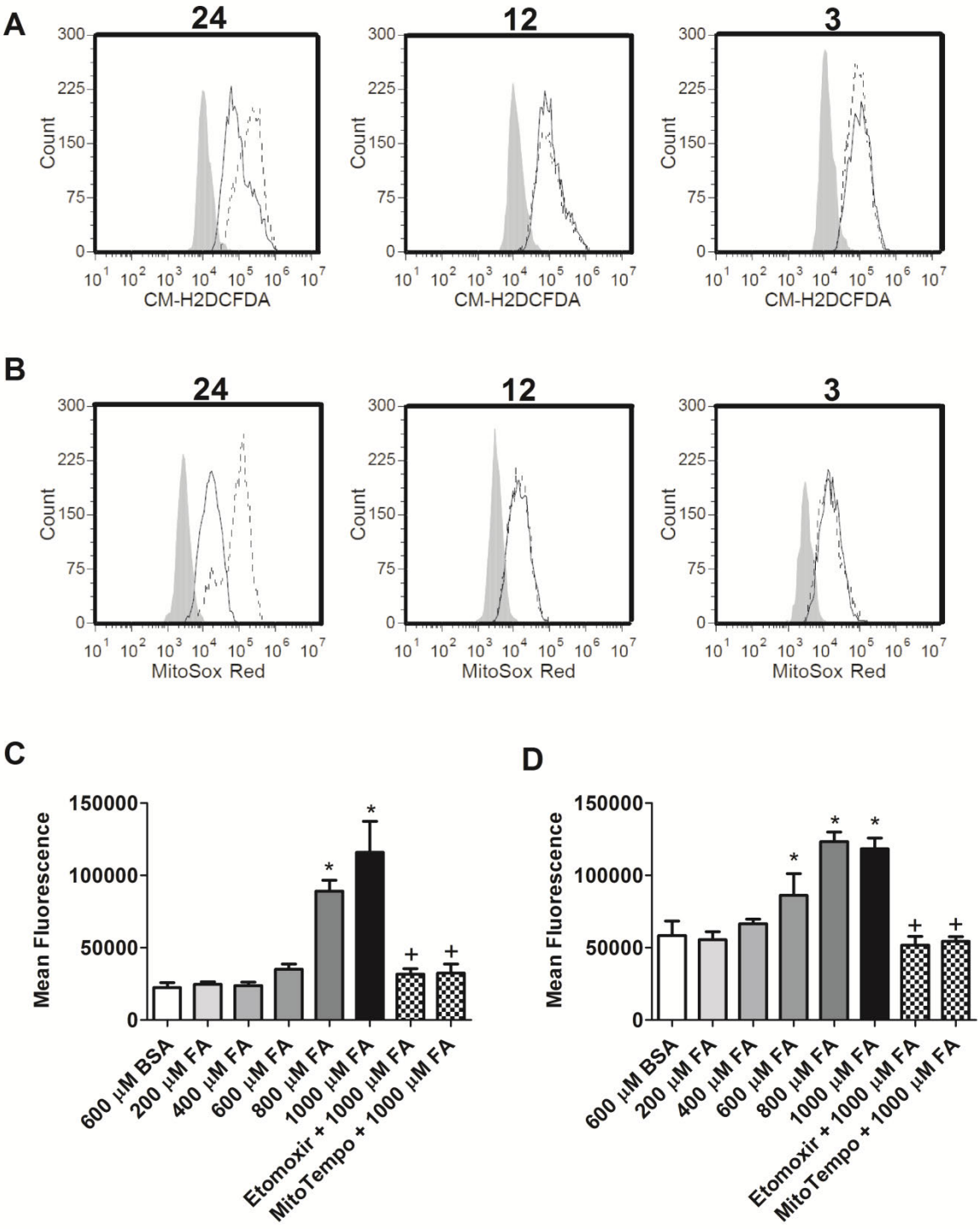
A
24
12
3
Count
CM-H2DCFDA
B
MitoSox Red
C
D
Mean Fluorescence
600 μM BSA
200 μM FA
400 μM FA
600 μM FA
800 μM FA
1000 μM FA
Etomoxir + 1000 μM FA
MitoTempo + 1000 μM FA

Figure 7. Fatty acids cause a transient increase in mitochondrial superoxide

Preadipocytes were preloaded with MitoSox Red and CRT flow cytometry was performed. After an initial baseline of 5 minutes with 600 µM BSA, FA were added and changes in MitoSox Red fluorescence was measured over time (A). At the end of 1 hour, the percent of cells with MitoSox Red fluorescence above baseline was counted (B). To determine the period at which increases in superoxide occur, preadipocytes were preloaded with MitoSox Red at different time points after the addition of FA. Transient increases in MitoSox Red fluorescence occurred within the first 60 minutes of FA exposure (C). The associated increase in MitoSox Red fluorescence was prevented by pretreatment with Etomoxir or MitoTempo (C). Arrows indicate the addition of FA. Percent of cells, AUC and mean fluorescence is expressed as $\pm$ SD (n=three independent experiments for B C D). * $P \leq 0.05$ when compared to 600 µM BSA. + $P \leq 0.05$ when compared to 1000 µM FA.

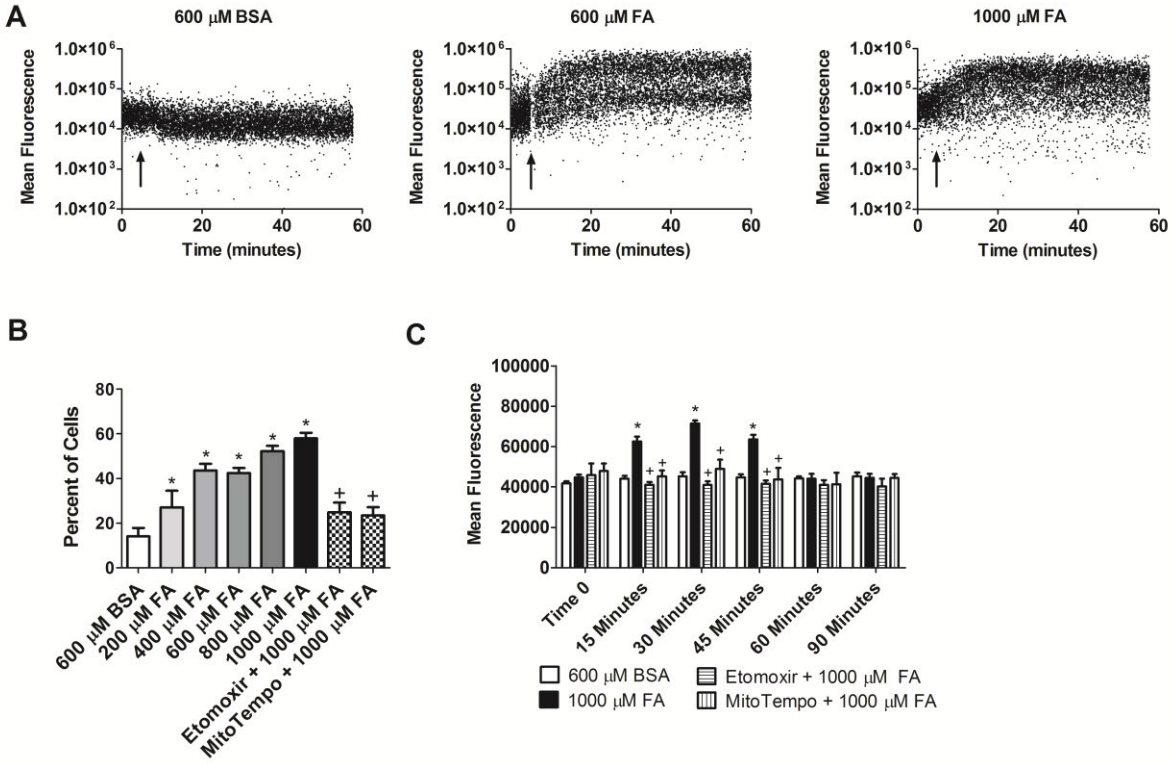
A
600 μM BSA
600 μM FA
1000 μM FA
Mean Fluorescence
Time (minutes)
B
Percent of Cells
600 μM BSA
200 μM FA
400 μM FA
600 μM FA
800 μM FA
1000 μM FA
Etomoxir + 1000 μM FA
MitoTempo + 1000 μM FA
C
Mean Fluorescence
Time 0
15 Minutes
30 Minutes
45 Minutes
60 Minutes
90 Minutes
600 μM BSA
1000 μM FA
Etomoxir + 1000 μM FA
MitoTempo + 1000 μM FA

Figure 8. Fatty acids cause a transient increase in mitochondrial H_2O_2 levels

Preadipocytes were transfected with the genetically encoded H_2O_2 sensor pHyPer Mito. Changes in pHyPer-Mito fluorescence upon exposure to 600 µM BSA(Black) or 1000 µM FA (Red) were measured over time using CRT flow cytometry and plotted in GraphPad Prism (A). Like changes in superoxide, analysis of mean fluorescence at a single time point revealed that increases in H_2O_2 occurred within 60 minutes (B), and could be prevented by pretreatment with Etomoxir or MitoTempo (B). Mean fluorescence is expressed as $\pm$ SD (n=three independent experiments for C and F). * $P \leq 0.05$ when compared to 600 µM BSA.

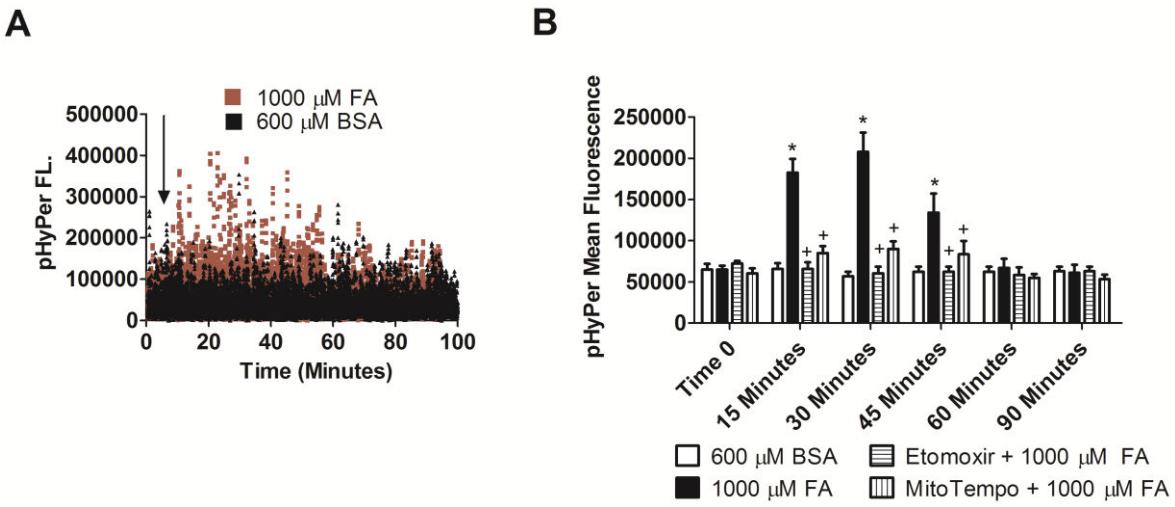
A
1000 μM FA
600 μM BSA
pHyPer FL.
500000
400000
300000
200000
100000
0
0
20
40
60
80
100
Time (Minutes)
B
pHyPer Mean Fluorescence
250000
200000
150000
100000
50000
0
Time 0
15 Minutes
30 Minutes
45 Minutes
60 Minutes
90 Minutes
600 μM BSA
1000 μM FA
Etomoxir + 1000 μM FA
MitoTempo + 1000 μM FA

Figure 9. Lipid peroxidation occurs within the first 3 hours of exposure to fatty acids

Preadipocytes were preloaded with MitoPerOx 30 minutes prior to performing CRT flow cytometry. MitoPerOx is a ratiometric dye that upon lipid peroxidation will shift its emission from 585/40 to 535/30 (A). Microscopy of preadipocytes treated with 600 µM BSA or 1000 µM FA for 1 hour shows an increase in emission of MitoPerOx with 1000 µM FA (B). To see if lipid peroxidation was occurring in a transient fashion, MitoPerOx fluorescence was measured at different intervals during the 150 minutes of FA exposure and revealed a statistically significant increase in MitoPerOx fluorescence (C) with 1000 µM FA, which could be prevented by pretreatment with MitoTempo or Carnosine (D). Like MitoSox Red and CM-H_2DCFDA, no change in the ratio of 530/585 was observed after 3 hours of FA exposure, suggesting that lipid peroxidation, like superoxide and H_2O_2 is transient. AUC and mean fluorescence is expressed as $\pm$ SD (n=three independent experiments for C and D). * $P \leq 0.05$ when compared to 600 µM BSA. + $P \leq 0.05$ when compared to 1000 µM FA.

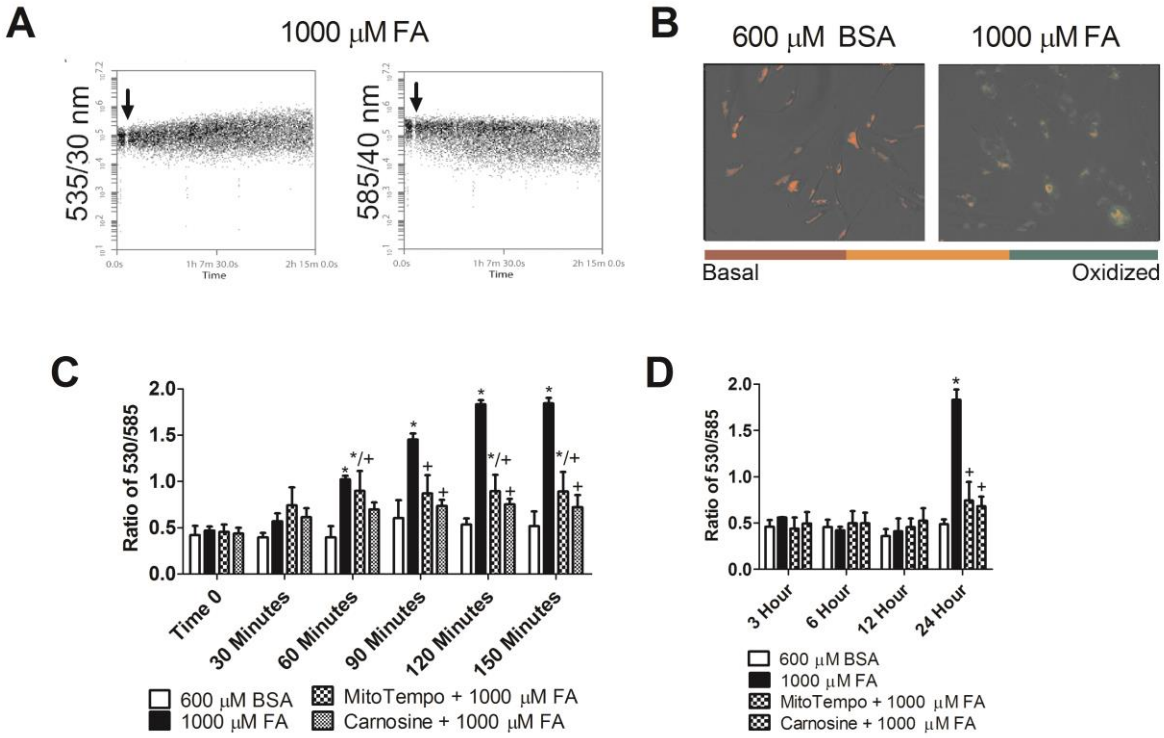
A
1000 μM FA
535/30 nm
585/40 nm
Time
B
600 μM BSA
1000 μM FA
Basal
Oxidized
C
Ratio of 530/585
Time 0
30 Minutes
60 Minutes
90 Minutes
120 Minutes
150 Minutes
600 μM BSA
1000 μM FA
MitoTempo + 1000 μM FA
Carnosine + 1000 μM FA
D
Ratio of 530/585
3 Hour
6 Hour
12 Hour
24 Hour
600 μM BSA
1000 μM FA
MitoTempo + 1000 μM FA
Carnosine + 1000 μM FA

Figure 10. Exposure to fatty acids cause an increase in mitochondrial crisis through loss of respiration, inner mitochondrial membrane potential, ATP, NAD^+ and NADH and opening of the mitochondrial permeability transition pore

Preadipocytes exposed to FA have a decrease in OCR over the course of 20 hours (A). Inner mitochondrial membrane potential as assessed by TMRE fluorescence revealed a decrease in the mean fluorescence after 24 hours, but not at 3 and 12 hours following FA exposure (B). Along with a decrease in OCR, ATP (C) and NAD^+ + NADH (D) levels were also decreased when exposed to 1000 µM FA over the course of 20 hours. Preadipocytes also had an increase in the percentage of cells with low Calcein AM fluorescence at 12 and 24 hours of FA exposure, suggesting that opening of the mPTP was occurring. Pretreatment with Etomoxir or MitoTempo followed by 1000 µM FA exposure prevented the loss of OCR (F), inner mitochondrial membrane potential (G), ATP (H), NAD^+ + NADH (I) and mPTP opening (J). (For A, C and D: Black=600 µM BSA, Green=200 µM, Dark Green=400 µM FA, Orange=600 µM FA, Red=800 µM FA, Dark Red=1000 µM FA). Time course experiments and 24 hour measurements are expressed as $\pm$ SD (n=three independent experiments for A, B, C, D, E, F, G, H, I and J). * $P \leq 0.05$ when compared to 600 µM BSA. + $P \leq 0.05$ when compared to 1000 µM FA.

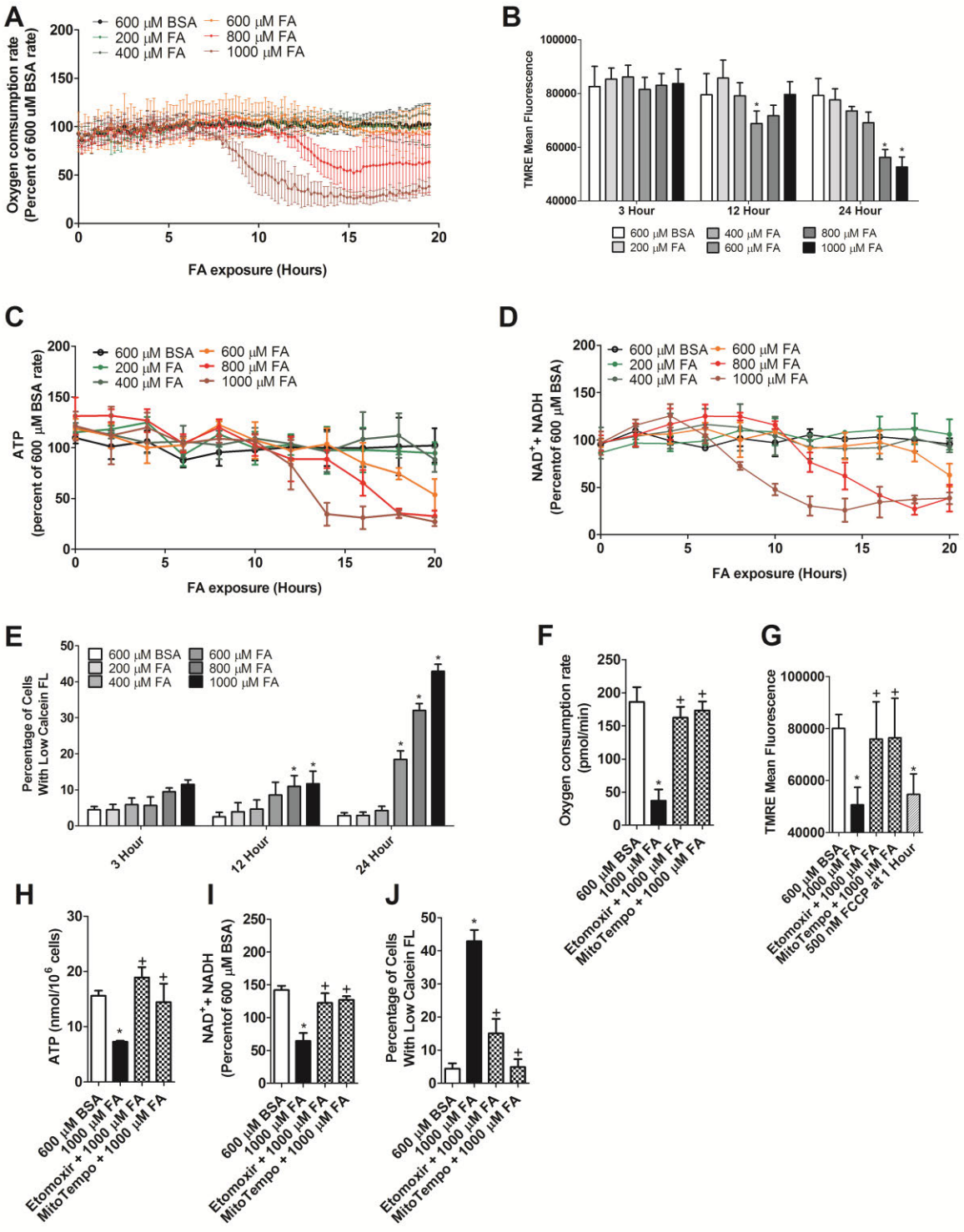
A
600 μM BSA
200 μM FA
400 μM FA
600 μM FA
800 μM FA
1000 μM FA
Oxygen consumption rate (Percent of 600 uM BSA rate)
FA exposure (Hours)
B
TMRE Mean Fluorescence
3 Hour
12 Hour
24 Hour
C
ATP (percent of 600 μM BSA rate)
FA exposure (Hours)
D
NAD+ + NADH (Percentof 600 μM BSA)
FA exposure (Hours)
E
Percentage of Cells With Low Calcein FL
F
Oxygen consumption rate (pmol/min)
G
TMRE Mean Fluorescence
600 μM BSA
1000 μM FA
Etomoxir + 1000 μM FA
MitoTempo + 1000 μM FA
500 nM FCCP at 1 Hour
H
ATP (nmol/10^6 cells)
I
NAD+ + NADH (Percentof 600 μM BSA)
J
Percentage of Cells With Low Calcein FL

Figure 11. Nicotinamide supplementation prevents the loss of mitochondrial fitness, oxidative stress and cell death associated with fatty acids at 24 hours

Preadipocytes were supplemented with 40 µM nicotinamide for 30 minutes prior to FA exposure. Nicotinamide pretreatment followed by 1000 µM FA, prevented the loss of OCR (A) inner mitochondrial membrane potential (B), ATP (C), NAD^+ and NADH (D) and mPTP opening (E). Nicotinamide pretreatment also prevented the increase in CM-H_2DCFDA (F) and MitoSox Red (G) fluorescence, as well as cell death (H) at 24 hours. Since loss of NAD^+ and NADH can occur through opening of the mPTP cells were pretreated with cyclosporin A and a decrease in mPTP opening was observed (I). Despite preventing the opening of the mPTP, cyclosporin A did not prevent the loss of NAD^+ and NADH that was associated with 1000 µM FA exposure (J). OCR, mean fluorescence, ATP, NAD^+ + NADH and percentage of cells is expressed as $\pm$ SD (n=three independent experiments for A, B, C, D, E, F, G, H, I and J). * $P \leq 0.05$ when compared to 600 µM BSA. + $P \leq 0.05$ when compared to 1000 µM FA.

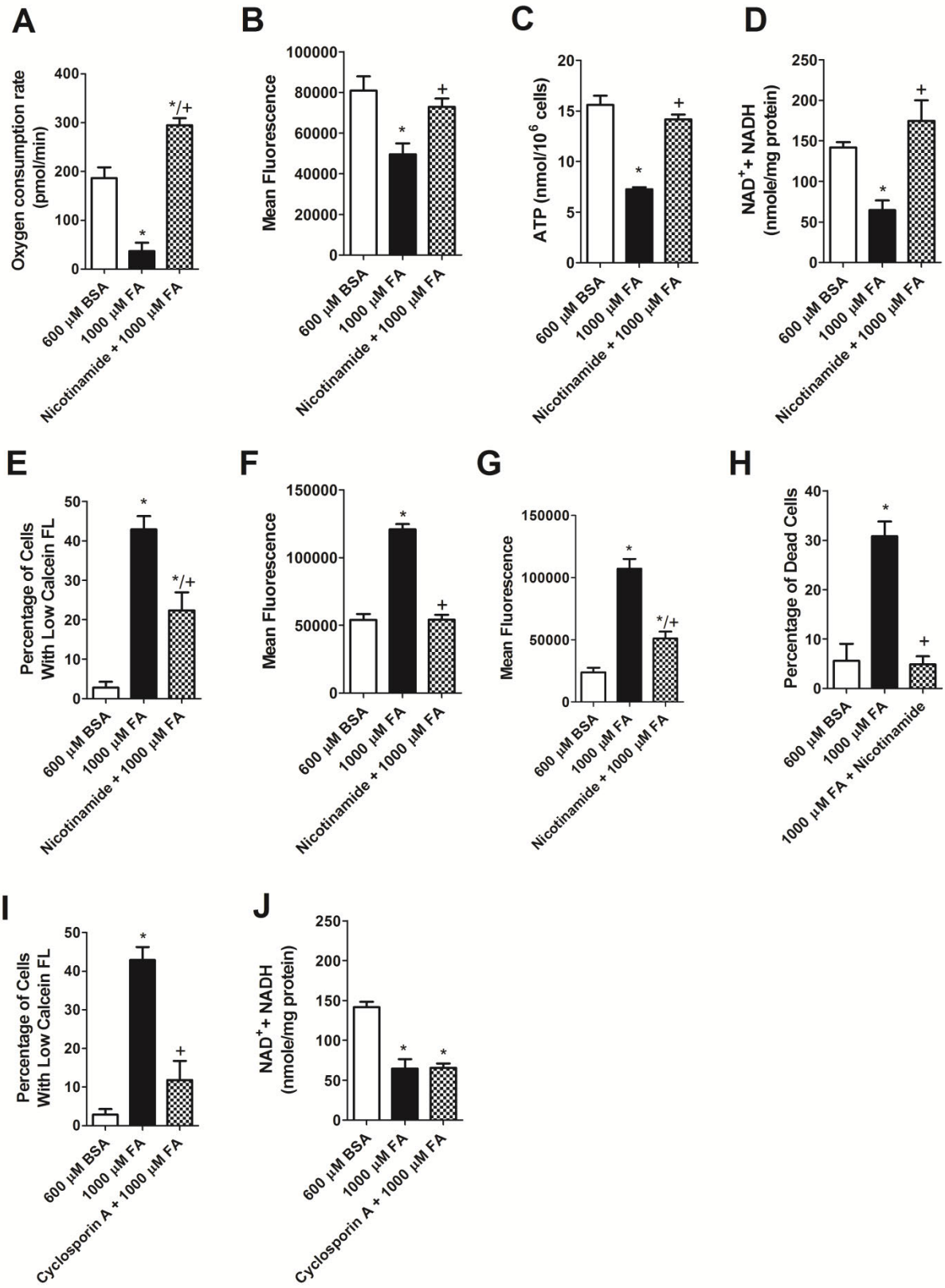
A
Oxygen consumption rate (pmol/min)
400
300
200
100
0
*
*/+
600 μM BSA
1000 μM FA
Nicotinamide + 1000 μM FA
B
Mean Fluorescence
100000
80000
60000
40000
20000
0
*
+
600 μM BSA
1000 μM FA
Nicotinamide + 1000 μM FA
C
ATP (nmol/10^6 cells)
20
15
10
5
0
*
+
600 μM BSA
1000 μM FA
Nicotinamide + 1000 μM FA
D
NAD+ + NADH (nmole/mg protein)
250
200
150
100
50
0
*
+
600 μM BSA
1000 μM FA
Nicotinamide + 1000 μM FA
E
Percentage of Cells With Low Calcein FL
50
40
30
20
10
0
*
*/+
600 μM BSA
1000 μM FA
Nicotinamide + 1000 μM FA
F
Mean Fluorescence
150000
100000
50000
0
*
+
600 μM BSA
1000 μM FA
Nicotinamide + 1000 μM FA
G
Mean Fluorescence
150000
100000
50000
*
*/+
600 μM BSA
1000 μM FA
Nicotinamide + 1000 μM FA
H
Percentage of Dead Cells
40
30
20
10
0
*
+
600 μM BSA
1000 μM FA
1000 μM FA + Nicotinamide
I
Percentage of Cells With Low Calcein FL
50
40
30
20
10
0
*
+
600 μM BSA
1000 μM FA
Cyclosporin A + 1000 μM FA
J
NAD+ + NADH (nmole/mg protein)
250
200
150
100
50
0
*
*
600 μM BSA
1000 μM FA
Cyclosporin A + 1000 μM FA

CHAPTER 5: SIRTUIN-1 ACTIVITY-DEPENDENT ANTIOXIDANT GENE EXPRESSION IN SUBCUTANEOUS ADIPOSE TISSUE CORRELATES TO INSULIN SENSITIVITY IN OBESE INDIVIDUALS

Carlyle Rogers, Barbara Davis and Jacques Robidoux

[1]Department of Pharmacology and Toxicology and [2]The East Carolina Diabetes and Obesity Institute, East Carolina University, Greenville, North Carolina.

Abstract

Adipose tissue dysfunction has been implicated as a major risk factor in the development of obesity-associated metabolic abnormalities such as systemic insulin resistance. One hypothesis as to why adipose tissue failure occurs is the inability of cells within adipose tissue to adapt and survive in an obesogenic environment. One mechanism that may explain why adipose tissue failure occurs is that the mitochondria are unable to sustain the reducing pressure of chronic nutrient energy imbalance. Therefore, the gene expression of antioxidant proteins, with an emphasis on mitochondrion-located enzymes, was measured from adipose tissue collected from thirty-two women covering a wide range of body mass indices and insulin sensitivity. Of the antioxidant genes measured, the expression of superoxide dismutase 2 (SOD2), peroxiredoxin 3 (PRDX3), thioredoxin reductase 2 (TXNRD2) and glutathione peroxidase 1 (GPX1) was lower in insulin-resistant obese individuals. Additionally, antioxidant gene expression and insulin sensitivity correlated positively with expression of the deacetylase sirtuin 1 (SIRT1), and the nuclear transcription factor forkhead member of the class O 1 (FOXO1), which could serve as part of the signaling pathway that links changes in nutrient availability, including fatty acids (FA), to antioxidant gene expression. In preadipocyte culture, FA exposure caused an increase in deacetylation of FOXO1 that was dependent on the formation of

mitochondrial superoxide or alkyl radicals. Furthermore, the expression of dominant negative SIRT1 and FOXO1 caused an exaggeration in FA-induced cell death. All together, these findings suggest that lower expression of SIRT1-FOXO1-regulated antioxidant gene expression is linked to insulin resistance and preadipocyte susceptibility to FA.

Introduction

Obesity has long been known to be an inherent risk factor for metabolic syndrome, diabetes and cardiovascular disease, with many of the associated metabolic changes being linked to the progression of insulin resistance and hyperinsulinemia (P. J. Anderson et al., 1997; Baik et al., 2000; McLaughlin, Abbasi, Lamendola, & Reaven, 2007). Despite the inherent risk of obesity, several studies have identified a subset of obese individuals, who despite an elevated body mass index (kg/m^2), remain relatively free from the perils of insulin resistance (Karelis et al., 2005; Klöting et al., 2010; Stefan et al., 2008). In the literature this subgroup of obese individuals has been identified as insulin-sensitive obese (ISO), and in addition to having normal glucose and insulin levels, present with lower plasma triglycerides, higher HDL cholesterol, and lower pro-inflammatory markers than insulin-resistant obese (IRO) and Type 2 Diabetic (T2DM) individuals (Brochu et al., 2001; Klöting et al., 2010). Despite a preponderance of evidence for improvements in physiological parameters, the exact mechanism that safeguards ISO individuals against obesity-related metabolic complications is unclear.

Although obesity can be classified as a necessary expansion of the body's adipose tissue to store an overabundance of calories, if caloric intake outpaces adipose tissue expansion an increase in the level of circulating non-esterified fatty acids (NEFA) can occur (Frayn, 2002; J. Smith et al., 2006). Consequently, an elevation of NEFA has been suggested as a risk factor for

ectopic fat accumulation and deterioration of glucose tolerance (Boden, 2008; Charles et al., 1997). Despite the recognized risk of NEFA on non-adipose tissue, the impact of elevated NEFA within adipose tissue has been overlooked since adipocytes possess the capability to increase the esterification rate of FA. In the context of obesity, however, the capacity of adipocytes to store FA may actually be lower (since it was found that a population of adipocytes that are slightly larger in size than preadipocytes but smaller than mature adipocytes are unable to store triacylglycerol) (McLaughlin, Sherman, et al., 2007). If the ability of adipocytes to esterify FA is reduced, then elimination of FA by oxidation may serve as the only protective mechanism against elevated circulating NEFA.

For adipocytes, and other cell types within adipose tissue such as preadipocytes and macrophages, FA oxidation serves to increase levels of NADH and $FADH_2$ for the synthesis of ATP (GM, 2000). In the absence of a concomitant increase in ATP demand, the likelihood of one-electron reduction of oxygen to form superoxide is increased (P Schönfeld & L Wojtczak, 2008). If superoxide or its byproduct (such as H_2O_2) is elevated above the antioxidant buffering capacity of the cell, formation of toxic by-products such as hydroxyl radicals and lipid peroxides can occur, leading to damage of mitochondrial components (Girotti, 1998; Murphy, 2009). Therefore, up-regulation of mitochondrial antioxidant genes may serve to protect against the elevation in ROS brought about by increased FA oxidation.

The purpose of the present scientific study was to investigate whether gene regulation associated with mitochondrial ROS detoxification differs in subcutaneous adipose tissue from insulin-sensitive non-obese (ISNO), ISO, IRO and T2DM individuals.

Materials and Methods

Subjects

All 32 subjects were women from eastern North Carolina, recruited through participating physicians performing abdominal surgery at Vidant Medical Center, and all subjects had given informed written consent. Subjects for this study were previously used in Rogers et al. to compare EGF Receptor (ERBB1) abundance in adipose tissue to markers of adipogenesis and proliferation (Rogers et al., 2012a). Their ages ranged from 25 to 61 years and their body mass indices (BMI) ranged from 20.7 to 54.7 kg/ m2. The protocol was approved by the East Carolina University Institutional Review Board (Appendix 1). All subjects were undergoing hysterectomies and were not taking drugs that could affect lipid or glucose homeostasis. BMI was calculated from body mass and height recorded at the time of surgery to the nearest 0.5 kg and centimeter, respectively. Fasting glucose was quantified from blood collected the day of the surgery using the 2300 Stat Plus System (Yellow Springs Instruments, Inc., Yellow Springs, OH). Insulin was quantified using the Beckman-Coulter Access Immunoassay System (Beckman-Coulter, Fullerton, CA). Abdominal subcutaneous adipose tissue (outside the fascia superficialis) was chosen because it constitutes the primary site of fatty acid storage and release, and hence would likely be a location where turnover is critical to maintaining fatty acid homeostasis (Koutsari & Jensen, 2006). The tissue was immediately frozen in liquid nitrogen, transported to the laboratory, and stored at -80^0 C. For comparison purposes, the subjects were subdivided into four groups: the insulin-sensitive lean (ISNO) [BMI_30 kg/m^2, homeostasis model of assessment for insulin resistance (HOMA-IR) _2.6 (actual highest value was 1.7), fasting insulin 10 _IU/ml, and fasting glucose_110 mg/dL]; the insulin-sensitive obese (ISO) (BMI_30 kg/m^2, HOMA-IR _2.6, fasting insulin _10 _IU/mLl, and fasting glucose _110 mg/dl);

the insulin-resistant obese (IRO) [BMI _30 kg/m^2, HOMA-IR _2.6 (actual lowest value was 3.0), fasting insulin _10_IU/mL, and fasting glucose_126 mg/dL], and the T2DM (fasting glucose ≥126 mg/dL on two occasions). The HOMA-IR cutoff of 2.6 was determined from our data bank of 38 lean individuals with normal glucose tolerance based on the commonly used 75th percentile, and it is in line with previously reported cutoffs (Ascaso et al., 2003). For some comparisons, the subjects from the first and fourth quartiles were compared with respect to insulin sensitivity, regardless of their body weight. Analysis of data from 81 subjects for which there were both HOMA-IR and iv glucose tolerance tests, minimal model values established that the first and last quartiles of HOMA have a sensitivity of 0.9 to identify subjects belonging to the last and first tertiles of SI, respectively. These are more stringent HOMA-IR cutoffs than the above-described insulin-sensitive and insulin-resistant cutoffs. For other comparisons, we compared the subjects from the first and fourth quartiles with respect to SIRT1 and FOXO1 protein levels.

Cell Culture

XA15A1 human preadipocytes (Lonza Walkersville, Inc., Walkersville, MD) were cultured as described in Skurk et al.,(Skurk et al., 2007) using Dulbecco's modified Eagle's medium: F12 (DMEM:F12; Mediatech, Manassas, VA) with 10% calf serum, 15 mM glucose, 33 µM biotin, 17 µM D-pantothenate, 100 nM insulin, and 10 nM hydrocortisone (all from Sigma Aldrich), 1 nM epidermal growth factor and 1 nM basic fibroblast growth factor (Gemini, West Sacrameto, CA). This medium also contained 50 IU/ml penicillin, 50 µg/ml of streptomycin and 2.5 µg/ml amphotericin B (Mediatech). The XA15A1 cells were propagated at 33 C. When the cells reached 80% confluence, growth factors were omitted from the media and the cells were placed at 37 C for at least 24 hours prior to the experiment. The XA15A1 cells

express a temperature-sensitive mutant of the SV 40 Large T-antigen (u19tsA58) and needs to be incubated at 37 C for 24 hours to revert to a phenotype that resembles that of primary cells and are able to differentiate. For experiments, the cells were transfected with plasmids coding for SIRT1 or FOXO1 dominant negative (DN) mutants obtained through the AddGene repository (Herscovitch et al., 2012; J. Nakae et al., 2000; Vaziri et al., 2001). The Sirt1 DN mutation causes an alteration of the catalytic site and leads to a loss in deacetylation activity (Vaziri et al., 2001). The Foxo1 DN mutant contains a deletion that truncates the transactivation domain (J. Nakae et al., 2000). Both the Sirt1 DN and Foxo1 DN plasmid encode for the puromycin resistance gene, for the selection of stably transfected cells. The two types of transfection were performed identically. Briefly, 5 x 10^6 cells were transfected in a 100 µL final volume of the nucleofection solution V containing 1µg of plasmid DNA and the application of the T-030 program from the Amaxa Nucleofactor 2b electroporator (Lonza Walkersville) list. For experiments using stably transfected cells, 10 ug/mL puromycin was added to the medium after 24 hours to select for cells that stably integrated the Puromycin resistance gene. The cells were used 4 to 6 passages later.

Preparation of Fatty Acids

A 50 mM stock of each single fatty acid was prepared in 0.1 M NaOH. Each fatty acid stock was added to Dulbecco's modified Eagle's medium: F12 (DMEM:F12) containing 600 µM BSA, 5% calf serum, 10 mM glucose, 33 µM biotin, 17 µM D-pantothenate, containing 50 IU/ml penicillin, 50 µg/ml of streptomycin, and 2.5 µg/ml amphotericin B to reach a mixture consisting of 40% oleate, 25% palmitate, 20% linoleate, and 15% stearate. Each concentration was pre-equilibrated for one hour with 600 µM BSA at 37^0C. For all experiments, cells were incubated in 600 µM BSA for at least 2 hours prior to the addition of the drugs or fatty acids (FA). To start

the experiment FA mixtures were added to the 600 µM BSA at a 2x concentration to equal a final FA concentration of 1x.

RNA Isolation, Reverse Transcription, and Quantitative Real-Time PCR

RNA was isolated from frozen adipose tissue samples or from cell culture samples after various treatments. Pieces of frozen adipose tissue of approximately 100 mg were allowed to unfreeze in 1 mL of RNA later ICE (Applied Biosystems, Foster City, CA). These pieces were homogenized and RNA isolated using the TriReagent procedure as described by the supplier (Sigma Aldrich). TriReagent was used, as well, for the cell culture experiments. First-strand cDNA was synthesized from 5 µg total RNA with the High-Capacity cDNA Reverse Transcription Kit (Applied Biosystems). Relative real-time TaqMan PCR was performed with primers and 6-carboxyfluorescein dye-labeled TaqMan probes (Applied Biosystems). Glyceraldehyde-3-phosphate dehydrogenase (GAPDH) was used as an endogenous control because it was found to be the most stable when compared to HPRT and POLII. Each reaction contained 5 ng cDNA from total RNA, in a total reaction volume of 10 µl. To prevent bias toward a specific group, the relative expression was determined by the comparative threshold method (Δct) using all samples as reference.

Cell Death

Cell death was measured by Calcein AM and Ethidium Homodimer-1 (Life Technologies, Grand Island, NY). Calcein AM is a live cell dye that accumulates in intact cells where it acquires a strong green fluorescence upon cleavage by intracellular esterases (Papadopoulos et al., 1994). Because intracellular esterase activity is quickly lost as cells die, little to no gain in fluorescence occurs in dead or dying cells. Ethidium Homodimer-1 is a dye

that enters the damaged plasma membrane and interacts with nucleic acids. As Ethidium Homodimer-1 interacts with nucleic acids the red fluorescence of the dye increases by 40 Fold, indicating dying or dead cells (Papadopoulos et al., 1994). At the end of the 6, 12 or 24 hour FA incubation periods, cells were collected and incubated for 15 minutes at room temperature in DPBS containing Calcein AM and Ethidium Homodimer 1 at a final concentration of 0.05 µM and 4 µM. To detect Calcein AM fluorescence an excitation wavelength of 488 and a 530± 30 nm emission filter was used. Ethidium Homodimer 1 fluorescence was detected using an excitation wavelength of 488 and a 675 ± 25 emission filter. After subtraction of auto-fluorescence, the live cell region was determined by examining an untreated sample and a sample containing only 600 µM BSA. Dead cells were determined by treating a control sample with 0.01% Triton-X for 15 minutes. All values for cell death represent the percent of dead cells found in the gated region of the cell population of interest.

Measurement of the Ratio of Acetylated versus Total FOXO1 Proteins

Following treatment with FA, $1.0x10^6$ cells were collected, fixed in 5% formaldehyde and permeabilized in 100% methanol. The non-specific binding of antibody on cells was blocked by incubating the cells for 60 minutes in an incubation buffer consisting of PBS containing 0.5 % BSA. After blocking, primary antibodies directed against total FOXO1 (sc-9808; Santa Cruz Biotechnology, Dallas, TX) or Ac-FOXO1 (sc-49437, Santa Cruz) were added at a 1:100 dilution ratio in the incubation buffer. Cells were washed once and incubated with a 1:1000 dilution of anti-goat IgG (H+L) Alexa Fluor 568 (A11057; Life technologies) and a 1:1000 dilution of anti-rabbit IgG (H+L) Alexa Fluor 488 (4412; Cell Signaling Technology) for 30 minutes to reveal the total and acetylated FOXO1 antibody, respectively. Alexa Fluor 488 has an excitation of 488 nm and an emission of 520 nm. Alexa Fluor 568 has an excitation of 568 nm

and an emission of 600 nm. After 30 minutes, cells were washed twice and suspended in 300 µL of PBS and analyzed on a flow cytometer. Auto fluorescence and nonspecific staining were determined by using either normal anti-rabbit IgG (Sc-2027; Santa Cruz) or normal anti-goat IgG (Sc-2028; Santa Cruz Biotechnology) as isotype controls, after gating on the live cell population. Gates were applied to each histogram that corresponded to either the 530 ±30 nm band pass filter or the 585 ±40 nm band pass filter. Mean fluorescence intensity (MFI) for each histogram was determined after gating. The ratio of Ac-Foxo MFI to Total-Foxo2 MFI was calculated and plotted using GraphPad Prism.

Statistical analysis

Statistical analysis was performed with PRISM (GraphPad Software, San Diego, CA) version 5.00 for Windows. Differences between ISL, ISNO, IRO and T2DM individuals were assessed by a one-way ANOVA, followed by Tukey's multiple comparison tests. Differences between the first and last quartiles of insulin sensitivity or gene expression were assessed using a two-tailed unpaired Student's T test. For in-vitro studies, differences between FA concentrations, 600 µM BSA and/or pretreatment with MitoTempo or Ex527 were assessed by a one-way ANOVA with a Tukey's multiple comparison test. All values are reported as $\pm$ SD. In all cases, a *P* value of less that 0.05 was used to indicate statistical significance between conditions.

Results

Subject Characteristics

Although previous studies have treated obese individuals as a homogenous population, not all obese individuals respond negatively to an obesogenic environment (Klöting et al., 2010; Samocha-Bonet, Chisholm, Tonks, Campbell, & Greenfield, 2012). Depending on where an individual's insulin sensitivity falls on the obesity continuum can dramatically influence his or her risk for developing metabolic and cardiovascular diseases (Klöting et al., 2010; Samocha-Bonet et al., 2012). Since protection or adaptation to an obesogenic environment should determine which extreme an individual is closer to, individuals belonging to the groups of ISNO (insulin-sensitive non-obese), ISO, IRO and T2DM were compared (Rogers et al., 2012b). Table 1 shows the basal characteristics of subjects following a 12-hour overnight fast. Plasma glucose levels were statistically increased in T2DM when compared to ISNO, ISO and IRO patients. Insulin levels were significantly increased in both IRO and T2DM when compared to ISNO, but not different between IRO and ISO individuals. Comparisons between ISNO and ISO showed no difference in HOMA-IR values, but there was a significant increase in the HOMA-IR value in both the IRO and T2DM group when compared to ISNO and ISO.

Antioxidant enzyme gene expression in adipose tissue correlates with insulin level and insulin sensitivity

Since chronic positive energy imbalance should put undue reducing pressure on the ETC and lead to exaggerated mitochondrial ROS production in all tissues including adipose tissue, we tested the hypothesis that ISO individuals maintain their adipose tissue metabolic fitness through higher antioxidant gene expression, while IRO individuals fail to maintain metabolic fitness due

to lower antioxidant gene expression. The expression level of antioxidant genes was evaluated by real-time PCR performed on cDNA obtained from RNA extracted from the subcutaneous adipose tissue of women of various ages, BMI, and insulin sensitivities. Figure 12A, C, E, G, I, and K shows the expression of six antioxidant genes in ISNO, ISO, IRO as well as in T2DM subjects. Figure 12 B, D, F, H, J, and L show the expression of these same genes in insulin-sensitive (ISI) and insulin-resistant (IRI) individuals irrespective of their weight. The characteristics of the subjects, classified as being ISI or IRI using the relatively stringent first and last quartiles of HOMA-IR as cut-offs are described in table 2. As show in figure 12 A and B, the expression of superoxide dismutase (SOD2) was lower in IRO than ISO individuals, and was decreased in IRI compared to ISI. Figure 12 C shows that the expression of catalase (CAT), the only non-mitochondrial protein of the list, was reduced in IRO and T2DM compared to ISO. However, no statistical difference was observed when comparing the upper and lower quartile of insulin sensitivity (Figure 12D). Peroxiredoxin 3 (PRDX3) expression correlated with HOMA-IR (r=-0.37, p=0.03),insulin (r=-0.38, p=0.03) and was lower in IRI compared to ISI (Figure 12F), (figure 12E). Thioredoxin reductase 2 (TXNRD2) expression, on the other hand, was lower in IRO and T2DM subjects (figure 12G) and lower in IRI compared to ISI (Figure 12H). Glutathione peroxidase 1 (GPX1) expression was was lower in IRI compared to ISI (figure 12J). Glutathione reductase (GSR) expression did not vary between any groups (Figure 12 K and L).

SIRT1 and FOXO1 gene expression correlate to insulin sensitivity and too some extent antioxidant gene expression

Although the cell, and in particular the mitochondrion, has several mechanisms that can buffer elevations in the level of ROS, the ability to resist repeated elevations of ROS requires an increase in the transcription of genes that can buffer ROS (Ikeuchi et al., 2005; Piantadosi &

Suliman, 2006; Sano & Fukuda, 2008). Therefore, finding the nuclear transcription factor(s) that regulate the transcription of antioxidant detoxification genes that correlated to insulin sensitivity was investigated. Although a plethora of factors have been shown to be part of the ROS hormetic stress response, the four genes we found in our study to be correlated with insulin sensitivity, SOD2, PRDX3, TXNRD2 and GPX1, are FOXO-regulated genes that contain a FOXO-binding element (FRE) (Biggs, Meisenhelder, Hunter, Cavenee, & Arden, 1999; Furuyama et al., 2000). Members of the forkhead member of the class O (FOXO) family of transcription factors have been shown to be recruited to the nucleus under oxidative stress conditions, and consequently favor the transcription of antioxidant genes after being deacetylated by the NAD+-dependent deacetylase sirtuins 1 (SIRT1) (Brunet et al., 2004; Kops et al., 2002; Nemoto & Finkel, 2002). Therefore, the prototypical stress response of SIRT1-FOXO1/3 could serve as one potential mechanism that links mitochondrial redox changes to transcription of antioxidant genes.

To test this hypothesis SIRT1 or FOXO1 mRNA expression was compared between ISNO, ISO, IRO or T2DM individuals. SIRT1 mRNA expression was significantly decreased in T2DM when compared to ISNO and IRO (Figure 13A) and was lower in IRI compared to ISI (Figure 13B). However, FOXO1 mRNA expression showed no significant difference between the ISNO, ISO, IRO and T2DM groups (Figure 13C). Nevertheless, FOXO1 mRNA expression was lower in IRI compared to ISI (Figure 13 D).

To investigate whether high or low SIRT1 or FOXO1 expression correlates to antioxidant gene expression, samples were separated into quartiles of low (first quartile) and high (last quartile) of SIRT1 or FOXO1 expression. The characteristics of the subjects from the first and last quartile of SIRT1 expression are described in Table 3. As found in Table 3, glucose, insulin,

and HOMA-IR values were higher in the lower quartile of SIRT1 expression. Similarly, the characteristics of the subjects from the first and last quartile of FOXO1 expression are described in Table 4. This table shows that only the HOMA-IR values were correlated with FOXO1 expression. As shown in Figure 14, individuals belonging to the high SIRT1 expression quartile also had a high SOD2, CAT, PRDX3, TXNRD2, GPX1 and FOXO1expression (Figure 14 A, B, C, D, E and G) compared to individuals from the low SIRT1 quartile. However, as shown in Figure 14F, no statically significant difference was found in GSR expression between the low and high SIRT1 expression quartiles. Like individuals from the upper quartile of SIRT1 expression, individuals from the upper FOXO1 quartile had an increase in SOD2, PRDX3 and GPX1 expression (Figure 15A, C and E). No difference in expression was found between CAT, TXNRD2 or SIRT1 (Figure 15B, D and G) when comparing the low and high FOXO1 quartile. Individuals belonging to the high FOXO1 expression quartile also had a surprising decrease in GSR expression (Figure 15F), compared to the low FOXO1 expression quartile.

Exposure to fatty acids in human preadipocytes cause an increase in deacetylation of FOXO1

After observing a positive correlation in the expression of SOD2, PRDX3 and GPX1 in the high expression quartile of SIRT1 and FOXO1, the ability of a mixture of fatty acids (FA) to stimulate the prototypical SIRT1-FOXO1 stress response in human preadipocytes was investigated. Preadipocytes were chosen because 1) protection of preadipocytes against lipotoxic insults is important in preserving adipose tissue turnover and function, 2) preadipocytes do not possess a high capacity to esterify FA, and therefore would be more susceptible to byproducts of mitochondrial FA oxidation, and 3) preadipocytes are found in locations near mature adipocytes leading to a constant exposure of FA (Carrière, Fernandez, Rigoulet, Pénicaud, & Casteilla, 2003; Frayn, 2002; Tchoukalova et al., 2007). To characterize what FA concentration may affect

the SIRT1-FOXO1 pathway, preadipocytes were treated with a mixture of FA in a FA to albumin ratio and concentration range that reflects the physiological relevant adipose tissue environment and evaluated for changes in the deacetylation of FOXO1 (Mittendorfer et al., 2003; Tahiri et al., 2007).

Preadipocytes were treated for 1, 2, 6, 12 or 24 hours with FA. Following FA treatment total protein level of FOXO1 (T-FOXO1) or acetylated FOXO1 (Ac-FOXO1) was measured. The ratio of Ac-FOXO1 to T-FOXO1 mean fluorescence intensity was shown to be significantly decreased at 6, 12 and 24 hours in 600 µM, 800 µM, and 1000 µM FA compared to 600 µM BSA indicating an increase in deacetylation was occurring (Figure 16A). To determine if the increase in FOXO1 deacetylation was occurring due to FA production of mitochondrial ROS, cells were pretreated with MitoTempo, a mitochondrial targeted superoxide and alkyl radical scavenger for 10 minutes followed by FA exposure. Compared to 600 µM BSA, when preadipocytes were pretreated with MitoTempo, no significant change in the ratio of Ac-FOXO1 to T-FOXO1 was observed at in any of the FA concentrations, suggesting that formation of superoxide or alkyl radicals plays a role in triggering deacetylation of FOXO1 (Figure 16B). In addition to ROS playing a role in deacetylation of FOXO1, pretreatment with the SIRT1 inhibitor EX-527, also prevented the increase in FOXO1 deacetylation that was observed with 1000 µM FA (Figure 16C).

Expression of dominant negative SIRT1 or FOXO1 further Exacerbates cell death induced by fatty acids

Although FA induced an increase in deacetylation in preadipocytes at the 24 hour time point, the protective effect of FOXO1 deacetylation was unknown, especially since FA exposure caused an increase in cell death in both 800 and 1000 µM FA at 24 hours (Figure 16D). To test this hypothesis, a stable cell line that expressed either a dominant negative (DN) SIRT1 or FOXO1, was treated with FA and the percentage of dead cells was measured. Compared to 1000 µM FA treatment in non-transfected cells, the SIRT1 DN demonstrated an almost a 2-fold increase in cell death when treated with 1000 µM FA (Figure 16D). The increase in cell death found in the SIRT1 DN was also present following 800 and 600 µM FA treatment. Interestingly, SIRT1 DN cells treated with 600 µM showed almost a 3-fold increase in cell death compared to non-transfected cells where no increase in cell death was observed (Figure 16C). In comparison to SIRT1 DN, the FOXO1 DN only showed an increase in cell death above non-transfected cells when treated with 1000 µM FA (Figure 16C). To confirm that the exacerbation in cell death was due to FA entry and ROS production within the mitochondria, pretreatment of preadipocytes with Etomoxir, a carnitine palmitoyl transferase I (CPT-I) inhibitor, that blocks the entry of fatty acyl-CoA into the mitochondria or MitoTempo was used. Pretreatment with Etomoxir or MitoTempo followed by 1000 µM FA, diminished the increase in cell death in non-transfected, SIRT1 DN and FOXO1 DN cells, suggesting the FA entry into the mitochondria and subsequent increases in superoxide or alkyl radical formation caused the associated increase in cell death (Figure 16D).

Discussion

This study is the first to demonstrate that mitochondrial antioxidant gene expression is altered depending on insulin sensitivity across a wide range of BMI. The findings suggest that decreased SIRT1 activity underlies a decrease in antioxidant gene expression. This lower antioxidant capacity would, in turn, increase the susceptibility of adipose tissue to chronic energy imbalance. This sensitivity to the cytotoxic effect of excess nutrients, in particular FA, may be linked to the loss of insulin sensitivity. Although subjects were matched for BMI and age as much as possible, the influence of age, BMI or the ability of obesity to accelerate aging within adipose tissue may have an effect on an individual's mitochondrial function and homeostasis.

Although the role of FOXO1 on antioxidant gene expression was a primary focus, FOXO1 has also been shown to increase insulin sensitivity through transcription of insulin receptor substrate 1 and modulation of energy homeostasis in adipose tissue through regulation of adipocyte size (Armoni et al., 2006; J Nakae et al., 2008). In other non-adipose tissue, however, increased nuclear FOXO1 may not be beneficial. For example, in the liver, inhibition of FOXO1 leads to improvement in hepatic insulin action (Altomonte et al., 2003). Furthermore, a mouse model that mimics overexpression of deacetylated FOXO1 leads to insulin resistance (Banks et al., 2011). Therefore, the changes observed in FOXO1 expression should be limited to the context of adipose tissue and not extrapolated to other tissues.

Despite uncovering strong associations between SIRT1, FOXO1 and antioxidant gene expression, not all genes were significantly changed. For example, despite having an FRE sequence, no change in Catalase (CAT) expression between the different quartiles of FOXO1 expression occurred. Furthermore, CAT and TXNRD2 were upregulated in the upper quartile

SIRT1 expression, but not FOXO1. Together these findings suggest that although the SIRT1-FOXO1 axis plays an important role in regulating mitochondrial antioxidant gene expression, other pathways may be involved. One alternative pathway that exists that can lead to increased expression of CAT, is the nuclear factor erythroid 2p45-related factor 2 (NFE2L2), which regulates induction of not only CAT, but also SOD2, GPX1 and GSR (Surh, Kundu, & Na, 2008). In addition to FOXO1, SIRT1 also functions to deacetylate peroxisome proliferator-activated receptor-coactivator (PGC1a) that can increase mitochondrial biogenesis and antioxidant gene expression including those presented in this paper (Nemoto, Fergusson, & Finkel, 2005). SIRT1 can also directly interact with nuclear factor-kappa B (NFkB) to limit formation of pro-inflammatory cytokines such as TNFa or to decrease the transcriptional activity of p53 by direct interaction that could favor adipocyte death and dysfunction (Vaziri et al., 2001; Yeung et al., 2004). The ability of SIRT1 to deacetylate other proteins besides FOXO1 may also explain why the SIRT1 DN had an increase in cell death at the 600 µM FA level, while the FOXO1 DN did not. Although FOXO1 is the dominant isoform in adipose tissue, FOXO3, which can also be deacetylated by SIRT1, governs transcription of mitochondrial antioxidant genes such as SOD2, and subsequently this could explain why the FOXO1 DN was not as detrimental as the SIRT1 DN after exposure to 600 µM FA (Brunet et al., 2004; van der Horst et al., 2004). In summary, insulin sensitivity correlates to antioxidant enzyme expression in subcutaneous adipose tissue.

Table 1. Characteristics of the subjects from the ISNO, ISO, IRO, and T2DM groups

(Modified from Rogers and al)

Table 1. Characteristics of the subjects from the ISL, ISO, IRO, and type 2 diabetes mellitus groups[$]

	ISNO[a]	**ISO**[b]	**IRO**[c]	**T2DM**
n	10	11	6	5
Age (year)	40.6 ± 6.4	43.3 ± 9.6	41.7 ± 8.9	52.4 ± 11.8
BMI (kg/m2)	25.5 ± 3.2	39.8 ± 6.9[a]	42.9 ± 9.3[a]	46.8 ± 3.2[a]
Glucose (mg/dL)	89.6 ± 9.4	93.7 ± 11.4	108.6 ± 16.4	149.7 ± 12.8[a,b,c]
Insulin (uIU/mL)	4.3 ± 2.3b	7.0 ± 1.9	20.1 ± 7.3[a]	12.8 ± 7.0[a,b]
HOMA	1.0 ± 0.5	1.6 ± 0.3	5.5 ± 2.3[a,b]	4.6 ± 2.4[a,b]

[$]Data are presented as mean ± SD. *a* P ≤0.05 when compared to ISNO. *b* P ≤0.05 when compared to ISO. *c* P ≤0.05 when compared to IRO.

Table 2. Characteristics of the subjects from the ISNO, ISO, IRO, and T2DM groups

Table 2. Characteristics of the subjects from the first and fourth quartiles of insulin sensitivity[$]

	First quartile	Last quartile
n	8	8
Age (year)	42.0 ± 10.0	44.1 ± 11.6
BMI (kg/m2)	25.9 ± 4.7	43.6 ± 7.7 *
Glucose (mg/dL)	91.3 ± 10.0	124.3 ± 18.4 *
Insulin (uIU/mL)	3.2 ± 1.3	19.6 ± 6.9 *
HOMA	0.7 ± 0.3	6.0 ± 2.1 *

[$]Data are presented as mean ± SD. P ≤0.05 when compared to the first quartile of insulin sensitivity

Table 3. Characteristics of the subjects from the first and fourth quartiles of SIRT1 gene expression

Table 3. Characteristics of the subjects from the first and fourth quartiles of SIRT1 Gene Expression[$]

	First Quartile	Last Quartile
n	8	8
SIRT1 Expression	0.5 ± 0.1	1.6 ± 0.1 *
Age (year)	44.1 ± 7.1	35.1 ± 7.0 *
BMI (kg/m2)	41.4 ± 7.1	34.7 ± 12.6
Glucose (mg/dL)	129.9 ± 25.8	87.8 ± 18.1 *
Insulin (uIU/mL)	17.1 ± 9.6	6.1 ± 4.4 *
HOMA	5.4 ± 2.8	1.2 ± 0.7 *

[$]Data are presented as mean ± SD. * P <0.05 when compared to the first quartile of SIRT1 gene expression.

Table 4. Characteristics of the subjects from the first and fourth quartiles of FOXO1 gene expression

Table 4. Characteristics of the subjects from the first and fourth quartiles of FOXO1 Gene Expression[$]

	First Quartile	Last Quartile
n	8	8
FOXO1 Expression	0.1 ± 0.1	2.4 ± 0.4 *
Age (year)	43.4 ± 7.3	39.0 ± 7.0
BMI (kg/m2)	37.1 ± 10.23	30.3 ± 9.1
Glucose (mg/dL)	93.7 ±29.1	92.2 ± 11.4
Insulin (uIU/mL)	12.1 ± 9.7	5.189 ± 3.6
HOMA	3.1 ± 1.1	1.2 ± 0.9 *

[$]Data are presented as mean ± SD. * P <0.05 when compared to the first quartile of FOXO1 gene expression

Figure 12. Antioxidant enzyme gene expression is lower in insulin-resistant individuals

Individuals were classified as ISNO, ISO, IRO or T2DM and mRNA levels of SOD2, CAT, PRDX3, TXRND2, DPX1 and GSR were quantified through rt-pcr using GAPDH as an endogenous control (Figure A-L). SOD2 (A) and TXNRD2 (G) showed a decrease in expression between ISNO and either IRO or T2DM, while SOD2 (A), CAT (C), and TXNRD2 (G) showed a difference in either IRO or T2DM when compared to ISO. PRDX3 (E), GPX1 (I) and GSR (L) showed no difference in the level of gene expression. Separating individuals into either the first or the fourth quartile of insulin sensitivity, regardless of age or BMI revealed significant differences between SOD2 (B), PRDX3 (F), TXNRD2 (H) and GPX1 (J), but not in CAT (D) and GSR (L). Results are expressed as mean + SD of 10 (ISNO), 11 (ISO), 6 (IRO) and 5 (T2DM) or 8 subjects per quartile. * $P < 0.05$ when compared to ISNO. + $P < 0.05$ when compared to ISO. $ $P < 0.05$ when compared to ISI.

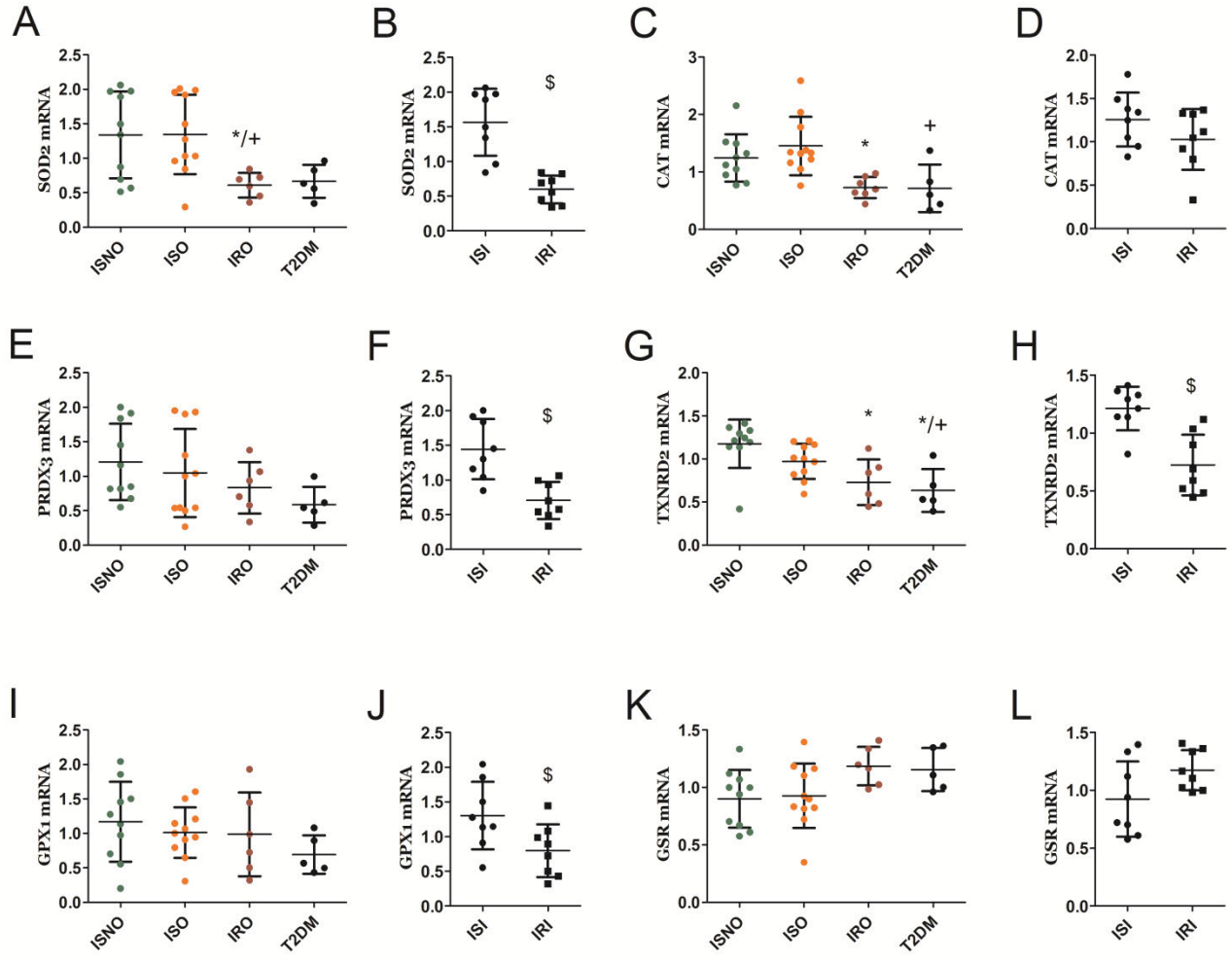
A
SOD2 mRNA
2.5
2.0
1.5
1.0
0.5
0.0
*/+
ISNO
ISO
IRO
T2DM
B
SOD2 mRNA
$
ISI
IRI
C
CAT mRNA
3
2
1
0
*
+
ISNO
ISO
IRO
T2DM
D
CAT mRNA
ISI
IRI
E
PRDX3 mRNA
ISNO
ISO
IRO
T2DM
F
PRDX3 mRNA
$
ISI
IRI
G
TXNRD2 mRNA
*
*/+
ISNO
ISO
IRO
T2DM
H
TXNRD2 mRNA
$
ISI
IRI
I
GPX1 mRNA
ISNO
ISO
IRO
T2DM
J
GPX1 mRNA
$
ISI
IRI
K
GSR mRNA
ISNO
ISO
IRO
T2DM
L
GSR mRNA
ISI
IRI

Figure 13. SIRT1 and FOXO1 gene expression correlate with insulin sensitivity

The mRNA expression levels of SIRT1 and FOXO1, were measured in ISNO, ISO, IRO or T2DM using RT-PCR. SIRT1 (A) was lower in T2DM when compared to ISNO or ISO individuals. No difference in the mRNA level of FOXO1(C) was observed between ISNO, ISO, IRO or T2DM individuals. After separating individuals into the first and fourth quartile of insulin sensitivity, the expression of SIRT1 (B) and FOXO1 (D) was significantly higher in the insulin-sensitive quartile. Results are expressed as mean $\pm$ SD of 10 (ISNO), 11 (ISO), 6 (IRO) and 5 (T2DM) or 8 subjects per quartile. * $P \leq 0.05$ when compared to ISNO. + $P \leq 0.05$ when compared to ISO. $ $P \leq 0.05$ when compared to ISI.

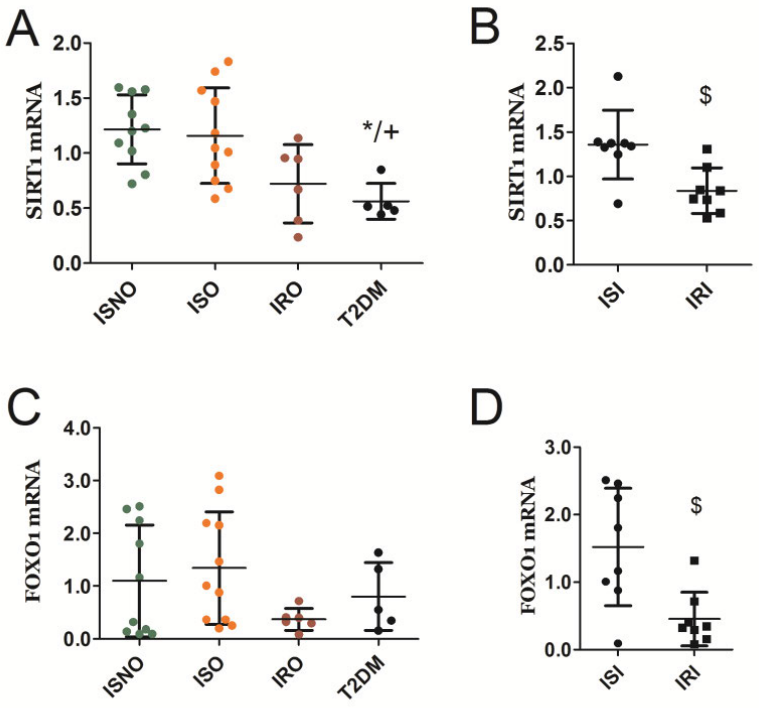
A
SIRT1 mRNA
2.0
1.5
1.0
0.5
0.0
*/+
ISNO
ISO
IRO
T2DM
B
SIRT1 mRNA
2.5
2.0
1.5
1.0
0.5
0.0
$
ISI
IRI
C
FOXO1 mRNA
4.0
3.0
2.0
1.0
0.0
ISNO
ISO
IRO
T2DM
D
FOXO1 mRNA
3.0
2.0
1.0
0.0
$
ISI
IRI

Figure 14. Individuals with high SIRT1 expression have an increase in antioxidant enzyme gene expression

SOD2 (A), CAT (B), PRDX3 (C), TXNRD2 (D), GPX1 (E) and FOXO1 (I) gene expression was higher in individuals who had increased SIRT1 expression. There was no difference in GSR (F) expression between the groups. Results are expressed as mean $\pm$ SD of 8 subjects per quartile. # $P \leq 0.05$ when compared to individuals belonging to the low SIRT1 expression quartile.

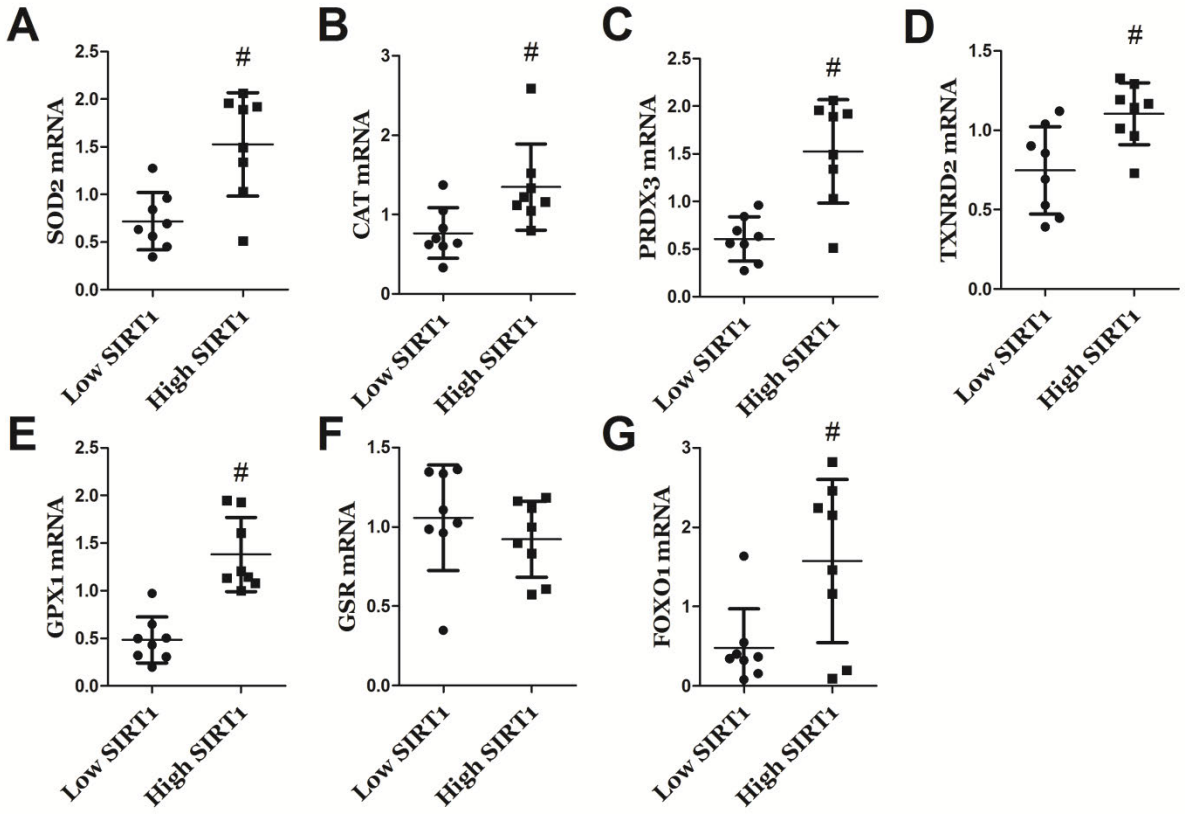
A
SOD2 mRNA
#
Low SIRT1
High SIRT1
B
CAT mRNA
#
Low SIRT1
High SIRT1
C
PRDX3 mRNA
#
Low SIRT1
High SIRT1
D
TXNRD2 mRNA
#
Low SIRT1
High SIRT1
E
GPX1 mRNA
#
Low SIRT1
High SIRT1
F
GSR mRNA
Low SIRT1
High SIRT1
G
FOXO1 mRNA
#
Low SIRT1
High SIRT1

Figure 15. Individuals with high FOXO1 expression are associated with an increase in antioxidant enzyme gene expression

SOD2 (A), PRDX3 (C), GPX1 (E) and GSR (F) gene expression was higher in individuals who had increased FOXO1 expression. There was no difference in CAT (B), TXNRD2 (D) or SIRT1 (G) expression between the groups. # $P \leq 0.05$ when compared to individuals belonging to the low FOXO1 expression quartile.

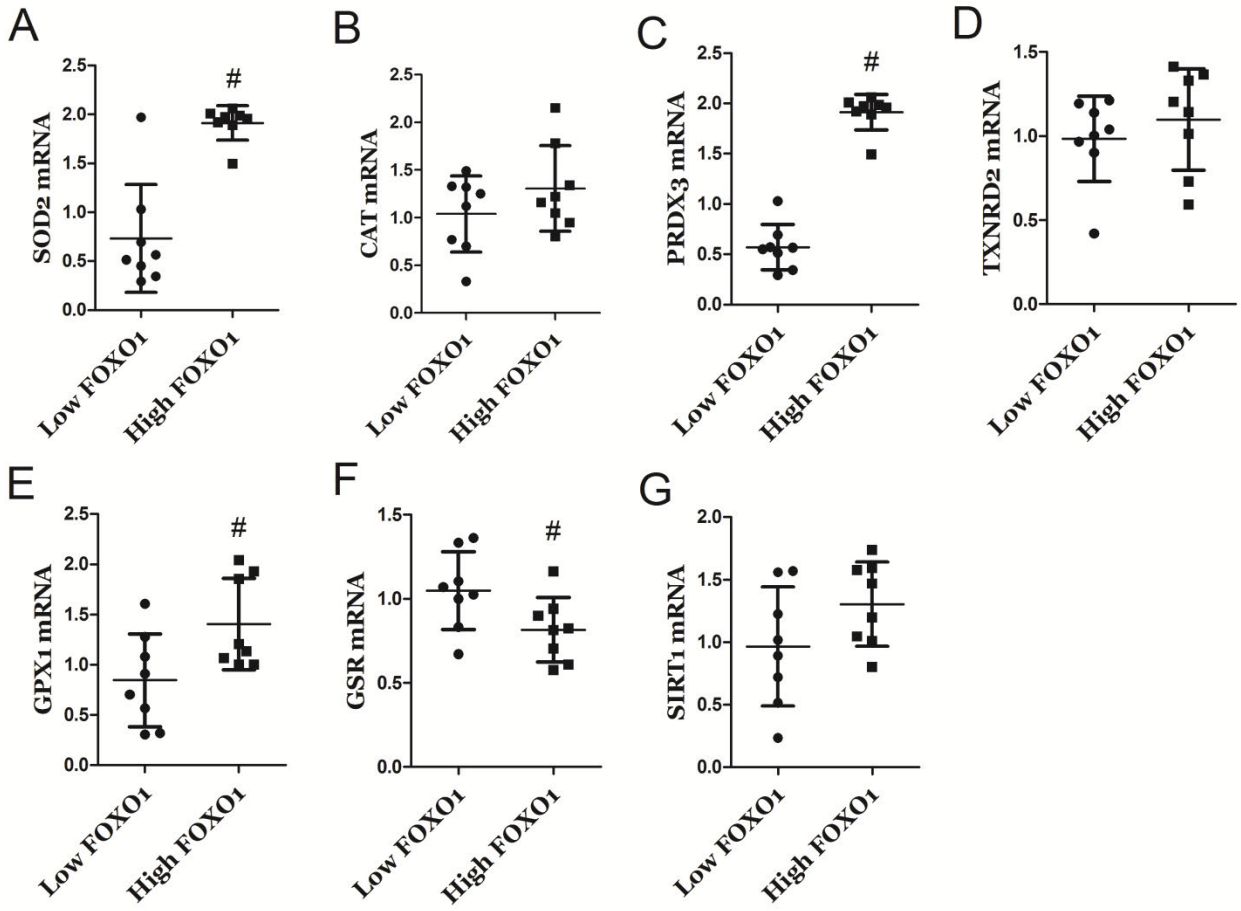
A
SOD2 mRNA
#
Low FOXO1
High FOXO1
B
CAT mRNA
Low FOXO1
High FOXO1
C
PRDX3 mRNA
#
Low FOXO1
High FOXO1
D
TXNRD2 mRNA
Low FOXO1
High FOXO1
E
GPX1 mRNA
#
Low FOXO1
High FOXO1
F
GSR mRNA
#
Low FOXO1
High FOXO1
G
SIRT1 mRNA
Low FOXO1
High FOXO1

Figure 16. FOXO1 and SIRT1 play a role in protecting human preadipocytes from cell death induced by fatty acids

(A) Preadipocytes were exposed to fatty acid for 1, 3, 6, 12 or 24 hours. After each time point cells were fixed and either total FOXO1 (Alexa Fluor 568) or acetylated FOXO1 (Alexa Fluor 488) protein levels were determined by flow cytometry. Analysis of the ratio of Ac-FOXO1 mean fluorescence intensity (MFI) to total-FOXO1 MFI revealed that fatty acid caused a decrease in acetylation as soon as 6 hours after treatment. Pretreatment with MitoTempo (B), a mitochondrial superoxide and alkyl radical scavenger, or EX-527 (C) a SIRT1 inhibitor, prevented the observed deacetylation of FOXO1. (D) Cells were stained with Calcein AM to detect live cells and Ethidium Homodimer 1 to detect dead cells. The percentage of dead cells was significantly increased in SIRT1 DN and FOXO1 DN following 1000 μM FA exposure when compared to 1000 μM FA exposure in non-transfected cells. Pretreatment with Etomoxir or MitoTempo prevented the increases in cell death that followed 1000 μM FA exposure. * $P \leq 0.05$ when compared to 600 μM BSA. + $P \leq 0.05$ when compared to 1000 μM FA.

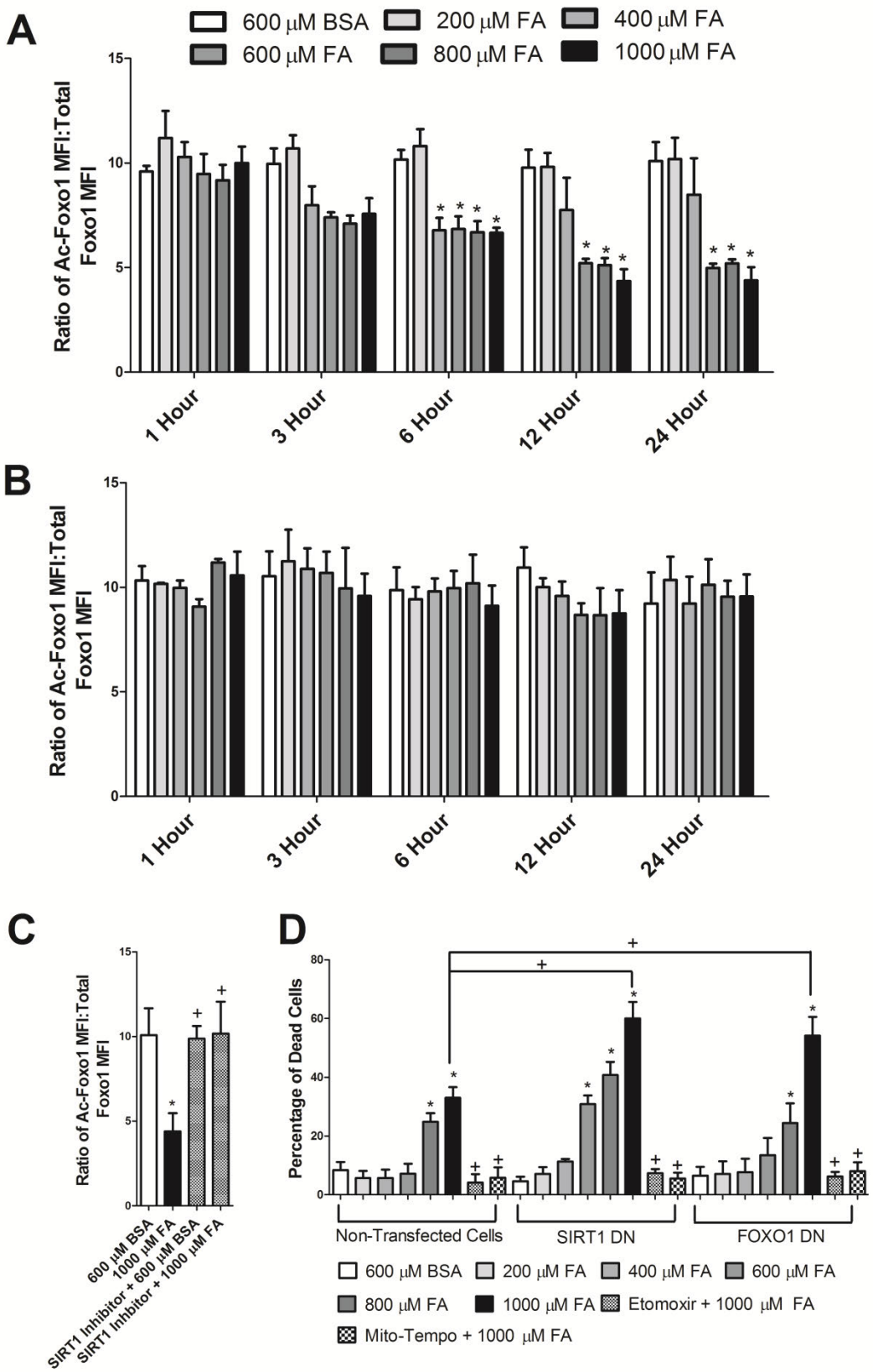
A
600 μM BSA
200 μM FA
400 μM FA
600 μM FA
800 μM FA
1000 μM FA
Ratio of Ac-Foxo1 MFI:Total Foxo1 MFI
1 Hour
3 Hour
6 Hour
12 Hour
24 Hour
B
C
600 μM BSA
1000 μM FA
SIRT1 Inhibitor + 600 μM BSA
SIRT1 Inhibitor + 1000 μM FA
D
Percentage of Dead Cells
Non-Transfected Cells
SIRT1 DN
FOXO1 DN
Etomoxir + 1000 μM FA
Mito-Tempo + 1000 μM FA

CHAPTER 6: INTEGRATED SUMMARY AND FUTURE DIRECTIONS

Major Findings

The aims of this study were to determine the impact of fatty acids (FA) on preadipocyte function with specific emphasis placed on how mitochondria integrate and adapt to concentrations of FA within the limits of daily FA exposure. Toward these objectives, the findings presented here are important for a number of reasons. First, this study shows that preadipocytes, despite belonging to the adipocyte lineage are susceptible to a physiologically relevant mixture of FA. Second, FA induce a transient increase in mitochondrial, but not cytosolic superoxide, H_2O_2 and lipid peroxidation within the first 2 hours of FA exposure that manifests into a loss of mitochondrial fitness over the course of 24 hours. Third, despite one-third of cells undergoing cell death, the majority of cells were able to survive the upper limit of FA exposure through a protective response initiated by a SIRT1-FOXO1 mediated increase in mitochondrial gene expression. Finally, global expression of SIRT1, FOXO1 and mitochondrial antioxidant genes is increased in adipose tissue of insulin sensitive individuals. Altogether these studies demonstrate for the first time how human preadipocytes are able to function during constant FA exposure and how preadipocyte mitochondrion susceptibility to FA can lead to the preadipocytes demise.

Future Directions

The studies presented within this dissertation describe the mechanisms that underlie preadipocyte susceptibility and survivability to FA. Of the numerous effects of FA exposure that were observed, a transient increase in superoxide and H_2O_2 was shown to be the initial step in priming preadipocytes for a loss in mitochondrial fitness through NAD+ depletion. However,

several questions of how FA influence preadipocytes are still unknown and call for future investigation.

First, in addition to Etomoxir and MitoTempo pretreatment, Nicotinamide supplementation also prevented the increase in preadipocyte cell death. However, like Etomoxir and MitoTempo, 2 hour post treatment with Nicotinamide failed to prevent FA induced cell death. Furthermore, the depletion of NAD^+ + NADH occurs 6-8 hours following FA exposure, suggesting that metabolism of nicotinamide to NAD+ may be affected. For nicotinamide to increase mitochondrial NAD+ pools, it first must be converted into nicotinamide mononucleotide (NMN) (Revollo et al., 2007; Rongvaux et al., 2003). Once NMN is formed it can freely enter mitochondria and be converted into NAD^+ by Nicotinamide mononucleotide adenylyl transferase (NMNAT3) (Nikiforov, Dölle, Niere, & Ziegler, 2011). If mitochondrial lipid peroxidation can occur within the first 2 hours of FA exposure, mitochondrial protein oxidation and loss of protein function could also occur (Davies, Fu, Wang, & Dean, 1999). If NMNAT3, is damaged by excessive ROS and is unable to convert NMN from nicotinamide to NAD+, no increase in mitochondrial NAD+ levels would occur (Nikiforov et al., 2011). Investigation into the function of NMNAT3 in the presence of FA would help to reveal if this is why nicotinamide is efficient at saving preadipocytes from cell death after 2 hours of FA exposure.

Second, how FA exposure signals from the mitochondria to the nucleus to increase antioxidant gene expression is still unclear. One potential pathway that could trigger increases in antioxidant genes is through JNK, as JNK inhibitor SP600125 prevented deacetylation of FOXO1. As H_2O_2 levels increase, antioxidant enzymes such as PRDX3 will interact with H_2O_2, leading to the formation of H_2O (Cox et al., 2009). Once PRDX3 becomes oxidized, TRX2 can reduce the oxidized cysteine groups of PRDX3 (Chae, Chung, et al., 1994; Chae, Uhm, et al.,

1994). However, for TRX2 to regenerate PRDX3, it first must dissociate from its complex with apoptosis signal-regulating kinase (ASK1) (Gotoh & Cooper, 1998; Hsieh & Papaconstantinou, 2006; Saitoh et al., 1998). Once TRX2 dissociates ASK1, ASK1 can then activate JNK (Nadeau, Charette, & Landry, 2009). Once activated, JNK can then interact with SIRT1 (Nasrin et al., 2009), which in turn deacetylates FOXO1. Furthermore, although this dissertation focused on the FOXO1 transcription, several other transcription factors that could influence antioxidant expression exist. Three additional transcription factors that may be involved in protection against FA exposure are nuclear factor E2-related factor 2 (NRF2), peroxisome proliferator-activated receptor-coactivator (PGC1 α), and peroxisome proliferator-activated receptor gamma (PPAR α). All three enzymes once activated can lead to an increase in genes involved in oxidant detoxification, FA oxidation and mitochondrial biogenesis(Lee, Calkins, Chan, Kan, & Johnson, 2003; H. Liang & Ward, 2006; T. Nguyen, Yang, & Pickett, 2004; Tyagi, Gupta, Saini, Kaushal, & Sharma, 2011) . Exploring the role of these transcription factors as well as the signals that are amplified in the mitochondria and released into the cytosol upon FA exposure, would help to reveal if a central node in the pathway exists that can be used to up regulate and defend against FA induced ROS.

Finally, this dissertation showed that pretreatment with the antioxidant Mito-Tempo or the NAD+ precursor Nicotinamide, prevented the increase in cell death that was associated with 1000 µM FA. Interestingly, variations of these compounds, CoEnzyme Q10 as an antioxidant (Ernster & Dallner, 1995; Potgieter, Pretorius, & Pepper, 2013) and Niacin for a precursor to NAD+ (Bogan & Brenner, 2008; Sauve, 2008), can be found in the vitamin section of the majority of health stores. Therefore, an individual who is at risk for the development of adipose tissue dysfunction could take a nutraceutical approach to decrease their risk. Future studies in an

animal model examining if pretreatment or post treatment with these compounds could prevent the associated increases in adipose tissue dysfunction associated with a high fat diet would add support to this hypothesis.

REFERENCES

Abbasi, F., Brown, B. J., Lamendola, C., McLaughlin, T., & Reaven, G. (2002). Relationship between obesity, insulin resistance, and coronary heart disease risk. *J Am Coll Cardiol, 40*(5), 937-943.

Accili, D., & Arden, K. C. (2004). FoxOs at the crossroads of cellular metabolism, differentiation, and transformation. *Cell, 117*(4), 421-426.

Ahmadian, M., Wang, Y., & Sul, H. S. (2010). Lipolysis in adipocytes. *Int J Biochem Cell Biol, 42*(5), 555-559.

Aldini, G., Dalle-Donne, I., Colombo, R., Maffei Facino, R., Milzani, A., & Carini, M. (2006). Lipoxidation-derived reactive carbonyl species as potential drug targets in preventing protein carbonylation and related cellular dysfunction. *ChemMedChem, 1*(10), 1045-1058.

Altomonte, J., Richter, A., Harbaran, S., Suriawinata, J., Nakae, J., Thung, S. N., et al. (2003). Inhibition of Foxo1 function is associated with improved fasting glycemia in diabetic mice. *Am J Physiol Endocrinol Metab, 285*(4), E718-728.

Anderson, E. J., Lustig, M. E., Boyle, K. E., Woodlief, T. L., Kane, D. A., Lin, C. T., et al. (2009). Mitochondrial H2O2 emission and cellular redox state link excess fat intake to insulin resistance in both rodents and humans. *J Clin Invest, 119*(3), 573-581.

Anderson, P. J., Chan, J. C., Chan, Y. L., Tomlinson, B., Young, R. P., Lee, Z. S., et al. (1997). Visceral fat and cardiovascular risk factors in Chinese NIDDM patients. *Diabetes Care, 20*(12), 1854-1858.

Andreyev, A., Kushnareva, Y., & Starkov, A. (2005). Mitochondrial metabolism of reactive oxygen species. *Biochemistry (Mosc), 70*(2), 200-214.

Armoni, M., Harel, C., Karni, S., Chen, H., Bar-Yoseph, F., Ver, M. R., et al. (2006). FOXO1 represses peroxisome proliferator-activated receptor-gamma1 and -gamma2 gene promoters in primary adipocytes. A novel paradigm to increase insulin sensitivity. *J Biol Chem, 281*(29), 19881-19891.

Arner, E., Westermark, P. O., Spalding, K. L., Britton, T., Rydén, M., Frisén, J., et al. (2010). Adipocyte turnover: relevance to human adipose tissue morphology. *Diabetes, 59*(1), 105-109.

Arner, P. (2005). Human fat cell lipolysis: biochemistry, regulation and clinical role. *Best Pract Res Clin Endocrinol Metab, 19*(4), 471-482.

Arner, P., Bernard, S., Salehpour, M., Possnert, G., Liebl, J., Steier, P., et al. (2011). Dynamics of human adipose lipid turnover in health and metabolic disease. *Nature, 478*(7367), 110-113.

Ascaso, J. F., Pardo, S., Real, J. T., Lorente, R. I., Priego, A., & Carmena, R. (2003). Diagnosing insulin resistance by simple quantitative methods in subjects with normal glucose metabolism. *Diabetes Care, 26*(12), 3320-3325.

Baik, I., Ascherio, A., Rimm, E. B., Giovannucci, E., Spiegelman, D., Stampfer, M. J., et al. (2000). Adiposity and mortality in men. *Am J Epidemiol, 152*(3), 264-271.

Banks, A. S., Kim-Muller, J. Y., Mastracci, T. L., Kofler, N. M., Qiang, L., Haeusler, R. A., et al. (2011). Dissociation of the glucose and lipid regulatory functions of FoxO1 by targeted knockin of acetylation-defective alleles in mice. *Cell Metab, 14*(5), 587-597.

Belousov, V. V., Fradkov, A. F., Lukyanov, K. A., Staroverov, D. B., Shakhbazov, K. S., Terskikh, A. V., et al. (2006). Genetically encoded fluorescent indicator for intracellular hydrogen peroxide. *Nat Methods, 3*(4), 281-286.

Bernardi, P., Penzo, D., & Wojtczak, L. (2002). Mitochondrial energy dissipation by fatty acids. Mechanisms and implications for cell death. *Vitam Horm, 65*, 97-126.

Biggs, W. H., Meisenhelder, J., Hunter, T., Cavenee, W. K., & Arden, K. C. (1999). Protein kinase B/Akt-mediated phosphorylation promotes nuclear exclusion of the winged helix transcription factor FKHR1. *Proc Natl Acad Sci U S A, 96*(13), 7421-7426.

Binas, B., Han, X. X., Erol, E., Luiken, J. J., Glatz, J. F., Dyck, D. J., et al. (2003). A null mutation in H-FABP only partially inhibits skeletal muscle fatty acid metabolism. *Am J Physiol Endocrinol Metab, 285*(3), E481-489.

Boden, G. (2008). Obesity and free fatty acids. *Endocrinol Metab Clin North Am, 37*(3), 635-646, viii-ix.

Bogan, K. L., & Brenner, C. (2008). Nicotinic acid, nicotinamide, and nicotinamide riboside: a molecular evaluation of NAD+ precursor vitamins in human nutrition. *Annu Rev Nutr, 28*, 115-130.

Bonnard, C., Durand, A., Peyrol, S., Chanseaume, E., Chauvin, M. A., Morio, B., et al. (2008). Mitochondrial dysfunction results from oxidative stress in the skeletal muscle of diet-induced insulin-resistant mice. *J Clin Invest, 118*(2), 789-800.

Brand, M. D. (2005). The efficiency and plasticity of mitochondrial energy transduction. *Biochem Soc Trans, 33*(Pt 5), 897-904.

Brand, M. D., & Nicholls, D. G. (2011). Assessing mitochondrial dysfunction in cells. *Biochem J, 435*(2), 297-312.

Brochu, M., Tchernof, A., Dionne, I. J., Sites, C. K., Eltabbakh, G. H., Sims, E. A., et al. (2001). What are the physical characteristics associated with a normal metabolic profile despite a high level of obesity in postmenopausal women? *J Clin Endocrinol Metab, 86*(3), 1020-1025.

Brunet, A., Bonni, A., Zigmond, M. J., Lin, M. Z., Juo, P., Hu, L. S., et al. (1999). Akt promotes cell survival by phosphorylating and inhibiting a Forkhead transcription factor. *Cell, 96*(6), 857-868.

Brunet, A., Park, J., Tran, H., Hu, L. S., Hemmings, B. A., & Greenberg, M. E. (2001). Protein kinase SGK mediates survival signals by phosphorylating the forkhead transcription factor FKHRL1 (FOXO3a). *Mol Cell Biol, 21*(3), 952-965.

Brunet, A., Sweeney, L. B., Sturgill, J. F., Chua, K. F., Greer, P. L., Lin, Y., et al. (2004). Stress-dependent regulation of FOXO transcription factors by the SIRT1 deacetylase. *Science, 303*(5666), 2011-2015.

Brömme, H. J., Zühlke, L., Silber, R. E., & Simm, A. (2008). DCFH2 interactions with hydroxyl radicals and other oxidants--influence of organic solvents. *Exp Gerontol, 43*(7), 638-644.

Carrière, A., Fernandez, Y., Rigoulet, M., Pénicaud, L., & Casteilla, L. (2003). Inhibition of preadipocyte proliferation by mitochondrial reactive oxygen species. *FEBS Lett, 550*(1-3), 163-167.

Caserta, F., Tchkonia, T., Civelek, V. N., Prentki, M., Brown, N. F., McGarry, J. D., et al. (2001). Fat depot origin affects fatty acid handling in cultured rat and human preadipocytes. *Am J Physiol Endocrinol Metab, 280*(2), E238-247.

Chae, H. Z., Chung, S. J., & Rhee, S. G. (1994). Thioredoxin-dependent peroxide reductase from yeast. *J Biol Chem, 269*(44), 27670-27678.

Chae, H. Z., Uhm, T. B., & Rhee, S. G. (1994). Dimerization of thiol-specific antioxidant and the essential role of cysteine 47. *Proc Natl Acad Sci U S A, 91*(15), 7022-7026.

Charles, M. A., Eschwège, E., Thibult, N., Claude, J. R., Warnet, J. M., Rosselin, G. E., et al. (1997). The role of non-esterified fatty acids in the deterioration of glucose tolerance in Caucasian subjects: results of the Paris Prospective Study. *Diabetologia, 40*(9), 1101-1106.

Choi, H., Kim, S., Mukhopadhyay, P., Cho, S., Woo, J., Storz, G., et al. (2001). Structural basis of the redox switch in the OxyR transcription factor. *Cell, 105*(1), 103-113.

Cinti, S. (2006). The role of brown adipose tissue in human obesity. *Nutr Metab Cardiovasc Dis, 16*(8), 569-574.

Cocco, T., Di Paola, M., Papa, S., & Lorusso, M. (1999). Arachidonic acid interaction with the mitochondrial electron transport chain promotes reactive oxygen species generation. *Free Radic Biol Med, 27*(1-2), 51-59.

Cox, A. G., Peskin, A. V., Paton, L. N., Winterbourn, C. C., & Hampton, M. B. (2009). Redox potential and peroxide reactivity of human peroxiredoxin 3. *Biochemistry, 48*(27), 6495-6501.

Curry, S., Brick, P., & Franks, N. P. (1999). Fatty acid binding to human serum albumin: new insights from crystallographic studies. *Biochim Biophys Acta, 1441*(2-3), 131-140.

Daitoku, H., Hatta, M., Matsuzaki, H., Aratani, S., Ohshima, T., Miyagishi, M., et al. (2004). Silent information regulator 2 potentiates Foxo1-mediated transcription through its deacetylase activity. *Proc Natl Acad Sci U S A, 101*(27), 10042-10047.

Davies, M. J., Fu, S., Wang, H., & Dean, R. T. (1999). Stable markers of oxidant damage to proteins and their application in the study of human disease. *Free Radic Biol Med, 27*(11-12), 1151-1163.

DeFronzo, R. A. (2004). Dysfunctional fat cells, lipotoxicity and type 2 diabetes. *Int J Clin Pract Suppl*(143), 9-21.

Di Paola, M., Cocco, T., & Lorusso, M. (2000). Arachidonic acid causes cytochrome c release from heart mitochondria. *Biochem Biophys Res Commun, 277*(1), 128-133.

Dinsa, G. D., Goryakin, Y., Fumagalli, E., & Suhrcke, M. (2012). Obesity and socioeconomic status in developing countries: a systematic review. *Obes Rev, 13*(11), 1067-1079.

Don, B. R., & Kaysen, G. (2004). Serum albumin: relationship to inflammation and nutrition. *Semin Dial, 17*(6), 432-437.

Drummen, G. P., Gadella, B. M., Post, J. A., & Brouwers, J. F. (2004). Mass spectrometric characterization of the oxidation of the fluorescent lipid peroxidation reporter molecule C11-BODIPY(581/591). *Free Radic Biol Med, 36*(12), 1635-1644.

Drynan, L., Quant, P. A., & Zammit, V. A. (1996). Flux control exerted by mitochondrial outer membrane carnitine palmitoyltransferase over beta-oxidation, ketogenesis and tricarboxylic acid cycle activity in hepatocytes isolated from rats in different metabolic states. *Biochem J, 317 (Pt 3)*, 791-795.

Edelhauser, H. F., Van Horn, D. L., Miller, P., & Pederson, H. J. (1976). Effect of thiol-oxidation of glutathione with diamide on corneal endothelial function, junctional complexes, and microfilaments. *J Cell Biol, 68*(3), 567-578.

Ernster, L., & Dallner, G. (1995). Biochemical, physiological and medical aspects of ubiquinone function. *Biochim Biophys Acta, 1271*(1), 195-204.

Fielding, B. A., Callow, J., Owen, R. M., Samra, J. S., Matthews, D. R., & Frayn, K. N. (1996). Postprandial lipemia: the origin of an early peak studied by specific dietary fatty acid intake during sequential meals. *Am J Clin Nutr, 63*(1), 36-41.

Fisher-Wellman, K. H., & Neufer, P. D. (2012). Linking mitochondrial bioenergetics to insulin resistance via redox biology. *Trends Endocrinol Metab, 23*(3), 142-153.

Frayn, K. N. (2002). Adipose tissue as a buffer for daily lipid flux. *Diabetologia, 45*(9), 1201-1210.

Frayn, K. N., Coppack, S. W., & Humphreys, S. M. (1993). Subcutaneous adipose tissue metabolism studied by local catheterization. *Int J Obes Relat Metab Disord, 17 Suppl 3*, S18-21; discussion S22.

Furuyama, T., Nakazawa, T., Nakano, I., & Mori, N. (2000). Identification of the differential distribution patterns of mRNAs and consensus binding sequences for mouse DAF-16 homologues. *Biochem J, 349*(Pt 2), 629-634.

Gao, C. L., Zhu, C., Zhao, Y. P., Chen, X. H., Ji, C. B., Zhang, C. M., et al. (2010). Mitochondrial dysfunction is induced by high levels of glucose and free fatty acids in 3T3-L1 adipocytes. *Mol Cell Endocrinol, 320*(1-2), 25-33.

Gastaldelli, A., Miyazaki, Y., Pettiti, M., Buzzigoli, E., Mahankali, S., Ferrannini, E., et al. (2004). Separate contribution of diabetes, total fat mass, and fat topography to glucose production, gluconeogenesis, and glycogenolysis. *J Clin Endocrinol Metab, 89*(8), 3914-3921.

Gastaldelli, A., Miyazaki, Y., Pettiti, M., Matsuda, M., Mahankali, S., Santini, E., et al. (2002). Metabolic effects of visceral fat accumulation in type 2 diabetes. *J Clin Endocrinol Metab, 87*(11), 5098-5103.

Gil, A., Olza, J., Gil-Campos, M., Gomez-Llorente, C., & Aguilera, C. M. (2011). Is adipose tissue metabolically different at different sites? *Int J Pediatr Obes, 6 Suppl 1*, 13-20.

Girotti, A. W. (1998). Lipid hydroperoxide generation, turnover, and effector action in biological systems. *J Lipid Res, 39*(8), 1529-1542.

GM, C. (2000). The Cell: A Molecular Approach, *The Mechanism of Oxidative Phosphorylation*. Sunderland (MA): Sinauer Associates.

Gotoh, Y., & Cooper, J. A. (1998). Reactive oxygen species- and dimerization-induced activation of apoptosis signal-regulating kinase 1 in tumor necrosis factor-alpha signal transduction. *J Biol Chem, 273*(28), 17477-17482.

Gottlieb, E., Armour, S. M., Harris, M. H., & Thompson, C. B. (2003). Mitochondrial membrane potential regulates matrix configuration and cytochrome c release during apoptosis. *Cell Death Differ, 10*(6), 709-717.

Gray, S., & Vidal-Puig, A. (2007). Adipose tissue expandability in the maintenance of metabolic homeostasis. *Nutr Rev, 65*(6 Pt 2), S7-12.

Guo, W., Wong, S., Xie, W., Lei, T., & Luo, Z. (2007). Palmitate modulates intracellular signaling, induces endoplasmic reticulum stress, and causes apoptosis in mouse 3T3-L1 and rat primary preadipocytes. *Am J Physiol Endocrinol Metab, 293*(2), E576-586.

Haidara, K., Morel, I., Abalea, V., Gascon Barre, M., & Denizeau, F. (2002). Mechanism of tert-butylhydroperoxide induced apoptosis in rat hepatocytes: involvement of mitochondria and endoplasmic reticulum. *Biochim Biophys Acta, 1542*(1-3), 173-185.

Hansen, J. M., Zhang, H., & Jones, D. P. (2006). Mitochondrial thioredoxin-2 has a key role in determining tumor necrosis factor-alpha-induced reactive oxygen species generation, NF-kappaB activation, and apoptosis. *Toxicol Sci, 91*(2), 643-650.

Hegele, R. A., Joy, T. R., Al-Attar, S. A., & Rutt, B. K. (2007). Thematic review series: Adipocyte Biology. Lipodystrophies: windows on adipose biology and metabolism. *J Lipid Res, 48*(7), 1433-1444.

Heilbronn, L., Smith, S., & Ravussin, E. (2004). Failure of fat cell proliferation, mitochondrial function and fat oxidation results in ectopic fat storage, insulin resistance and type II diabetes mellitus. *Int J Obes Relat Metab Disord, 28 Suppl 4*, S12-21.

Heimberg, M., Dunn, G. D., & Wilcox, G. (1974). The derivation of plasma-free fatty acids from dietary neutral fat in man. *J Lab Clin Med, 83*(3), 393-402.

Herscovitch, M., Perkins, E., Baltus, A., & Fan, M. (2012). Addgene provides an open forum for plasmid sharing. *Nat Biotechnol, 30*(4), 316-317.

Higuchi, M., Dusting, G. J., Peshavariya, H., Jiang, F., Hsiao, S. T., Chan, E. C., et al. (2012). Differentiation of Human Adipose-Derived Stem Cells into Fat Involves Reactive Oxygen Species and Forkhead Box O1 Mediated Upregulation of Antioxidant Enzymes. *Stem Cells Dev*.

Houstis, N., Rosen, E. D., & Lander, E. S. (2006). Reactive oxygen species have a causal role in multiple forms of insulin resistance. *Nature, 440*(7086), 944-948.

Hsieh, C. C., & Papaconstantinou, J. (2006). Thioredoxin-ASK1 complex levels regulate ROS-mediated p38 MAPK pathway activity in livers of aged and long-lived Snell dwarf mice. *FASEB J, 20*(2), 259-268.

Huang, H., Regan, K. M., Lou, Z., Chen, J., & Tindall, D. J. (2006). CDK2-dependent phosphorylation of FOXO1 as an apoptotic response to DNA damage. *Science, 314*(5797), 294-297.

Huang, H., & Tindall, D. (2007). Dynamic FoxO transcription factors. *J Cell Sci, 120*(Pt 15), 2479-2487.

Hubbard, B. P., Gomes, A. P., Dai, H., Li, J., Case, A. W., Considine, T., et al. (2013). Evidence for a common mechanism of SIRT1 regulation by allosteric activators. *Science, 339*(6124), 1216-1219.

Ikeuchi, M., Matsusaka, H., Kang, D., Matsushima, S., Ide, T., Kubota, T., et al. (2005). Overexpression of mitochondrial transcription factor a ameliorates mitochondrial deficiencies and cardiac failure after myocardial infarction. *Circulation, 112*(5), 683-690.

Imai, S. (2011). Dissecting systemic control of metabolism and aging in the NAD World: the importance of SIRT1 and NAMPT-mediated NAD biosynthesis. *FEBS Lett, 585*(11), 1657-1662.

Kampf, J. P., Parmley, D., & Kleinfeld, A. M. (2007). Free fatty acid transport across adipocytes is mediated by an unknown membrane protein pump. *Am J Physiol Endocrinol Metab, 293*(5), E1207-1214.

Karelis, A. D., Faraj, M., Bastard, J. P., St-Pierre, D. H., Brochu, M., Prud'homme, D., et al. (2005). The metabolically healthy but obese individual presents a favorable inflammation profile. *J Clin Endocrinol Metab, 90*(7), 4145-4150.

Karlsson, M., Kurz, T., Brunk, U. T., Nilsson, S. E., & Frennesson, C. I. (2010). What does the commonly used DCF test for oxidative stress really show? *Biochem J, 428*(2), 183-190.

Kiens, B., & Roepstorff, C. (2003). Utilization of long-chain fatty acids in human skeletal muscle during exercise. *Acta Physiol Scand, 178*(4), 391-396.

Kim, H. K., Della-Fera, M., Lin, J., & Baile, C. A. (2006). Docosahexaenoic acid inhibits adipocyte differentiation and induces apoptosis in 3T3-L1 preadipocytes. *J Nutr, 136*(12), 2965-2969.

Kim, J. Y., van de Wall, E., Laplante, M., Azzara, A., Trujillo, M. E., Hofmann, S. M., et al. (2007). Obesity-associated improvements in metabolic profile through expansion of adipose tissue. *J Clin Invest, 117*(9), 2621-2637.

Kim, M. Y., Kim, E. J., Kim, Y. N., Choi, C., & Lee, B. H. (2011). Effects of α-lipoic acid and L-carnosine supplementation on antioxidant activities and lipid profiles in rats. *Nutr Res Pract, 5*(5), 421-428.

Kitamura, Y. I., Kitamura, T., Kruse, J. P., Raum, J. C., Stein, R., Gu, W., et al. (2005). FoxO1 protects against pancreatic beta cell failure through NeuroD and MafA induction. *Cell Metab, 2*(3), 153-163.

Klöting, N., Fasshauer, M., Dietrich, A., Kovacs, P., Schön, M. R., Kern, M., et al. (2010). Insulin-sensitive obesity. *Am J Physiol Endocrinol Metab, 299*(3), E506-515.

Kops, G. J., Dansen, T. B., Polderman, P. E., Saarloos, I., Wirtz, K. W., Coffer, P. J., et al. (2002). Forkhead transcription factor FOXO3a protects quiescent cells from oxidative stress. *Nature, 419*(6904), 316-321.

Koutsari, C., Ali, A. H., Mundi, M. S., & Jensen, M. D. (2011). Storage of circulating free fatty acid in adipose tissue of postabsorptive humans: quantitative measures and implications for body fat distribution. *Diabetes, 60*(8), 2032-2040.

Koutsari, C., & Jensen, M. D. (2006). Thematic review series: patient-oriented research. Free fatty acid metabolism in human obesity. *J Lipid Res, 47*(8), 1643-1650.

Koutsari, C., Snozek, C. L., & Jensen, M. D. (2008). Plasma NEFA storage in adipose tissue in the postprandial state: sex-related and regional differences. *Diabetologia, 51*(11), 2041-2048.

Lambertucci, R., Hirabara, S., Silveira, L. R., Levada-Pires, A., Curi, R., & Pithon-Curi, T. (2008). Palmitate increases superoxide production through mitochondrial electron transport chain and NADPH oxidase activity in skeletal muscle cells. *J Cell Physiol, 216*(3), 796-804.

Langley, E., Pearson, M., Faretta, M., Bauer, U. M., Frye, R. A., Minucci, S., et al. (2002). Human SIR2 deacetylates p53 and antagonizes PML/p53-induced cellular senescence. *EMBO J, 21*(10), 2383-2396.

Lee, J. M., Calkins, M. J., Chan, K., Kan, Y. W., & Johnson, J. A. (2003). Identification of the NF-E2-related factor-2-dependent genes conferring protection against oxidative stress in primary cortical astrocytes using oligonucleotide microarray analysis. *J Biol Chem, 278*(14), 12029-12038.

Lei, X. G. (2002). In vivo antioxidant role of glutathione peroxidase: evidence from knockout mice. *Methods Enzymol, 347*, 213-225.

Li, M., Luo, J., Brooks, C. L., & Gu, W. (2002). Acetylation of p53 inhibits its ubiquitination by Mdm2. *J Biol Chem, 277*(52), 50607-50611.

Li, Z., Bowerman, S., & Heber, D. (2005). Health ramifications of the obesity epidemic. *Surg Clin North Am, 85*(4), 681-701, v.

Liang, H., & Ward, W. F. (2006). PGC-1alpha: a key regulator of energy metabolism. *Adv Physiol Educ, 30*(4), 145-151.

Liang, M., & Pietrusz, J. L. (2007). Thiol-related genes in diabetic complications: a novel protective role for endogenous thioredoxin 2. *Arterioscler Thromb Vasc Biol, 27*(1), 77-83.

Lidell, M. E., Betz, M. J., Leinhard, O. D., Heglind, M., Elander, L., Slawik, M., et al. (2013). Evidence for two types of brown adipose tissue in humans. *Nat Med*.

Loskovich, M. V., Grivennikova, V. G., Cecchini, G., & Vinogradov, A. D. (2005). Inhibitory effect of palmitate on the mitochondrial NADH:ubiquinone oxidoreductase (complex I) as related to the active-de-active enzyme transition. *Biochem J, 387*(Pt 3), 677-683.

Lu, S. C. (2000). Regulation of glutathione synthesis. *Curr Top Cell Regul, 36*, 95-116.

Malik, A. I., & Storey, K. B. (2011). Transcriptional regulation of antioxidant enzymes by FoxO1 under dehydration stress. *Gene, 485*(2), 114-119.

Markvicheva, K. N., Bilan, D. S., Mishina, N. M., Gorokhovatsky, A. Y., Vinokurov, L. M., Lukyanov, S., et al. (2011). A genetically encoded sensor for H2O2 with expanded dynamic range. *Bioorg Med Chem, 19*(3), 1079-1084.

Mather, M., & Rottenberg, H. (2001). Polycations induce the release of soluble intermembrane mitochondrial proteins. *Biochim Biophys Acta, 1503*(3), 357-368.

McLaughlin, T., Abbasi, F., Lamendola, C., & Reaven, G. (2007). Heterogeneity in the prevalence of risk factors for cardiovascular disease and type 2 diabetes mellitus in obese individuals: effect of differences in insulin sensitivity. *Arch Intern Med, 167*(7), 642-648.

McLaughlin, T., Sherman, A., Tsao, P., Gonzalez, O., Yee, G., Lamendola, C., et al. (2007). Enhanced proportion of small adipose cells in insulin-resistant vs insulin-sensitive obese individuals implicates impaired adipogenesis. *Diabetologia, 50*(8), 1707-1715.

MITCHELL, P. (1961). Coupling of phosphorylation to electron and hydrogen transfer by a chemi-osmotic type of mechanism. *Nature, 191*, 144-148.

Mitchell, P., & Moyle, J. (1968). Proton translocation coupled to ATP hydrolysis in rat liver mitochondria. *Eur J Biochem, 4*(4), 530-539.

Mittendorfer, B., Liem, O., Patterson, B. W., Miles, J. M., & Klein, S. (2003). What does the measurement of whole-body fatty acid rate of appearance in plasma by using a fatty acid tracer really mean? *Diabetes, 52*(7), 1641-1648.

Modur, V., Nagarajan, R., Evers, B. M., & Milbrandt, J. (2002). FOXO proteins regulate tumor necrosis factor-related apoptosis inducing ligand expression. Implications for PTEN mutation in prostate cancer. *J Biol Chem, 277*(49), 47928-47937.

Moro, C., Bajpeyi, S., & Smith, S. R. (2008). Determinants of intramyocellular triglyceride turnover: implications for insulin sensitivity. *Am J Physiol Endocrinol Metab, 294*(2), E203-213.

Murphy, M. P. (2009). How mitochondria produce reactive oxygen species. *Biochem J, 417*(1), 1-13.

Nadeau, P. J., Charette, S. J., & Landry, J. (2009). REDOX reaction at ASK1-Cys250 is essential for activation of JNK and induction of apoptosis. *Mol Biol Cell, 20*(16), 3628-3637.

Nakae, J., Barr, V., & Accili, D. (2000). Differential regulation of gene expression by insulin and IGF-1 receptors correlates with phosphorylation of a single amino acid residue in the forkhead transcription factor FKHR. *EMBO J, 19*(5), 989-996.

Nakae, J., Cao, Y., Oki, M., Orba, Y., Sawa, H., Kiyonari, H., et al. (2008). Forkhead transcription factor FoxO1 in adipose tissue regulates energy storage and expenditure. *Diabetes, 57*(3), 563-576.

Nasrin, N., Kaushik, V. K., Fortier, E., Wall, D., Pearson, K. J., de Cabo, R., et al. (2009). JNK1 phosphorylates SIRT1 and promotes its enzymatic activity. *PLoS One, 4*(12), e8414.

Nemoto, S., Fergusson, M. M., & Finkel, T. (2005). SIRT1 functionally interacts with the metabolic regulator and transcriptional coactivator PGC-1{alpha}. *J Biol Chem, 280*(16), 16456-16460.

Nemoto, S., & Finkel, T. (2002). Redox regulation of forkhead proteins through a p66shc-dependent signaling pathway. *Science, 295*(5564), 2450-2452.

Nguyen, M., Satoh, H., Favelyukis, S., Babendure, J., Imamura, T., Sbodio, J., et al. (2005). JNK and tumor necrosis factor-alpha mediate free fatty acid-induced insulin resistance in 3T3-L1 adipocytes. *J Biol Chem, 280*(42), 35361-35371.

Nguyen, T., Yang, C. S., & Pickett, C. B. (2004). The pathways and molecular mechanisms regulating Nrf2 activation in response to chemical stress. *Free Radic Biol Med, 37*(4), 433-441.

Nikiforov, A., Dölle, C., Niere, M., & Ziegler, M. (2011). Pathways and subcellular compartmentation of NAD biosynthesis in human cells: from entry of extracellular precursors to mitochondrial NAD generation. *J Biol Chem, 286*(24), 21767-21778.

Nonn, L., Williams, R. R., Erickson, R. P., & Powis, G. (2003). The absence of mitochondrial thioredoxin 2 causes massive apoptosis, exencephaly, and early embryonic lethality in homozygous mice. *Mol Cell Biol, 23*(3), 916-922.

Novgorodtseva, T. P., Karaman, Y. K., Zhukova, N. V., Lobanova, E. G., Antonyuk, M. V., & Kantur, T. A. (2011). Composition of fatty acids in plasma and erythrocytes and eicosanoids level in patients with metabolic syndrome. *Lipids Health Dis, 10*, 82.

Olshansky, S. J. (2005). Projecting the future of U.S. health and longevity. *Health Aff (Millwood), 24 Suppl 2*, W5R86-89.

Orrenius, S., Gogvadze, V., & Zhivotovsky, B. (2007). Mitochondrial oxidative stress: implications for cell death. *Annu Rev Pharmacol Toxicol, 47*, 143-183.

Ott, M., Robertson, J. D., Gogvadze, V., Zhivotovsky, B., & Orrenius, S. (2002). Cytochrome c release from mitochondria proceeds by a two-step process. *Proc Natl Acad Sci U S A, 99*(3), 1259-1263.

Paolisso, G., Gambardella, A., Balbi, V., Ammendola, S., D'Amore, A., & Varricchio, M. (1995). Body composition, body fat distribution, and resting metabolic rate in healthy centenarians. *Am J Clin Nutr, 62*(4), 746-750.

Paolisso, G., Tataranni, P. A., Foley, J. E., Bogardus, C., Howard, B. V., & Ravussin, E. (1995). A high concentration of fasting plasma non-esterified fatty acids is a risk factor for the development of NIDDM. *Diabetologia, 38*(10), 1213-1217.

Papadopoulos, N. G., Dedoussis, G. V., Spanakos, G., Gritzapis, A. D., Baxevanis, C. N., & Papamichail, M. (1994). An improved fluorescence assay for the determination of lymphocyte-mediated cytotoxicity using flow cytometry. *J Immunol Methods, 177*(1-2), 101-111.

Petronilli, V., Miotto, G., Canton, M., Colonna, R., Bernardi, P., & Di Lisa, F. (1998). Imaging the mitochondrial permeability transition pore in intact cells. *Biofactors, 8*(3-4), 263-272.

Piantadosi, C. A., & Suliman, H. B. (2006). Mitochondrial transcription factor A induction by redox activation of nuclear respiratory factor 1. *J Biol Chem, 281*(1), 324-333.

Pories, W., & Dohm, G. (2009). Full and durable remission of type 2 diabetes? Through surgery? *Surg Obes Relat Dis, 5*(2), 285-288.

Potgieter, M., Pretorius, E., & Pepper, M. S. (2013). Primary and secondary coenzyme Q10 deficiency: the role of therapeutic supplementation. *Nutr Rev, 71*(3), 180-188.

Prime, T. A., Forkink, M., Logan, A., Finichiu, P. G., McLachlan, J., Li Pun, P. B., et al. (2012). A ratiometric fluorescent probe for assessing mitochondrial phospholipid peroxidation within living cells. *Free Radic Biol Med, 53*(3), 544-553.

Pushpa-Rekha, T. R., Burdsall, A. L., Oleksa, L. M., Chisolm, G. M., & Driscoll, D. M. (1995). Rat phospholipid-hydroperoxide glutathione peroxidase. cDNA cloning and identification of multiple transcription and translation start sites. *J Biol Chem, 270*(45), 26993-26999.

Ravussin, E., & Smith, S. (2002). Increased fat intake, impaired fat oxidation, and failure of fat cell proliferation result in ectopic fat storage, insulin resistance, and type 2 diabetes mellitus. *Ann N Y Acad Sci, 967*, 363-378.

Revollo, J. R., Grimm, A. A., & Imai, S. (2007). The regulation of nicotinamide adenine dinucleotide biosynthesis by Nampt/PBEF/visfatin in mammals. *Curr Opin Gastroenterol, 23*(2), 164-170.

Rogers, C., Moukdar, F., McGee, M. A., Davis, B., Buehrer, B. M., Daniel, K. W., et al. (2012a). EGF receptor (ERBB1) abundance in adipose tissue is reduced in insulin-resistant and type 2 diabetic women. *J Clin Endocrinol Metab, 97*(3), E329-340.

Rogers, C., Moukdar, F., McGee, M. A., Davis, B., Buehrer, B. M., Daniel, K. W., et al. (2012b). EGF Receptor (ERBB1) Abundance in Adipose Tissue Is Reduced in Insulin-Resistant and Type 2 Diabetic Women. *J Clin Endocrinol Metab*.

Rongvaux, A., Andris, F., Van Gool, F., & Leo, O. (2003). Reconstructing eukaryotic NAD metabolism. *Bioessays, 25*(7), 683-690.

Sabin, M. A., De Hora, M., Holly, J. M., Hunt, L. P., Ford, A. L., Williams, S. R., et al. (2007). Fasting nonesterified fatty acid profiles in childhood and their relationship with adiposity, insulin sensitivity, and lipid levels. *Pediatrics, 120*(6), e1426-1433.

Saitoh, M., Nishitoh, H., Fujii, M., Takeda, K., Tobiume, K., Sawada, Y., et al. (1998). Mammalian thioredoxin is a direct inhibitor of apoptosis signal-regulating kinase (ASK) 1. *EMBO J, 17*(9), 2596-2606.

Samocha-Bonet, D., Chisholm, D. J., Tonks, K., Campbell, L. V., & Greenfield, J. R. (2012). Insulin-sensitive obesity in humans - a 'favorable fat' phenotype? *Trends Endocrinol Metab, 23*(3), 116-124.

Sano, M., & Fukuda, K. (2008). Activation of mitochondrial biogenesis by hormesis. *Circ Res, 103*(11), 1191-1193.

Sauve, A. A. (2008). NAD+ and vitamin B3: from metabolism to therapies. *J Pharmacol Exp Ther, 324*(3), 883-893.

Schaap, F. G., Binas, B., Danneberg, H., van der Vusse, G. J., & Glatz, J. F. (1999). Impaired long-chain fatty acid utilization by cardiac myocytes isolated from mice lacking the heart-type fatty acid binding protein gene. *Circ Res, 85*(4), 329-337.

Schönfeld, P., & Bohnensack, R. (1997). Fatty acid-promoted mitochondrial permeability transition by membrane depolarization and binding to the ADP/ATP carrier. *FEBS Lett, 420*(2-3), 167-170.

Schönfeld, P., & Struy, H. (1999). Refsum disease diagnostic marker phytanic acid alters the physical state of membrane proteins of liver mitochondria. *FEBS Lett, 457*(2), 179-183.

Schönfeld, P., & Wojtczak, L. (2007). Fatty acids decrease mitochondrial generation of reactive oxygen species at the reverse electron transport but increase it at the forward transport. *Biochim Biophys Acta, 1767*(8), 1032-1040.

Schönfeld, P., & Wojtczak, L. (2008). Fatty acids as modulators of the cellular production of reactive oxygen species. *Free Radic Biol Med, 45*(3), 231-241.

Schönfeld, P., & Wojtczak, L. (2008). Fatty acids as modulators of the cellular production of reactive oxygen species. *Free Radic Biol Med, 45*(3), 231-241.

Sethi, J., & Vidal-Puig, A. (2007). Thematic review series: adipocyte biology. Adipose tissue function and plasticity orchestrate nutritional adaptation. *J Lipid Res, 48*(6), 1253-1262.

Shadid, S., Koutsari, C., & Jensen, M. D. (2007). Direct free fatty acid uptake into human adipocytes in vivo: relation to body fat distribution. *Diabetes, 56*(5), 1369-1375.

Shah, N. R., & Braverman, E. R. (2012). Measuring Adiposity in Patients: The Utility of Body Mass Index (BMI), Percent Body Fat, and Leptin. *PLoS One, 7*(4), e33308.

Skulachev, V. (1996). Role of uncoupled and non-coupled oxidations in maintenance of safely low levels of oxygen and its one-electron reductants. *Q Rev Biophys, 29*(2), 169-202.

Skurk, T., Ecklebe, S., & Hauner, H. (2007). A novel technique to propagate primary human preadipocytes without loss of differentiation capacity. *Obesity (Silver Spring), 15*(12), 2925-2931.

Smith, G. R., & Shanley, D. P. (2010). Modelling the response of FOXO transcription factors to multiple post-translational modifications made by ageing-related signalling pathways. *PLoS One, 5*(6), e11092.

Smith, J., Al-Amri, M., Dorairaj, P., & Sniderman, A. (2006). The adipocyte life cycle hypothesis. *Clin Sci (Lond), 110*(1), 1-9.

Spalding, K. L., Arner, E., Westermark, P. O., Bernard, S., Buchholz, B. A., Bergmann, O., et al. (2008). Dynamics of fat cell turnover in humans. *Nature, 453*(7196), 783-787.

Stefan, N., Kantartzis, K., Machann, J., Schick, F., Thamer, C., Rittig, K., et al. (2008). Identification and characterization of metabolically benign obesity in humans. *Arch Intern Med, 168*(15), 1609-1616.

Stillwell, W., Jenski, L. J., Crump, F. T., & Ehringer, W. (1997). Effect of docosahexaenoic acid on mouse mitochondrial membrane properties. *Lipids, 32*(5), 497-506.

Subauste, A., & Burant, C. (2007). Role of FoxO1 in FFA-induced oxidative stress in adipocytes. *Am J Physiol Endocrinol Metab, 293*(1), E159-164.

Subauste, A. R., & Burant, C. F. (2007). Role of FoxO1 in FFA-induced oxidative stress in adipocytes. *Am J Physiol Endocrinol Metab, 293*(1), E159-164.

Surh, Y. J., Kundu, J. K., & Na, H. K. (2008). Nrf2 as a master redox switch in turning on the cellular signaling involved in the induction of cytoprotective genes by some chemopreventive phytochemicals. *Planta Med, 74*(13), 1526-1539.

Tahiri, Y., Karpe, F., Tan, G. D., & Cianflone, K. (2007). Rosiglitazone decreases postprandial production of acylation stimulating protein in type 2 diabetics. *Nutr Metab (Lond), 4*, 11.

Tchoukalova, Y., Koutsari, C., & Jensen, M. (2007). Committed subcutaneous preadipocytes are reduced in human obesity. *Diabetologia, 50*(1), 151-157.

Tyagi, S., Gupta, P., Saini, A. S., Kaushal, C., & Sharma, S. (2011). The peroxisome proliferator-activated receptor: A family of nuclear receptors role in various diseases. *J Adv Pharm Technol Res, 2*(4), 236-240.

Unger, R. H., Clark, G. O., Scherer, P. E., & Orci, L. (2010a). Lipid homeostasis, lipotoxicity and the metabolic syndrome. *Biochim Biophys Acta, 1801*(3), 209-214.

Unger, R. H., Clark, G. O., Scherer, P. E., & Orci, L. (2010b). Lipid homeostasis, lipotoxicity and the metabolic syndrome. *Biochim Biophys Acta, 1801*(3), 209-214.

van der Horst, A., Tertoolen, L. G., de Vries-Smits, L. M., Frye, R. A., Medema, R. H., & Burgering, B. M. (2004). FOXO4 is acetylated upon peroxide stress and deacetylated by the longevity protein hSir2(SIRT1). *J Biol Chem, 279*(28), 28873-28879.

Varlamov, O., Somwar, R., Cornea, A., Kievit, P., Grove, K. L., & Roberts, C. T. (2010). Single-cell analysis of insulin-regulated fatty acid uptake in adipocytes. *Am J Physiol Endocrinol Metab, 299*(3), E486-496.

Vaziri, H., Dessain, S. K., Ng Eaton, E., Imai, S. I., Frye, R. A., Pandita, T. K., et al. (2001). hSIR2(SIRT1) functions as an NAD-dependent p53 deacetylase. *Cell, 107*(2), 149-159.

Vines, A., McBean, G. J., & Blanco-Fernández, A. (2010). A flow-cytometric method for continuous measurement of intracellular Ca(2+) concentration. *Cytometry A, 77*(11), 1091-1097.

Wallace, D. C., Fan, W., & Procaccio, V. (2010). Mitochondrial energetics and therapeutics. *Annu Rev Pathol, 5*, 297-348.

Wang, T., Si, Y., Shirihai, O. S., Si, H., Schultz, V., Corkey, R. F., et al. (2010). Respiration in adipocytes is inhibited by reactive oxygen species. *Obesity (Silver Spring), 18*(8), 1493-1502.

Wang, T., Zang, Y., Ling, W., Corkey, B. E., & Guo, W. (2003). Metabolic partitioning of endogenous fatty acid in adipocytes. *Obes Res, 11*(7), 880-887.

Wojtczak, L. (1976). Effect of long-chain fatty acids and acyl-CoA on mitochondrial permeability, transport, and energy-coupling processes. *J Bioenerg Biomembr, 8*(6), 293-311.

Woods, Y. L., Rena, G., Morrice, N., Barthel, A., Becker, W., Guo, S., et al. (2001). The kinase DYRK1A phosphorylates the transcription factor FKHR at Ser329 in vitro, a novel in vivo phosphorylation site. *Biochem J, 355*(Pt 3), 597-607.

Wu, J., Boström, P., Sparks, L. M., Ye, L., Choi, J. H., Giang, A. H., et al. (2012). Beige adipocytes are a distinct type of thermogenic fat cell in mouse and human. *Cell, 150*(2), 366-376.

Yamazaki, E., Inagaki, M., Kurita, O., & Inoue, T. (2005). Kinetics of fatty acid binding ability of glycated human serum albumin. *J Biosci, 30*(4), 475-481.

Yang, N. C., Ho, W. M., Chen, Y. H., & Hu, M. L. (2002). A convenient one-step extraction of cellular ATP using boiling water for the luciferin-luciferase assay of ATP. *Anal Biochem, 306*(2), 323-327.

Yeop Han, C., Kargi, A. Y., Omer, M., Chan, C. K., Wabitsch, M., O'Brien, K. D., et al. (2010). Differential effect of saturated and unsaturated free fatty acids on the generation of monocyte adhesion and chemotactic factors by adipocytes: dissociation of adipocyte hypertrophy from inflammation. *Diabetes*, *59*(2), 386-396.

Yeung, F., Hoberg, J. E., Ramsey, C. S., Keller, M. D., Jones, D. R., Frye, R. A., et al. (2004). Modulation of NF-kappaB-dependent transcription and cell survival by the SIRT1 deacetylase. *EMBO J, 23*(12), 2369-2380.

APPENDIX A: HUMAN INSTITUTIONAL AND REVIEW BOARD APPROVAL LETTER

EAST CAROLINA UNIVERSITY
University & Medical Center Institutional Review Board Office
1L-09 Brody Medical Sciences Building· Mail Stop 682
600 Moye Boulevard · Greenville, NC 27834
Office **252-744-2914** · Fax **252-744-2284** · www.ecu.edu/irb

Notification of Initial Approval (Committee)

From: Biomedical IRB
To: Jacques Robidoux
CC:

Barbara Davis
Date: 11/3/2011
Re: UMCIRB 11-001086
Fatty acids and redox homeostasis in adipocytes

I am pleased to inform you that at the convened meeting on 10/26/2011 12:00 PM of Biomedical IRB , the committee voted to approve the above study. Approval of the study and the consent form(s) is for the period of 10/26/2011 to 10/25/2012.

The Biomedical IRB deemed this study Greater than Minimal Risk.

Changes to this approved research may not be initiated without UMCIRB review except when necessary to eliminate an apparent immediate hazard to the participant. All unanticipated problems involving risks to participants and others must be promptly reported to the UMCIRB. The investigator must submit a continuing review/closure application to the UMCIRB prior to the date of study expiration. The investigator must adhere to all reporting requirements for this study.

The approval includes the following items:

Name	Description	Modified	Version
4-Informed Consent.docx | History	Consent Forms	10/28/2011 11:52 AM	0.02
CR_Research_Plan_AHA_2011.pdf | History	Study Protocol or Grant Application	10/17/2011 4:57 PM	0.01
Fat Metabolism Flyer.docx | History	Recruitment Documents/Scripts	10/17/2011 8:52 PM	0.02
Literature_Cited[1].pdf | History	Study Protocol or Grant Application	10/17/2011 4:58 PM	0.01

The following UMCIRB members were recused for reasons of potential for Conflict of Interest on this research study:

None

The following UMCIRB members with a potential Conflict of Interest did not attend this IRB meeting:

R. Hickner

APPENDIX B: APPROVED CONSENT FORMS FOR RESEARCH INVOLVING HUMAN SUBJECTS

East Carolina University

Consent to Participate in Research that is Greater than Minimal Risk

Information to Consider Before Taking Part in This Research

Title of Research Study: Fatty acids and redox homeostasis in adipocytes

Principal Investigator: Jacques Robidoux, PhD.
Department of Pharmacology and Toxicology, East Carolina Diabetes and Obesity Institute, Brody School of Medicine
Address: 6S10 Brody School of Medicine, Greenville, NC 27834
Telephone #: 252-744-2741 (Lab), 252-744-5909 (Office)

Research performed at the East Carolina Diabetes and Obesity Institute (ECDOI) aims to provide understanding, to prevent or to treat metabolic disorders with an emphasis on diabetes and obesity. Our goal is to try to find ways to improve the quality of life. To accomplish this, we need the help of people who are willing to take part in this research.

The person who is in charge of this research project is called the Principal Investigator. Dr. Jacques Robidoux is the Principal Investigator of this project. Dr. Robert Hickner and Dr. Darrell Neufer are his collaborators. Artie Carlyle Rogers is a graduate student. Angela Clark is a registered nurse. Barbara Davis is the study coordinator. They will perform some of the procedures. Dr. Robert J. Tanenberg is overseeing the medical issues associated with the project.

The person explaining the research to you may be someone other than Jacques Robidoux, PhD. Artie Carlyle Rogers or Barbara Davis may be explaining the research to you as well as asking you to take part in this study.

You may have questions that this form does not answer. If you do have questions, feel free to ask the person explaining the study to you. You may have questions later and you should ask those questions, as you think of them. There is no time limit for asking about this research.

You do not have to take part in this research. Take your time and think about the information that is provided. If you want, have a friend or family member go over this form with you before you decide whether or not to participate. It is up to you. If you choose to be in the study, then you should sign the form when you feel comfortable that you understand the information provided below. If you do not want to take part in the study, you should not sign this form. That decision is yours and it is okay to decide not to volunteer.

This form explains why this research is being done, what will happen during the research, and what you will need to do if you decide to participate in this research.

Why is this research being done?

The purpose of this research study is to understand the reasons why some overweight/obese individuals develop insulin resistance and type 2 diabetes. Insulin resistance is a state in which you need more insulin (a hormone released by your pancreas) to keep your blood glucose (sugar) in the normal range. Type 2 diabetes develops when your body does not produce enough insulin to overcome insulin resistance. We are especially interested in trying to understand why some overweight or obese individuals do not develop these metabolic disorders. We are asking you to take part in this research. However, the decision is yours to make. By doing this research, we hope to learn new ways to prevent insulin resistance and ultimately type 2 diabetes.

Why am I being invited to take part in this research?

You are being invited to take part in this research because you are a man or a premenopausal woman, 18-45 years old and overweight or obese. If you volunteer to take part in this study, you will be one of about 60 people to do so.

Are there reasons I should not take part in this research?

I understand I should not volunteer for this study if I am diabetic, a smoker, under 18 or over 45 years of age, take part in regular physical activity (greater than 45 minutes per day, more than 2 days per week), I am pregnant, lactating or trying to get pregnant, taking any hormone therapy (including hormonal birth control), taking drugs to control my blood glucose, lipids, or blood pressure, or if I am actively trying to lose weight.

Where is the research going to take place and how long will it last?

The research procedures will be conducted at the East Carolina Heart Institute (ECHI). You will need to come to the ECHI rooms 2377/2379 up to three times. The initial screening visit takes about 40 minutes. The second screening visit takes slightly more than 2 hours. The third visit takes about 2 hours. The total amount of time you will be asked to volunteer for this study could be up to 5-6 hours over a period of 2-3 months.

What will I be asked to do?

<u>Initial Screening visit</u> (about 40 minutes)

FOR THIS VISIT AND ALL OTHER VISITS YOU WILL BE FASTING
<u>(no food or drink other than water after 10pm the night before).</u>

If you consume anything, please call us. We will have to reschedule the screening procedure at the next available date. If you eat, the data collected will not be valid!

Medical and Family History Questionnaire: Before beginning the study, you will complete a medical and family history questionnaire to provide information on your ancestry, medical history of your blood related family, and your health and medical status. Completion of the questionnaire will take approximately 20 minutes.

We will ask that you do not change your activity level, dietary habits or any medication you are taking during the time you are taking part in this study. If this becomes a concern during your participation we ask you to contact us and let us know as soon as possible.

Determination of fasting and glucose and insulin levels. Because we want to understand the difference between insulin-sensitive and insulin-resistant individual we will draw blood from you to measure your plasma glucose (sugar), nonesterified fatty acids (lipids) and insulin (hormone) levels. Blood samples will be drawn from an intravenous (IV) catheter placed in a vein in your arm by, or under the supervision of, Angela Clark RN, a registered nurse. This procedure will take less than 5 minutes and the blood sample will amount to about half of a teaspoon (2.7 mL).

Height and weight measurements. Height and weight will be taken by having you stand on a medical scale with a height rod. This test will last less than 5 minutes.

Waist to Hip ratio. Waist and hip circumferences will be taken with a tape measure against the skin around the waist and hip regions. This test will last less than 5 minutes.

Second Screening visit (about 2 ½ hours)

Only if the first screening visit suggests that you are very insulin-sensitive or very insulin-resistant will you be invited to participate in the second procedure.

FOR THIS VISIT YOU WILL BE FASTING
(no food or drink other than water after 10pm the night before).

If you consume anything, please call us. We will have to reschedule the screening procedure at the next available date. If you eat, the data collected will not be valid!

Two hour, five-sample oral glucose tolerance test (OGTT). Blood samples will be drawn from an intravenous (IV) catheter placed in a vein in your arm by, or under the supervision of, Angela Clark RN, a registered nurse. These blood samples will be taken just before and 30, 60, 90, 120 minutes after ingestion of 75g glucose. These samples will be used to determine blood concentration of glucose, nonesterified fatty acids, and insulin. The total amount of blood drawn

as part of this study will be approximately 2.5 teaspoons (5 X 2.7 mL). This amount is very small compared to the total amount (about a gallon) of blood that you have.

Third visit: Fat biopsies (about 2 hours)

FOR THIS VISIT YOU WILL BE FASTING
(no food or drink other than water after 10pm the night before).

If you consume anything, please call us. We will have to reschedule the screening procedure at the next available date. If you eat, the data collected will not be valid!

Adipose tissue (fat) biopsies. You will undergo two biopsies: 1) to determine the level of oxidized proteins (which may be a cause of insulin resistance) and the expression of genes that could protect or lead to insulin resistance; 2) to isolate fat cell precursors (cells that can develop into fat cells) that will be grown in the laboratory. These cells will be exposed to lipids and we will measure the cell's response to lipids. For this procedure, a small amount of anesthesia (less than 1 teaspoon of 1% Lidocaine) will be injected in a ½ inch area under the skin of your abdomen a few inches to the left side of your belly button. About 1 teaspoon of saline (salt water) will also be injected under the skin. Adipose tissue (fat) will be aspirated (sucked out) using a needle with suction provided by a large syringe. Less than a gram (one fifth of a teaspoon) of subcutaneous adipose tissue will be collected this way. This procedure will, if you still consent, be repeated on the right side of your belly button. Because there is an extremely remote risk of allergic reaction to the Lidocaine anesthesia, risk will be minimized by using subjects who have had prior exposure to Lidocaine or Novocaine anesthesia or by having a physician available during the biopsy procedure for those subjects who have not had previous exposure to "caine-type" anesthetics. You should tell us now if you are allergic to "caine-type" anesthetics. For example, if you have had an allergic reaction to an injection at the dentist's office. You should also tell us now whether or not you have been exposed to a caine-type anesthetic (for example at the dentist office or during a prior biopsy). Robert Hickner, Ph.D, will perform the biopsies under the medical coverage of Dr. Robert Tanenberg, MD

What possible risks or discomforts might I experience if I take part in the research?

There are always risks (the chance of harm) when taking part in research. We know about the following risks or discomforts you may experience if you choose to volunteer for this study. These are called side effects. The following side effects are known to occur in some people:

Medical history: Risk of feeling embarrassed or a loss of privacy. To minimize these risks, you will fill out the forms in a private area. All information collected will not be associated with your name, will be kept confidential, and your name will not appear on any forms containing any data obtained from you. You will be given an identification number which will be your only identifier

throughout the study including the archiving of your samples and the analysis of the data obtained from these samples.

Weight and circumference measurement. Risk of feeling embarrassed or a loss of privacy. To minimize these risks, these measurements will be performed in a private area. All information collected will not be associated with your name, will be kept confidential, and your name will not appear on any forms containing any data from you. You will be given an identification number which will be your only identifier throughout the study including the archiving of your samples and the analysis of the data obtained from these samples.

Overnight fasting may cause hunger and possibly dizziness. By scheduling the research procedures from 8 -10 AM this discomfort will be minimal and will be relieved within minutes after the procedures when you will be allowed to drink and eat.

Risks associated with an IV catheter and blood draw are small and can include hematoma (minor swelling and bruising) and infection**.** The insertion of the IV catheter will be performed by qualified personnel to reduce these risks.

Fat Biopsies - Robert Hickner, Ph.D, will perform the fat biopsies with Dr. Robert J. Tanenberg, MD providing medical coverage. There is a small risk of hematoma or infection around the biopsy site, as well as mild tenderness and bruising. The risk will be minimized by using sterile procedures and applying pressure to the biopsy site until the minor bleeding has stopped. You will feel mild pain, similar to the pain you feel when receiving a shot in the arm, during the injection of numbing medication (Lidocaine) under the skin over your abdominal adipose tissue before the adipose tissue biopsy**.** Because there is an extremely remote risk of allergic reaction to the Lidocaine anesthesia, risk will be minimized by using subjects who have had prior exposure to Lidocaine or Novocaine anesthesia or by having a physician available during the biopsy procedure for those subjects who have not had previous exposure to "caine-type" anesthetics. You cannot participate in this research if you knowingly have heart disease or any condition that could result in excessive bleeding.

There is also the risk of potential embarrassment during the collection of adipose tissue biopsies. This risk will be minimized by the involvement of minimal staff associated with the procedure and conducting the procedure in a private room or behind a privacy curtain.

There is always a chance that any medical intervention may cause you some discomfort or harm and the procedures in this study are no different. We will do everything possible to keep you from being harmed. There may be other risks or side effects that occur which we do not know about at this time.

It is important for you to tell us as quickly as possible if you experience a side effect.

Are there any reasons you might take me out of the research?

There may be reasons we will need to take you out of the study, even if you want to stay in. We may find out that it is not safe for you to stay in the study. It may be that the side effects are so severe that we need to stop the study or take you out of the study to reduce your risk of harm. If we find that the research might harm you or that it is not providing enough of a benefit to justify the risks you are taking, we will contact you immediately with an explanation of why you can no longer participate and give you copies of results from any screening or research tests that would be of interest to you or your primary care physician. We may also find that you cannot come for your study visits as scheduled. If that is found to be true, we will need to take you out of the study. Finally there are scientific reasons. The principal reasons are that you are not clearly insulin-sensitive or sensitive-resistant. Because we want to understand the difference between these two groups we will have to stop your participation in the study if you do not clearly fall into these two groups.

What are the possible benefits I may experience from taking part in this research?

There may be no personal benefit from your participation but the information gained by doing this research may help others in the future.

Will I be paid for taking part in this research?

We will pay you for the time you volunteer while being in this study. Compensation will be provided according to the visits you complete as part of the study. $25 will be provided for the consent visit, $50 for the second (first screening visit), $75 for the third (second screening visit), $75 for the fourth (fat biopsy visit); for a possible total of $225. Appropriate compensation will be provided after completion of the study or after your participation in the study has stopped for any reason.

What will it cost me to take part in this research?

It will not cost you any money to be part of the research; it will only cost your personal time. You will be responsible for providing your own transportation to and from the ECHI for each study related visit. There is no service provided that requires a cost on your or on our part. The cost of this research is assumed by the researcher's funding.

Who will know that I took part in this research and learn personal information about me?

To do this research, you may meet with the study coordinator, research nurses, and study staff including Dr. Hickner who will perform the biopsies and Dr. Robert J. Tanenberg, who oversees

the medical aspects of the research. All other individuals that do not have physical contact with you, which include these same individuals and others when processing the samples, the data from the samples, or the data from the questionnaires you filed, will only know you by your identification number. These people are ECU staff and the people and organizations listed below.

The research team, including the Principal Investigator, study coordinator, research nurses, and all other research staff or students involved in conducting the study.
All of the research sites' staff. These are the research and medical staff at the ECHI
Any agency of the federal, state, or local government that regulates this research. This includes the Department of Health and Human Services (DHHS), the North Carolina Department of Health, and the Office for Human Research Protections
The ECU University & Medical Center Institutional Review Board (UMCIRB) and the staff who have responsibility for overseeing your welfare during this research, and other ECU office staff who oversee this research.

How will you keep the information you collect about me secure and how long will you keep it?

The confidentiality of information collected from volunteers of this study will be ensured by numeric coding of all data. Data will be secured on password encrypted computers, in the office of Dr. Robidoux and in a secondary backup file contained in a locked filing cabinet also in Dr Robidoux's office. The data will be kept for at least 10 years. Samples will be stored in freezers for at least 10 years. It is possible that the information collected in this study will be used in professional publications, conference presentations or for future research projects, but all data will be stripped of any personal identifiers so no one will associate you with the research project.

What if I decide I do not want to continue in this research?

Participating in this study is voluntary. If you decide not to participate in this research after it has already started, you may stop at any time. You will not be penalized or criticized for stopping.

What if I get sick or hurt while I am in this research?

If you are harmed while taking part in this study:

If you believe you have been hurt or if you get sick because of something that is done during the study, you should call and tell us immediately. There are procedures in place to help attend to your injuries or provide care for you. Costs associated with this care will be billed in the ordinary manner, to you or your insurance company. However, some insurance companies will not pay

bills that are related to research costs. You should check with your insurance company about this. Medical costs that result from research-related harm may also not qualify for payments through Medicare, or Medicaid. You should talk to the study coordinator, the principal investigator or Dr. Robidoux about this, if you have concerns.

If you need emergency care:

Call 911 for help. It is important that you tell the doctors, the hospital or emergency room staff that you are taking part in a research study and the name of the Principal Investigator. If possible, take a copy of this consent form with you when you go.

Call Barbara Davis at [redacted] days or nights and weekends, Artie Carlyle Rogers at [redacted] days or nights and weekends or Dr. Jacques Robidoux at [redacted] days or nights and weekends. We need to know if you are hurt or ill.

If you do NOT need emergency care, but have been hurt or get sick:

Call Barbara Davis at [redacted] days or nights and weekends, Artie Carlyle Rogers at [redacted] days or nights and weekends or Dr. Jacques Robidoux at [redacted] days or nights and weekends. We need to know that you are hurt or ill. As necessary, go to your regular doctor. It is important that you tell your regular doctor that you are participating in a research study.

Who should I contact if I have questions?

The people conducting this study will be available to answer any questions concerning this research, now or in the future. You may call Barbara Davis at [redacted] days or nights and weekends, Artie Carlyle Rogers at [redacted] days or nights and weekends or Dr. Jacques Robidoux at [redacted] days or nights and weekends.

If you have questions about your rights as someone taking part in research, you may call the ECU Institutional Review Board Office at phone number 252-744-2914 (days). If you would like to report a complaint or concern about this research study, you may call the Director of UMCIRB Office, at 252-744-1971 (days).

Is there anything else I should know?

You can limit the amount and type of information that is shared and you must make this request in writing. We will make sure that no information is linked to your name except for the files containing your name and your identification number. These files (the original and the backup file) will not be shared and will be locked in Dr. Robidoux's office. The identification number associated data will be accessed and used by the research staff and may be shared with other ECU researchers and other organizations as is deemed necessary. Research information

continues to be reviewed long after study completion, so it is difficult to say when the use of your information will stop. There is not an expiration date for the use of your information for this study.

I have decided I want to take part in this research. What should I do now?

The person obtaining informed consent will ask you to read the following and if you agree, you should sign this form:

I have read (or had read to me) all of the above information.
I have had an opportunity to ask questions about things in this research I did not understand and have received satisfactory answers.
I understand that I can stop taking part in this study at any time.
By signing this informed consent form, I am not giving up any of my rights.
I have been given a copy of this consent document, and it is mine to keep.

_____ _____

Participant's Name (PRINT) Signature Date

Person Obtaining Informed Consent: I have conducted the initial informed consent process. I have orally reviewed the contents of the consent document with the person who has signed above, and answered all of the person's questions about the research.

_____

Person Obtaining Consent (PRINT) Signature Date

Jacques Robidoux
_____

Principal Investigator (PRINT) Signature Date

(If other than person obtaining informed consent)

APPENDIX C: FLOW CYTOMETRY DOTPLOT SHOWS NO CHANGE IN FSC OR SSC

Figure 17. (A) Analysis of 600 μM BSA and 100 μM H2O2 showed no shift in the forward or side scatter at 5, 15, and 30 minutes. (B) Flow cytometry gates were applied between 600 μM BSA and 100 μM H2O2 were kept constant during the course of the experiment. (C) The density plot of CM-H2DCFDA fluorescence vs. time of 100 μM H2O2 was sectioned into different (D) quadrants. Each quadrant was (E) pseudo-colored and plotted on the (F) forward scatter vs. side scatter dot plot to determine if the change in fluorescence associated with 100 μM H2O2 occurred in a single cell homogenous fashion. (G) Overlay of the gated region with the pseudo-colored dot plot revealed that the selected population exhibited a homogenous response to H2O2.

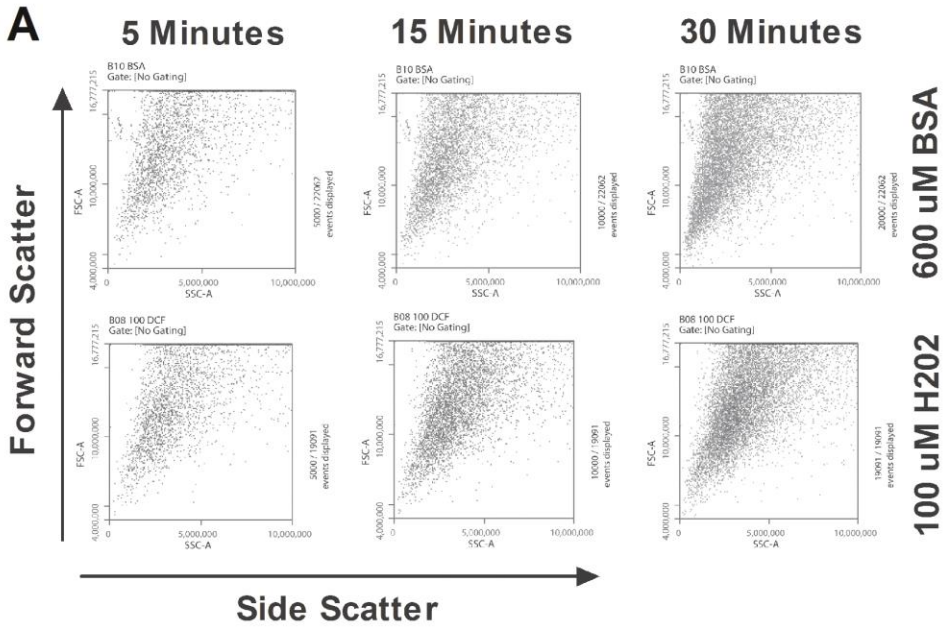
A
5 Minutes
15 Minutes
30 Minutes
600 uM BSA
100 uM H202
Forward Scatter
Side Scatter
B10 BSA
Gate: [No Gating]
B08 100 DCF
Gate: [No Gating]
FSC-A
SSC-A

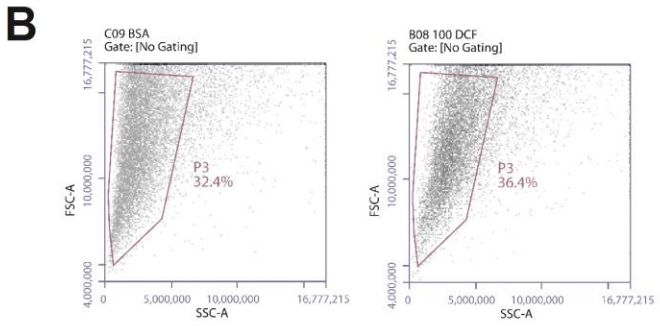
B
C09 BSA
Gate: [No Gating]
B08 100 DCF
Gate: [No Gating]
P3
32.4%
P3
36.4%
FSC-A
SSC-A

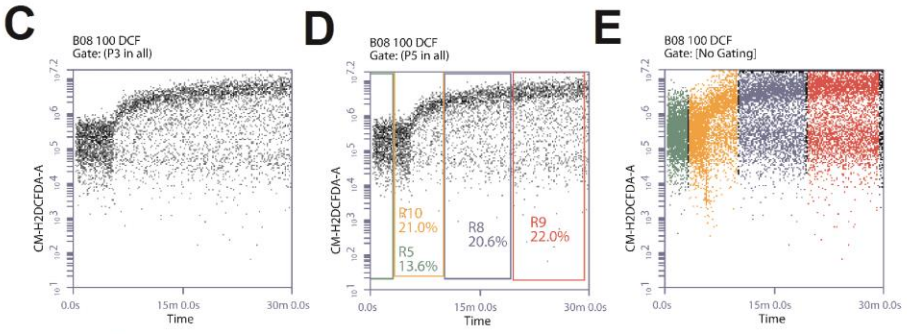
C
B08 100 DCF
Gate: (P3 in all)
D
B08 100 DCF
Gate: (P5 in all)
R10
21.0%
R5
13.6%
R8
20.6%
R9
22.0%
E
B08 100 DCF
Gate: [No Gating]
CM-H2DCFDA-A
Time

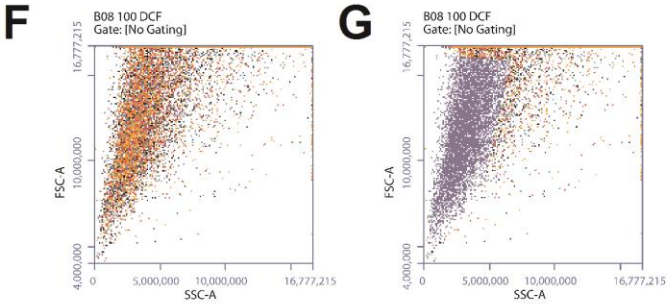
F
B08 100 DCF
Gate: [No Gating]
G
B08 100 DCF
Gate: [No Gating]
FSC-A
SSC-A

APPENDIX D: ISOTYPE STAINING OF TOTAL AND AC-FOXO1 ANTIBODIES IN PREADIPOCYTES

Figure 18. To ensure the fluorescence we observed was not due to background, we incubated cells in antibodies targeting total Foxo1, Ac-Foxo1, non-specific IgG rabbit and IgG goat antibodies. Data indicate that the fluorescent signal obtained is not due to non-specific staining.

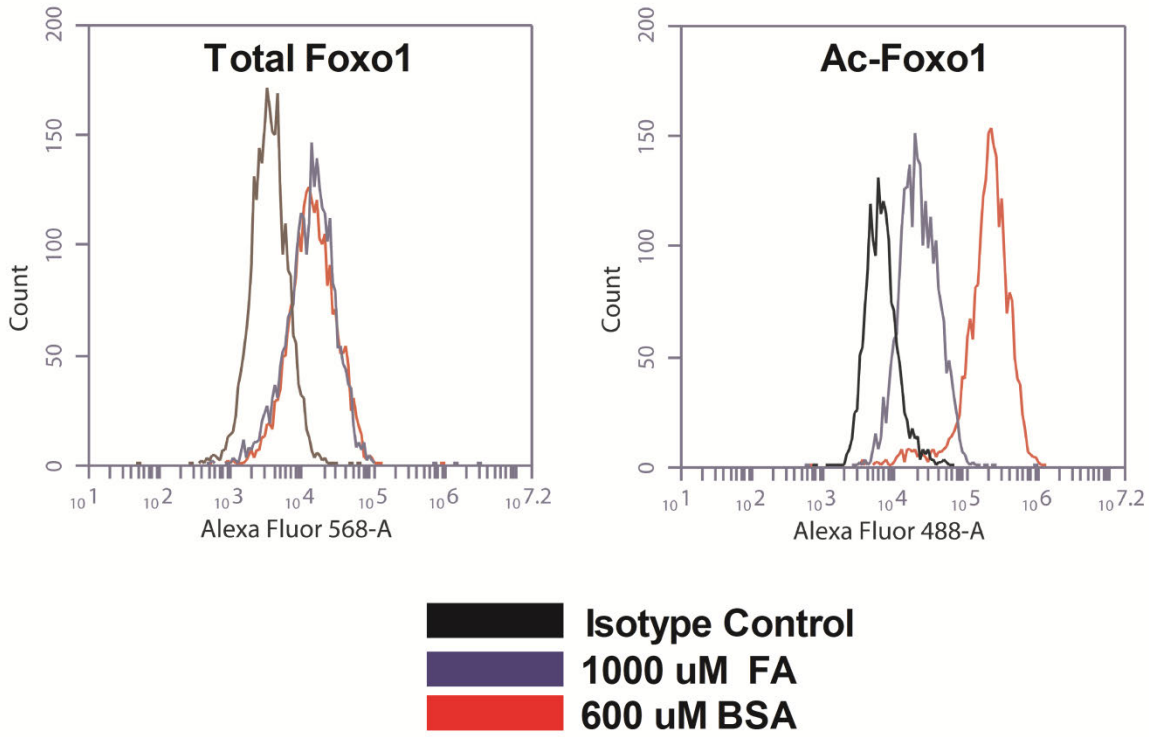
Total Foxo1
Count
Alexa Fluor 568-A
Ac-Foxo1
Count
Alexa Fluor 488-A
Isotype Control
1000 uM FA
600 uM BSA